Discovery of Naturally Occurring Sphingomyelin Synthase Inhibitors: Structural Activity Relationship Validation and Inspiring Sphingo-mimic Studies

（スフィンゴ脂質代謝を制御する天然有機化合物の探索とその機能解明に関する研究）

A Thesis

Submitted for the Degree of

Doctor of Life Science

Mahadeva Swamy M.M

Laboratory of Chemical Biology

Transdisciplinary Life Science Course

Graduate School of Life Science

Hokkaido University, Japan

March, 2018

Table of contents

Chapter-3: Daurichromenic acid, a novel SMS inhibitor: stereochemical studies of rhododaurichromanic acid A and Hongoquercin A

Abbreviations

APP: amyloid precursor protein

BSS: dextran sodium sulfate

Cdase: ceramidase

Cer: ceramide

CERK: ceramide kinase

CerS: ceramide synthase

$CHCl_3$: chloroform

CHO cells: chinese hamster ovary cells

DA: daurichromenic acid

DCC: *N,N'*-Dicyclohexylcarbodiimide

DIEAP: *N,N*-Diisopropylethylamine

DMAP: 4-Dimethylaminopyridine

DMF: *N,N*-dimethylformamide

ER: endopasmic reticulam

ERK: extracellular signal-regulated kinase

ESIMS: electrospray ionization mass spectrometry

Et_3N: triethylamine

EtOAc: ethylacetate

GA: ginkgolic acid

GBA-1: acid β-glucosidase

GCS: glucosyl ceramide synthase

GPCRs: G protein coupled receptors

GSL: glycosphingolipid

HATU: 1-[Bis(dimethylamino)methylene]-1*H*-1,2,3-triazolo[4,5-b]pyridinium-3-oxide hexafluorophosphate

HBTU: 3-[Bis(dimethylamino)methyliumyl]-3*H*-benzotriazol-1-oxide hexafluorophosphate

HRMS: high resolution mass spectrometry

IBX: 2-Iodoxybezoic acid

IC_{50}: concentration for 50% inhibition of enzyme activity

LPP: lipid phosphate phosphatase

MeOH: methanol

NMR: nuclear magnetic resonance

nSMase2: neutral sphingomyelinase 2

Pd/C: palladium on carbon

PS: phosphotidylserine

r.t: room temperature

SAR: structural activity relationship

SM: sphingomyelin

SMase: sphingomyelinase

SMS: sphingomyelin synthase

SMSr: sphingomyelin synthase related protein

SPHK: sphingosine kinase

SPP: sphingosine phosphate phosphatase

S1P: sphingosine 1-phosphate

S1PRs: sphingosine 1-phosphate receptors

TBAF: tetra-*N*-butyl ammonium fluoride

TBDPSCl: *tert*-butyldiphenylsilyl chloride

TFA: trifluoroacetic acid

TLC: thin layer chromatography

Chapter 1

Introduction

1.1 Sphingolipids

Sphingolipds are one of the major categories of lipids which are principle constituents of eukaryotic cell membrane.[1] Sphingolipids are defined by the presence of a sphingoid base backbone, sphingosine. Sphingosine is (2*S*, 3*R*, 4*E*)-2-aminooctadec-4-ene-1,3-diol (it is also called D-*erythro*-sphingosine and sphing-4-enine). Sphingosine is only one of many sphingoid bases found in nature, which vary in alkyl chain length and branching, the number and positions of double bonds, the presence of additional hydroxyl groups, and other features. The main mammalian sphingoid bases are dihydrosphingosine and sphingosine.

Sphingolipids were first discovered from brain extract in 1870s and were named after the mythological Sphinx due to their enigmatic nature. Sphingolipids are known to protect cell surface from harmful environmental factors by forming plasma membrane lipid bilayer. Sphingolipids are synthesized in a pathway that begins in endoplasmic reticulam (ER) and completed in the Golgi apparatus, but these sphingolipids are enriched in plasma membrane and in endosomes, where they perform their function.[2] Sphingolipids play an important role in signal transmission and cell recognition and some of the sphingolipids are involved in are involved in cellular processes such as apoptosis, cell proliferation, differentiation, senescence, inflammation, autophagy, migration and immunity.[3] General structure of sphingolipids is as follows (**Figure 1**).

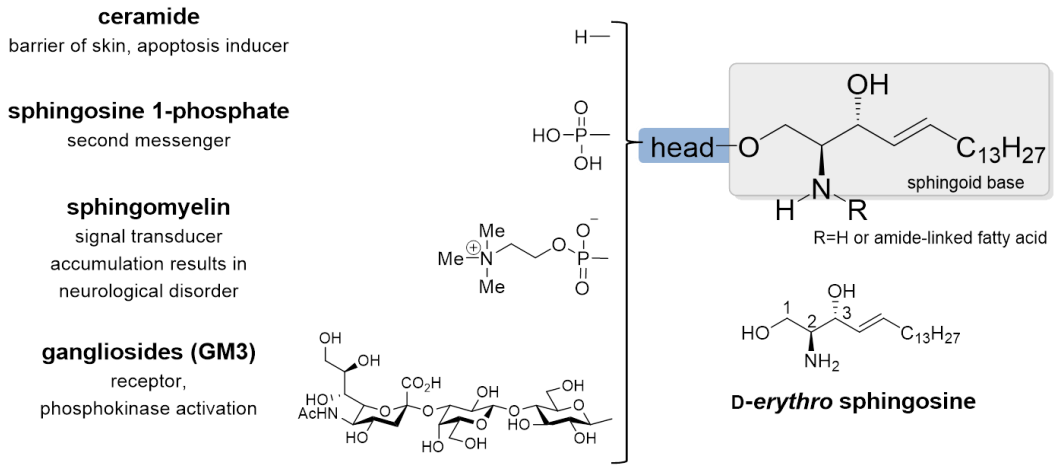

Figure 1: general structure of sphingolipids

1.2 Importance of sphingolipids & biosynthesis

Sphingolipids are essential components of cellular membranes and are involved in diverse cell functions. Especially the sphingolipids ceramide (Cer), sphingomyelin (SM) and sphingosine 1-phosphate (S1P) have been shown to be important mediators in the signaling cascades involved in many cellular processes. The structure and metabolism of main sphingolipids are as follows (**Figure 2**)

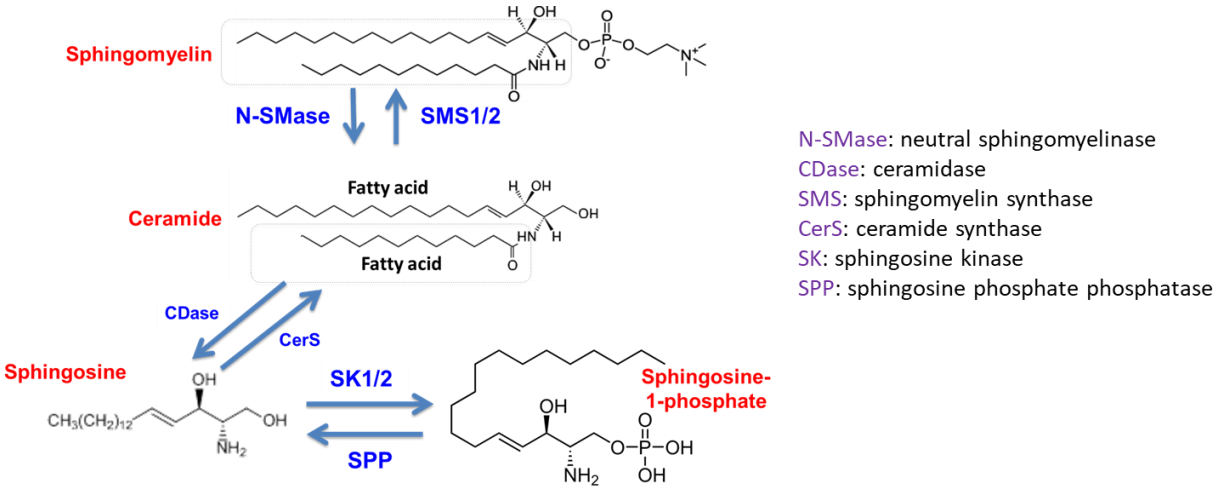

Figure 2: structure and metabolism of important sphingolipids

Ceramide (Cer)

A Cer is composed of sphingosine and a fatty acid which are found in cell membrane with high concentration. In cells Cer is synthesized mainly by three pathways (**figure 3**)

1) **Sphingomyelin hydrolysis**: involves hydrolysis of SM by sphingomyelinase
2) **De novo pathway**: begins with the condensation of palmitate and serine to form 3-keto-dihydrosphingosine catalyzed by serine palmitoyltransferse and ends by formation of ceramide from dihydro-ceramide by dihydroceramide desaturase.
3) **Salvage pathway**: involves the synthesis of ceramide from sphingosine by ceramide synthase and from glucosyl ceramide by acid β-glucosidase.

As a bioactive sphingolipid, Cer has been implicated in variety of physiological functions including apoptosis, cell growth arrest, differentiation, cell senescence, cell migration and

adhesion.[4] It has been reported that Cer accumulation is found during the treatment of cells with chemotherapeutic agents and UV light.[5] Suggesting that Cer has apoptosis inducing effect on cancer cells. Due to this effect Cer is termed as "**tumor suppressor lipid"**. Among sphingolipids Cer was first reported to induce cell death and differentiation in human leukemia HL-60 cells.[6,7] To confirm the mechanism of Cer induced cell death, the subcellular compartmentalization of active ceramide, the putative diverse function among ceramide molecular species and its regulation by metabolic enzymes have been investigated in several kinds of cancer.[8,9]

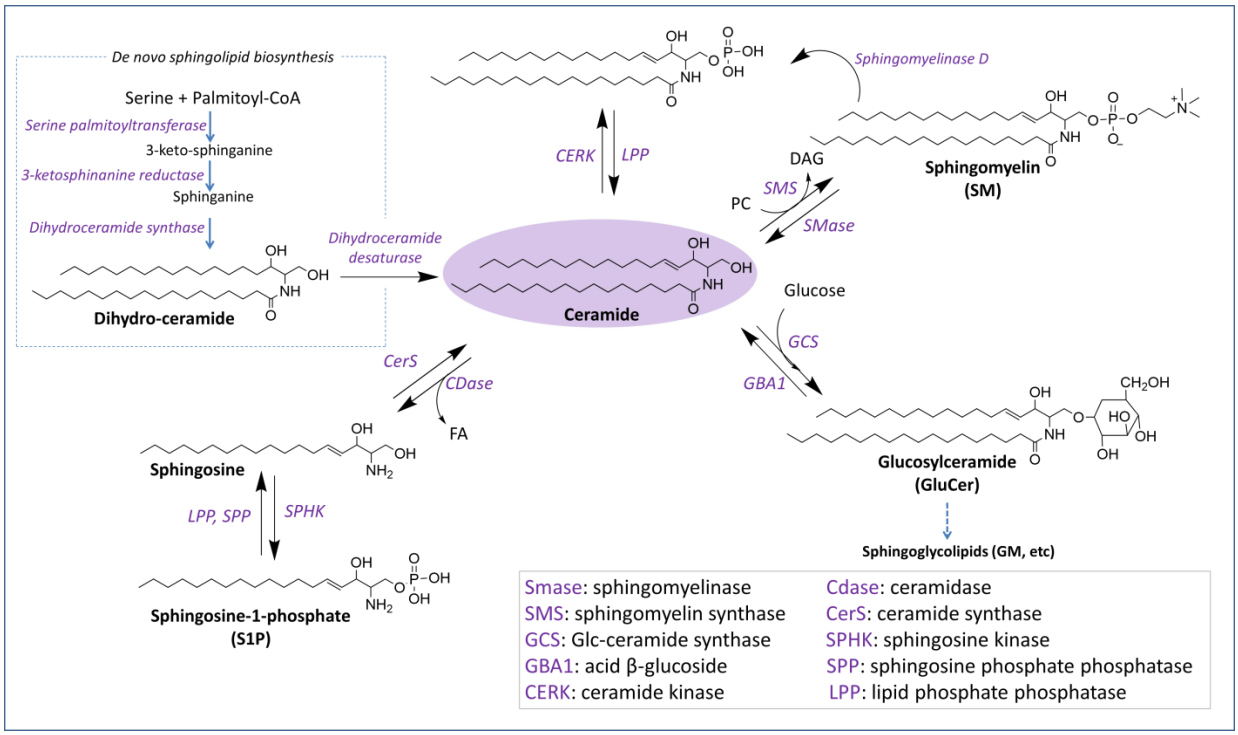

Figure 3: structure of sphingolipids and their biosynthesis

Sphingomyelin (SM)

SM is an important sphingolipid regulates membrane fluidity and microdomain structure. SM represents about 85% of all sphingolipids in human and it is a major component of plasma membrane lipis (10 to 20%). It is composed of ceramide and a phosphocholine as head group. SM participates in many signaling pathway and it has a significant structural and functional roles in cells. SM synthesis involves enzymatic transfer of phosphocholine group to a ceramide by sphingomyelin synthase (SMS). The functions of SM are as follows

1) SM, along with other sphingolipids, are associated with the formation of lipid raft which gives more structural rigidity compared to other part of the plasma membrane lipid bilayer. Lipid raft could be involved in the many cellular processes such as signal transduction, trafficking and cell polarization.[10] Excessive SM in the lipid raft may lead to insulin resistance.[11]
2) Even though lots of reports support the involvement of SM in signal transduction process the mechanism is still remained elusive. The degradation of SM in the plasma membrane by Sphingomyelinase (SMase) to produce ceramide which is involved in apoptotic signaling pathway.
3) SM is the major component of myelin sheath which surrounds and electrically insulates nerve cell axon. The deficiency of sphingomyelin in nerve cells leads to multiple sclerosis which affects the signal transmission process.

The accumulation of SM is found in rare heredity disease called Niemann-pick disease which is caused due to the deficiency of SMase. As a result of this, SM deposition is found in the liver, spleen, lungs, bone marrow and brain leads to irreversible neurological disorders. An excess accumulation sphingomyelin in the blood cell membrane leads to more lipid accumulation in the outer leaflet of the red blood cell membrane which leads to abnormally shaped red cells called acanthocytes.

Sphingosine 1-phosphate (S1P)

S1P is generated from sphingosine by the action of sphingosine kinase. It is involved in proliferation, migration and pro-apoptotic effects. S1P is a signaling molecule for sphingosine-1-phosphate receptors ($S1P_1$-$S1P_5$) which belongs to the family of G protein coupled receptors (GPCRs). GPCRs represent a major drug target in all the clinical areas and currently about 40% of drugs in the market target GPCRs.[12] GPCRs, $S1P_1$-$S1P_5$ recognize the lipid S1P, which regulates variety of cellular functions and out of five S1PRs, $S1P_1$ is the most important physiologically, especially in the vascular and immune system.[13] In mammals, $S1P_1$, $S1P_2$ and $S1P_3$ are expressed ubiquitously, whereas $S1P_4$ and $S1P_5$ are restricted to certain tissues. $S1P_4$ found in lymphoid tissues and lung whereas $S1P_5$ found in brain and skin.

After S1P binds to S1P receptors and activates downstream signaling pathways leads to many cellular processes such as proliferation, cell migration, and cytoskeletal rearrangement.[13] Each S1P receptors coupled with specific G protein, which when activated, dissociates into α and βV subunits and transfer signal toward downstream pathways. The important functions of Cer, SM and S1P is as shown below (**Figure 4**)

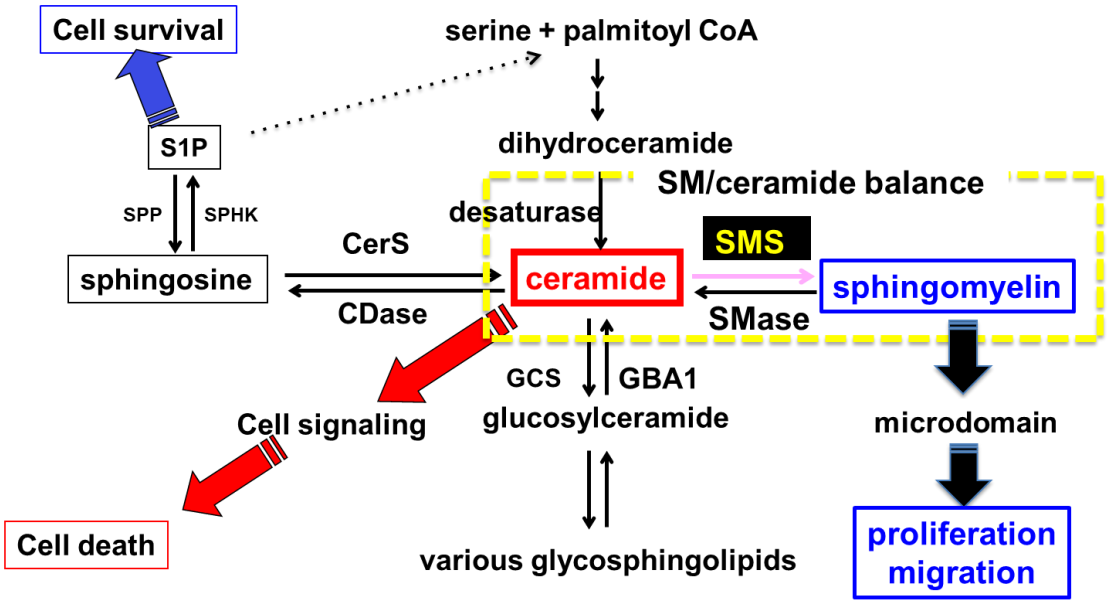

Figure 4: important functions of Cer, SM and S1P

S1P is synthesized in most cells, but it is irreversibly degraded by intracellular S1P lyase or dephosphorylated by S1P phosphatases. S1P levels are extremely low in most tissues. Notably S1P present in blood with low-micromolar range and are mainly contributed by erythrocytes and the lymph, where S1P levels are in hundred-nanomolar range. $S1P_1$ interaction with S1P is very critical for immunomodulation. $S1P_1$ is expressed in most of the immune cells but other S1P receptors expressions are limited. The S1P in lymphoid tissue is relatively low compared with the lymph, therefore S1P gradient is firmed. The expressed $S1P_1$ on T cell in the lymphoid organ is responsive to the S1P gradient and promotes T cell egress from the lymphoid organ to lymph through the endothelial barrier[14] (**Figure 5**).

After activation of the T cell in the lymphoid organ by encountering an antigen-expressing dendritic cell or by type 1 interferon stimulation, $S1P_1$ expression is decreased. Mechanisms include direct protein–protein interaction with CD69, which is induced upon type 1 interferon stimulation, and down regulation of the transcription factor Kruppel-like factor 2 (KLF2), which is a direct activator of the $S1P_1$ gene. Effector T cells eventually re-express $S1P_1$ and thereby egress from the lymph node to the lymph and into the peripheral tissues. If the levels of S1P are increased in lymphoid tissues, by inhibition of S1P lyase or by inflammation, or in the presence of synthetic $S1P_1$ ligands such as FTY720, T-cell egress might be blocked by several possible mechanisms: dissipation of the S1P gradient, down modulation of $S1P_1$ on T cells by ligand-induced internalization and $S1P_1$-mediated closure of egress ports on the endothelium by enhancement of junctional contacts (**Figure 5**).

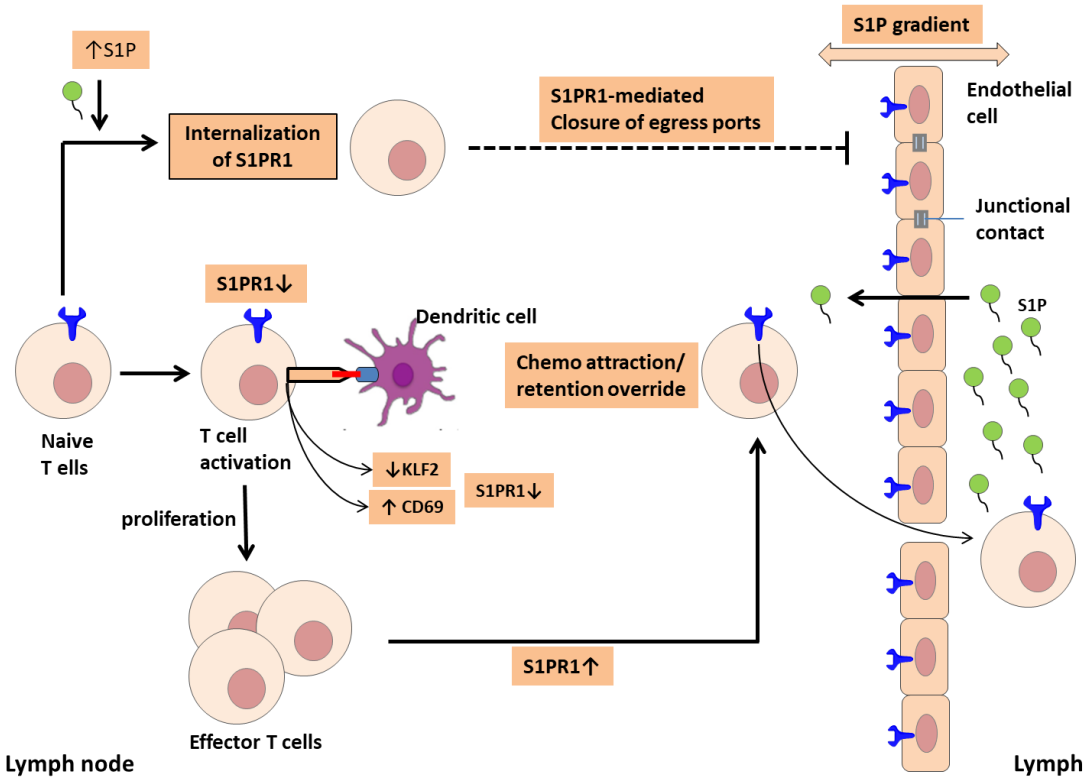

Figure 5: $S1P_1$-mediated lymphocyte egress from lymph nodes

1.3 Sphingomyelin synthase

Sphingomyelin Synthase (SMS), an enzyme which catalyzes the conversion of ceramide and phosphatidylcholine to Sphingimyelin (SM) and diacylglycerol (**Figure 6A**). The SMS substrate, ceramide and catalytic product SM are emerged has key components of cell membrane, which are involved diverse cell functions such as cell adhesion, migration, cell growth, inflammation and angiogenesis.[15] There are three isoforms of SMS; sphingomyelin synthase 1 (SMS1), sphingomyelin synthase 2 (SMS2), sphingomyelin synthase-related protein (SMSr). SMS1 is responsible for the bulk SM production in the Golgi apparatus.[16] and has significant role in maintaining cell homeostasis.[17] SMSr is localized in endoplasmic reticulum (ER) which is a suppressor of ceramide-induced mitochondrial apoptosis.[18] In a recent report, the deficiency of plasma membrane protein SMS2 attenuates the development of obesity, fatty liver and type 2 diabetes.[19] The SMS2 activity has been involved in other metabolic disorders such as insulin resistance.[20] SMS2 activity also associated with the generation of amyloid-beta peptide,[21] HIV-1 envelop-mediated membrane fusion[22] and induction of colitis-associated colon cancer.[23] Thus, SMS2 is expected to be potential target for the treatment of many diseases.

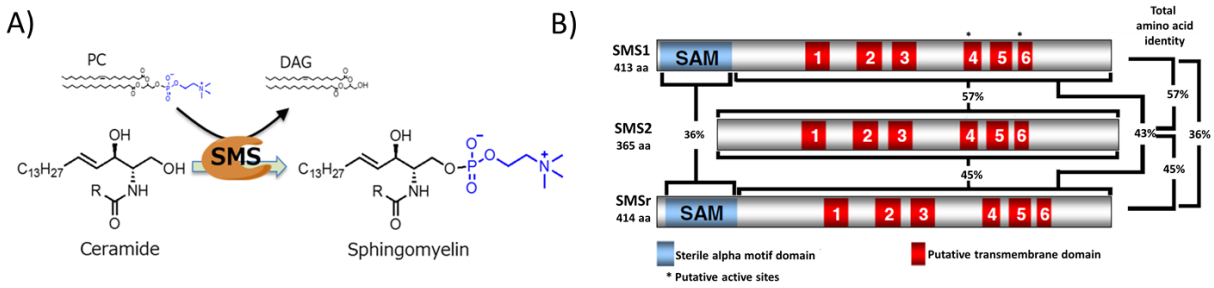

Figure 6: A) catalytic conversion of ceramide to sphingomyelin by SMS B) domain architecture of SMS isoforms

SMS1, SMS2, and SMSr have six transmembrane (TM) domains and their N- and C-termini are facing cytosol (**Figure 6B**). In SMS1 and SMSr, there is a sterile alpha motif (SAM) at N-terminus. The SAM domain may play a role in cellular functions such as development, signal transduction, and transcriptional regulation through protein–protein or protein–lipid interaction.[24] The proteins, which interact with SAM domain of SMS1, have not identified, and SAM domain function is unclear.

1.4 SMS and related disorders

SMS has been involved in many disorders especially in metabolic disorders such as obesity, insulin resistance, fatty liver formation, and type 2 diabetes.[19] Mitsutake et al, recently reported that the deficiency of SMS2 decreases the formation of fatty liver. SMS2 knock out (KO) experiments in high fat diet induced mice results suggest that there is drastic decrease in the deposition of fat around liver compared to wild type (**Figure 7A**). Furthermore in SMS2 KO mice there is significant decrease in liver triglycerides (TG) when compared with wild type and it is comparable with SMS2 KO normal diet type (**Figure 7B**). When authors tried to find out the reason for SMS2 mediated fat deposition, they found significance decrease in the expression of long chain free fatty acid transporter gene CD36 and there is significant increase in CD36 expression of high fat diet induced wild type mice.

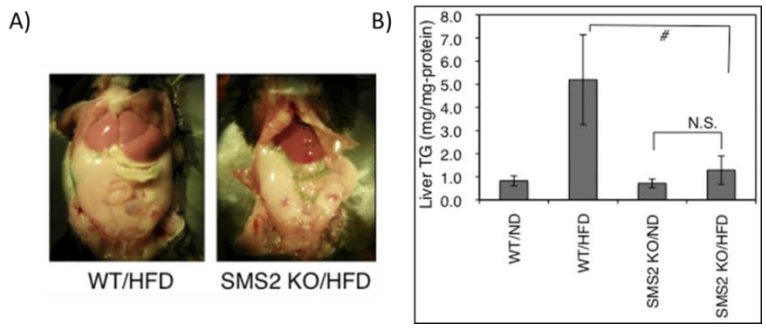

Figure 7: A) SMS2 KO studies of high fat diet induced mouse in liver B) triglycerides level in liver

Amyloid β-peptide (Aβ), the pathogenic agent of Alzheimer disease, is a physiological metabolite whose levels are constantly controlled in normal human brain. Aβ is derived from a sequential proteolysis of the transmenbrane amyloid precursor protein (APP), a process which is dependent on the distribution of lipids present in the plasma membrane. Recent studies have demonstrated that the extracellular Aβ is associated with exosomes, small membrane vesicles of endosomal origin. The fate of Aβ in association with exosome is largely unknown. K. Yuyama et.al[25] recently demonstrated that the secretion of neuronal exosomes is modulated by the activities of sphingolipid metabolizing enzymes, neutral sphingomyelinase 2 (nSMase2) and SMS2. Up-regulation of exosome secretion from neuronal cells by treatment of SMS2 siRNA enhanced Aβ uptake into microglial cells and significantly decreased extracellular levels of Aβ (**Figure 8**). Their findings indicate a novel

mechanism responsible for clearance of Aβ through its association with exosomes. The potent and selective SMS2 inhibitors are well in need to modulate exosome production by the inhibition of SMS2 in neuronal cells. This strategy will be a way to identify a small molecule drug for the treatment of Alzheimer's disease.

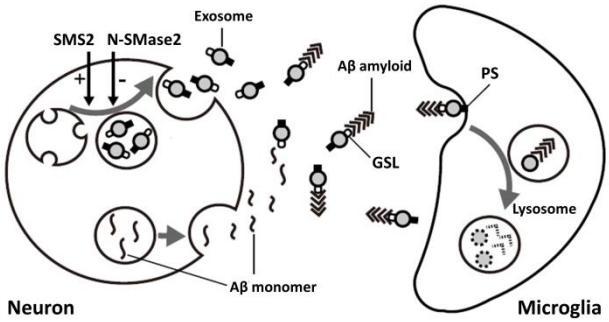

Figure 8: Schematic representation of role of exosome secretion in Aβ metabolism

Exosomes and Aβ peptides are generated and released from neurons into the extracellular space. In extracellular space exosome enhances Aβ amyloidogenesis by glycospingolipids (GSLs) in its surface and subsequent incorporation of Aβ fibrils into microglia in a phosphatidylserine (PS) dependent manner to degrade Aβ.

The elevation of Aβ generation is also associated with the increase in SMS activity.[26] The SMS is significantly expressed in AD brain especially in hippocampus not in cerebellum. To understand the role of SMS in AD, CHO-APP cells were treated with the SMS inhibitor D609, as a result there is dose and time dependent decrease in Aβ deposition (**Figure 9**). The decrease in Aβ level occurred without changes in APP expression or cell viability.

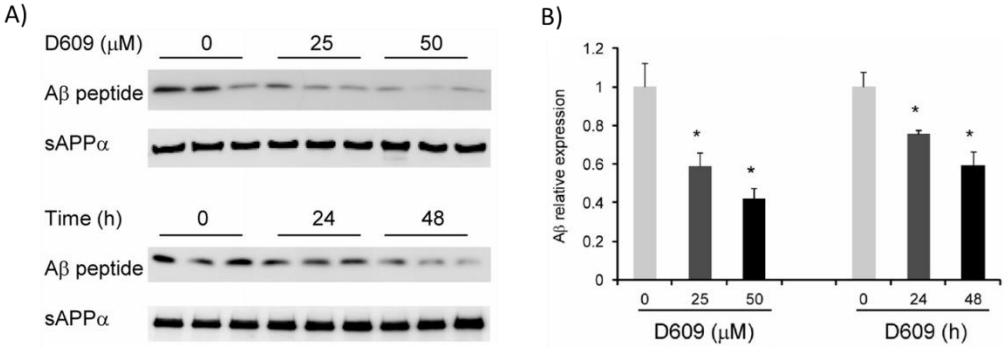

Figure 9: Impact on Aβ generation by SMS inhibition A) time and dose dependent treatment of D609 on CHO-APP cells and measurement of Aβ deposition B) quantification data

Ceramide is known to be apoptosis inducer sphingolipid and ceramide accumulation has been found during chemotherapy. A lower level of ceramide with higher activities of GCS and SMS was detected in drug resistant human leukemia 60 (HL-60) cells than IN HL-60 cells. It has been observed lower level of ceramide in case of chemo resistant leukemia patients that chemosensitive patients. The GCS and SMS activity are two fold higher in case of chemoresistant HL-60 cells[27] (**figure 10**). These results suggest that the apoptotic mechanism of drug resistant leukemia patients regulated ceramide content, GCS and SMS activity.

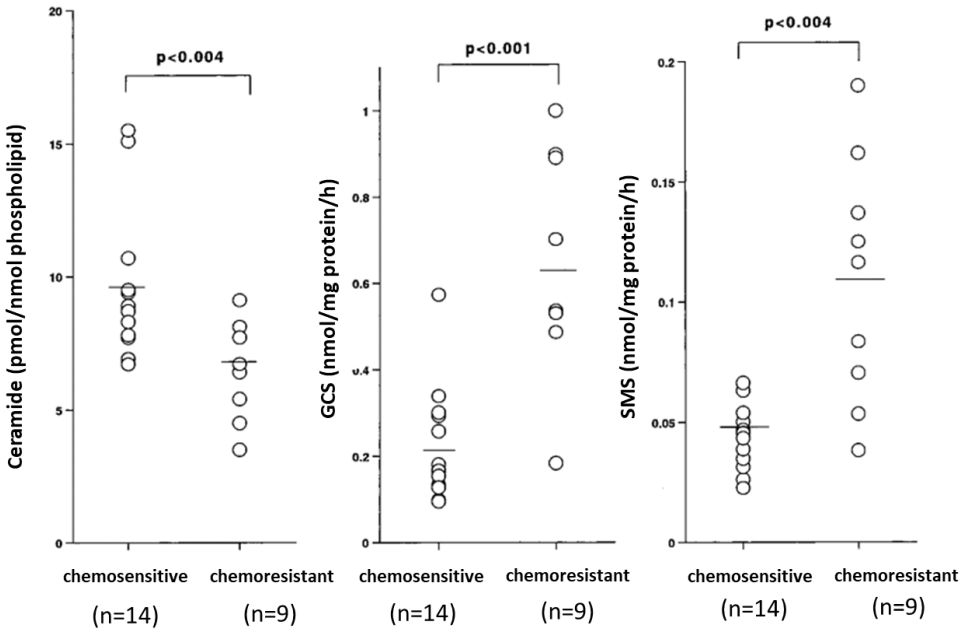

Figure 10: ceramide level, GCS and SMS activity in chemosensitive and chemoresistant HL-60 cells

The role of sphingolipids and sphingolipid metabolizing enzymes in metabolic disorders are being known. Many studies suggest that the abnormalities of sphingolipid metabolism may be involved in inflammation and carcinogenesis.[28] Very recent study colon cancer and sphingolipid metabolizing enzyme reports SMS2 deficiency inhibits DSS (dextran sodium sulfate)-induced colitis and subsequent colitis-associated colon cancer via inhibition of colon epithelial cell–mediated inflammation.[29] The increase in ceramide or decrease in SM or both plays a role in the suppression of colon inflammation and colitis-associated colon cancer need to be clarified. The effect of SMS1 on colon inflammation and colitis-associated colon cancer is not known.

1.5 SMS inhibitors and function

So far, few small molecule inhibitors are reported. D609 is the first known SMS inhibitor which was originally identified as anticancer and antiviral agent.[30] Unfortunately, it is not practically useful because of its less potency towards SMS and high instability. In search of new small molecule with high potency and stability X. Deng *et al.* identified two relatively selective SMS2 inhibitor by virtual screening.[31] One of inhibitor **D2** found to effective *in vivo* in regulation ceramide and SM concentration by inhibiting SMS in plasma membrane. As a result of SMS inhibition there is increase in ceramide concentration and decrease in SM concentration, but SMS inhibitor **D2** was not studies in terms of metabolic disorders and others. Even though **D2** is relatively effective towards SMS2, it can't be used for therapeutic application because of it less potency. Very recently, research group from takeda pharmaceutical company, Japan could able to identify highly potent and selective SMS2 inhibitor **1**, **2** & **3** by synthetic method.[32] But these inhibitors *in vivo* efficacy in diseased condition need to be identified.

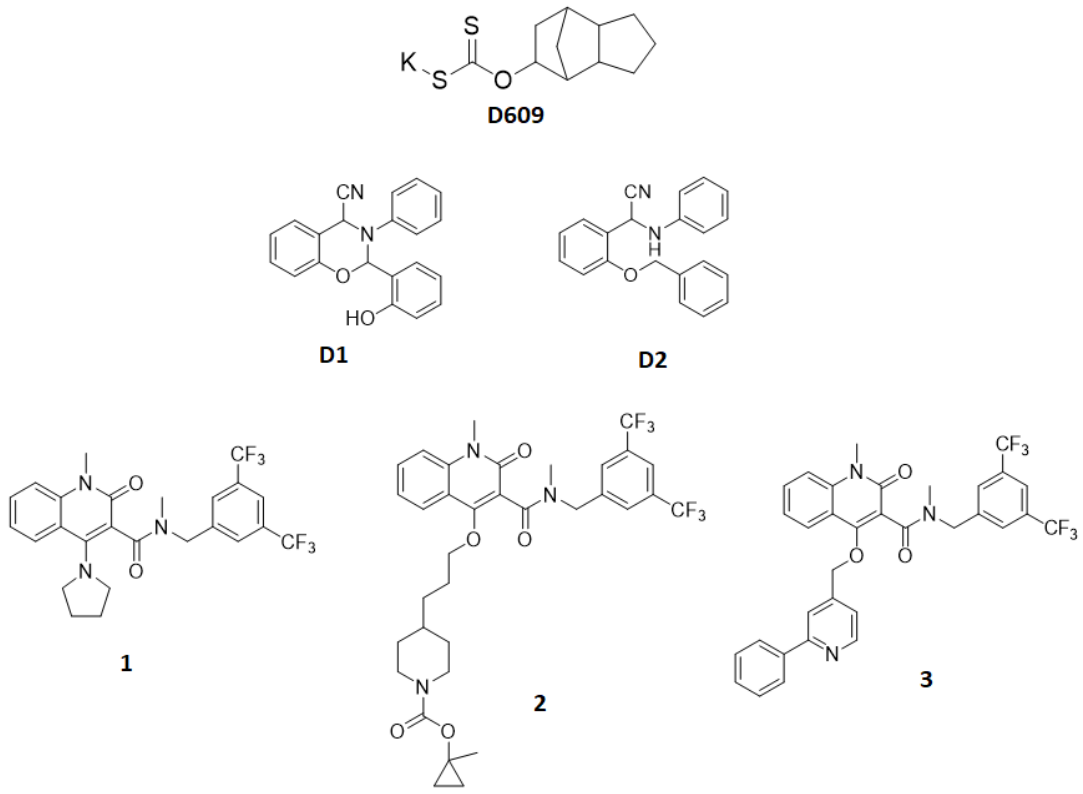

Figure-11: reported SMS small molecule inhibitors

1.6 References:

1) E. Fahy, S. Subramaniam, H. A. Brown, C. K. Glass, A. H. Merrill Jr., R. C. Murphy, C. R. Raetz, D. W. Russell, Y. Seyama, W. Shaw, T. Shimizu, F. Spener, G. van Meer, M. S.VanNieuwenhze, S. H. White, J. L. Witztum, and E. A. Dennis, ***J. Lipid Res***., 2005, 46, 839
2) A. H. Futerman, ***Biochim. Biophys. Acta***, 2006, 1758, 1885
3) M. Adada, D. Canals, Y. A Hannun, and L. M Obeid, ***Biochim. Biophys. Acta***, 2014, 1841, 727
4) Y. A. Hannun and L. M. Obeid, ***Mol. Cell Biol.***, 2008, 9, 139
5) J. A. Rotolo, J. Zhang, M. Donepudi, H. Lee, Z. Fuks, and R. Kolesnick, ***J. Biol. Chem.***, 2004, 280, 26425
6) L. M. Obeid, C. M. Linardic, L. A. Karolak, and Y. A Hannun, ***Science***, 1993, 259, 1769
7) T. Okazaki, R. M. Bell, and Y. A. Hannun, ***J. Biol. Chem.***, 1989, 264, 19076
8) C. R. Gault, L. M. Obeid, and Y. A. Hannun, ***Adv. Exp. Med. Biol.***, 2010, 688, 1
9) J. W. Park, W. J. Park, and A. H. Futerman, ***Biochim. Biophys. Acta***, 2014, 1841, 671
10) M. Giocondi, S. Boichot, T. Plenat, and C. Le Grimellec, ***Ultramicroscopy***, 2004, 100, 135
11) Z. Li, H. Zhang, J. Liu, C. P. Liang, Y. Li, Y. Li, G. Teitelman, T. Beyer, H. H. Bui, D. A. Peake, Y. Zhang, P. E. Sanders, M. S. Kuo, T. S. Park, G. Cao, and X. C. Jiang, ***Mol. Cell Biol.***, 2011, 31, 4205
12) S. Park and D. Im. ***Biomol. Ther.***, 2017, 25, 80
13) A. Kihara, S. Mitsutake, Y. Mizutani, and Y. Igarashi, ***Prog. Lipid Res.***, 2007, 46, 126
14) J. Rivera, R. L. Proia and A. Olivera, ***Nat. Rev. Immuno***., 2008, 8, 753
15) Y. A. Hannun and L. M. Obeid, ***Nature reviews***, 2008, 9, 139
16) F. G. Tafesse, P. Ternes, and J. C. M. Holthuis, ***J. Biol. Chem.***, 2003, 281, 29421
17) F. G. Tafesse, K. Huitema, M. Hermansson, S. Poel, J. Dikkenberg, A. Uphoff, P. Somerharju, and J. C. M. Holthuis. ***J. Biol. Chem.***, 2007, 282, 17537
18) G. Tafesse, A. M. Vacaru, E. F. Bosma, M. Hermansson, A. Jain, A. Hilderink, P. Somerharju, and J. C. M. Holthuis, ***J. Cell Sci.***, 2014, 127, 445

19) S. Mitsutake, K. Zama, H. Yokota, T. Yoshida, M.i Tanaka, M. Mitsui, M. Ikawa, M. Okabe, Y. Tanaka, T. Yamashita, H.i Takemoto, T. Okazaki, K. Watanabe, and Y. Igarashi, ***J. Biol. Chem.***, 2011, 286, 28544

20) Z. Li, H. Zhang, J. Liu, C. Liang, Y. Li, Y. Li, G. Teitelman, T.Beyer, H. H. Bui, D. A. Peake, Y. Zhang, P. E. Sanders, M. Kuo, T. Park, G. Cao, and X. Jiang, ***Mol. Cell. Biol.***, 2001, 21, 4205

21) J. T. Hsiao, Y. Fu, A. Hill, G. M. Halliday, and W. S. Kim, ***PLOS ONE***, 8, e74016

22) Y. Hayashi, Y. Nemoto-Sasaki, T. Tanikawa, S. Oka, K. Tsuchiya, K. Zama, S. Mitsutake, T. Sugiura, and A. Yamashita, ***J. Biol. Chem.***, 2014, 289, 30842

23) T. Ohnishi, C. Hashizume, M. Taniguchi, H. Furumoto, J. Han, R. Gao, S. Kinami, T. Kosaka, and T. Okazaki, ***The FASEB J.***, 2017, 31, 3816

24) M. Taniguchi and T. Okazaki, ***Biochim. Biophys. Acta***, 2014, 1841, 692

25) K. Yuyama, H. Sun, S. Mitsutake, and Y. Igarashi, ***J. Biol. Chem.***, 2012, 287. 10977

26) J. T. Hsiao, Y. Fu, A. F. Hill, G. M. Halliday, W. S. Kim, ***PLOS ONE***, 2013, 8, e74016

27) M. Itoh, T. Kitano, M. Watanabe, T. Kondo, T. Yabu, Y. Taguchi, K. Iwai, M. Tashima, T. Uchiyama, and T. Okazaki, ***Clin. Canc. Res.***, 2003, 8, 415

28) H. Furuya, Y. Shimizu, and T. Kawamori, ***Canc. Meta. Rev.***, 2011, 30, 567

29) T. Ohnishi, C. Hashizume, M. Taniguchi, H. Furumoto, J. Han, R. Gao, S. Kinami, T. Kosaka, and T. Okazaki, ***The FASAB J.***, 2017, 31, 3816

30) C. Luberto and Yusuf A. Hannun, ***J. Biol. Chem.***, 1998, 273, 14550

31) X. Deng, F. Lin, Y. Zhang, Y. Li, L. Zhou, B. Lou, Y. Li, J. Dong, T. Ding, X. Jiang, R. Wang, D. Ye, Eur. ***J. Med. Chem.***, 2014, 73, 1 73

32) R. Adachi, K. Ogawa, S. Matsumoto, T. Satou, Y. Tanaka, J. Sakamoto, T. Nakahata, R. Okamoto, M. Kamaura, T. Kawamoto, ***Eur. J. Med. Chem.***, 2017, 136, 283

Chapter 2

Structure-inspired design of S1P mimic from natural sphingomyelin synthase inhibitor

2.1 Abstract

A Sphingolipid, Sphingomyelin (SM) is a vital component of cellular membrane has significant structural and functional roles in the cell. Its production involves the catalytic conversion of ceramide and phosphatidylcholine by sphingomyelin synthase (SMS). The SMS isoform, SMS1 play a crucial role to maintain cell homeostasis but the plasma membrane enzyme, SMS2 activity involved in metabolic syndrome and Alzheimer's disease, thus SMS2 may serve as potential therapeutic target. To understand the SMS biology under these circumstances we have identified ginkgolic acid (GA, 15:1) as a first natural and potent inhibitor of SMS2 by screening library of medicinal plants. Herein, we have reported the total synthesis and structural activity relationship (SAR) studies of GA (15:1) to identify the role of functional groups and a long hydrophobic chain. Interestingly, GA (15:1) structure resembles sphingosine and ceramide (substrate of SMS), due to their structural resemblance, we have proposed that GA (15:1) behaves like sphingosine and named as sphingo-mimic. The sphingo-mimic nature of GA (15:1) has been chemically proved by synthesizing various ceramide mimics and also obtained few selective SMS2 inhibitors. The sphingo-mimic nature of ginkgolic acid inspired us to synthesize a phosphate derivative of GA, its agonist/anatagonist effect on $S1P_1$ has been carried out by cell-based assay. Phospho-GA mimics S1P structurally and modulates $S1P_1$ by inducing ERK phosphorylation and internalization. The S1P mimicking nature of phospho-GA was further confirmed by docking studies, which shows phospho-GA adopts similar binding pose to the bound ligand ML5. Collectively, we have reported GA as a first natural SMS inhibitor, which is natural sphingo-mimic.

2.2 Introduction

Sphingomyelin Synthase (SMS), an enzyme which catalyzes the conversion of ceramide and phosphatidylcholine to Sphingimyelin (SM) and diacylglycerol. Sphingolipids, SM and ceramide are emerged has key components of cell membrane, which are involved diverse cell functions such as cell adhesion, migration, cell growth, inflammation and angiogenesis.[1] The SMS isoform SMS1 (sphingomyelin synthase 1) is responsible for the bulk SM production in the Golgi apparatus[2] and has significant role in maintaining cell homeostasis. In a recent report, the deficiency of plasma membrane protein SMS2 (sphingomyelin synthase 2) attenuates the development of obesity, fatty liver and type 2 diabetes.[3] The SMS2 activity also involved in other metabolic disorders such as insulin resistance[4] and atherosclerosis.[5] SMS2 activity also associated with the generation of amyloid-beta peptide,[6] HIV-1 envelop-mediated membrane fusion[7] and induction of colitis-associated colon cancer.[8] Thus, SMS2 is expected to be potential target for the treatment of many diseases. So far there are very few SMS inhibitors are available in the literature 1) D609 (tricyclo[5.2.1.0(2,6)]-decan-8-yl dithiocarbonate), a first known small molecule inhibitor for SMS[9] which was originally identified as antiviral,[10] antitumor[11] reagent. Due to its instability and weak inhibitory activity (IC_{50} on SMS2 is 224 µM) SMS is not potential target of D609 2) D1 (75 µM on SMS2) and D2 (14 µM on SMS2) were identified recently as SMS inhibitors,[12] which are not potent for therapeutic application. Very recently, Adachi *et.al*[13] discovered synthetic selective human SMS2 inhibitors. These inhibitors further needs to be explored in inflammatory responses and atherosclerosis.

Natural products have been emerging as source of potential drug candidates since few decades.[14] Identifying a drug from the natural source to target enzymes involved in human diseases is a big challenge in the field of chemical biology, which indicated that natural products play a significant role in the field of drug discovery and process development.[15] To identify an inhibitor of SMS2 by high throughput screening of medicinal plants, we screened methanol extracts of leaves, stem, and roots of around 600 medicinal plants from Hokkaido by cell based SMS assay. Few plant extracts showed inhibitory activity against SMS2 and we found that *ginkgo biloba* (stem) extract showed better inhibitory activity against SMS2. *Ginkgo biloba* is variously used as a natural medicine, functional food, and dietary

supplement. Particularly, *ginkgo biloba* leaves were traditionally applied to treat asthma, cough, and enuresis in China for thousands of years.[16]

Bio-assay guided fractionation, purification and characterization by spectroscopic techniques identified GA (15:1) **1** as first natural and potent inhibitor of SMS2 with IC_{50} 1.5 µM, but it fails to show selectivity towards SMS2 with that of SMS1 (IC_{50} 1.5 µM). Ginkgolic acid, a blanket term which belongs to family of closely related compounds consisting of salicylic acid with 13 or 15-carbon alkyl chain and 15-carbon alkyl chain with monoene or diene.[17] GA is known to inhibit protein SUMOylation.[18] Recently, GA has been shown to suppress the development of pancreatic cancer.[19] More recently, GA has been reported to protect against Aβ-induced synaptic dysfunction in the hippocampus[20] and inhibits the cell proliferation, migration of lung cancer cells.[21]

2.3 Results and discussion

To compare natural and synthetic ginkgolic acid (15:1) against SMS2 activity, we synthesized ginkgolic acid (15:1) by novel methodology (**scheme-1**) and both turned out to be equally potent. To elucidate the role of functional groups and the long hydrophobic chain with an unsaturation of ginkgolic acid (15:1), compounds **2-5** (**Fig. 1A**) were synthesized, their SMS inhibitory activities were measured (**Fig. 1B**). Bioassay data suggested that GA (15:0) **2**, without unsaturation in the hydrophobic chain showed no significant difference in the SMS2 inhibitory activity with that of **1.** Compound **3** with reduced chain length to eight showed less potency towards SMS2. The methyl ester of GA (15:1) **4** and compound **5** turned out to be inactive derivatives of GA (15:1). As a result, carboxylic acid group and long hydrophobic chain of GA are very essential for inhibitory activity of SMS2 and SMS2 attains 100% inhibition at 10 µM concentration of GA (15:1).

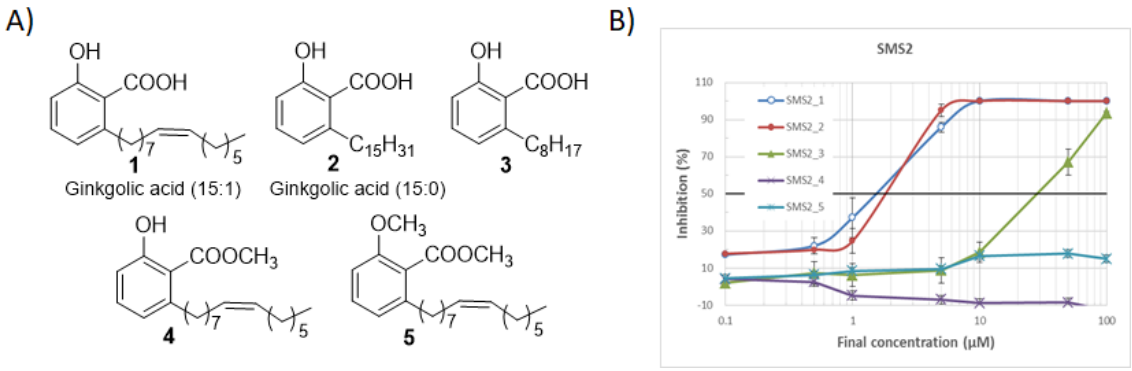

Fig. 1: **A)** structure of ginkgolic acid (15:1) and SAR studies **B)** SMS assay of compounds **1-5**

Total Synthesis of Ginkgolic acid (15:1): So far three reports showed the total synthesis of GA (15:1).[22,23,24] Herein, we reported synthesis of GA (15:1) in eight steps starting from 2,6-dihydroxy benzoic acid by novel methodology. Compounds **6** and **7** were synthesized according to ref- 25. Compound **8** was synthesized by palladium catalyzed reaction (heck reaction) of **7** with hydroxyl group protected *7*-octene-*1*-ol in the presence of K_2CO_3[17] followed by deprotection of hydroxyl group with TBAF (tetra-*N*-butyl ammonium fluoride) to get **9**. The hydrogenation of double bond was carried out using Pd/C, H_2 to obtain **10**. Compound **11** which was synthesized by oxidation of **10** using IBX (2-iodoxybenzoic acid) followed by Wittig reaction of **11** and heptyltriphenylphosphonium ion in the presence of

NaH to get **12**.[26] Finally, GA (15:1) was obtained by hydrolysis of **12**. The natural and synthetic GA (15:1) is equally potent SMS inhibitor.

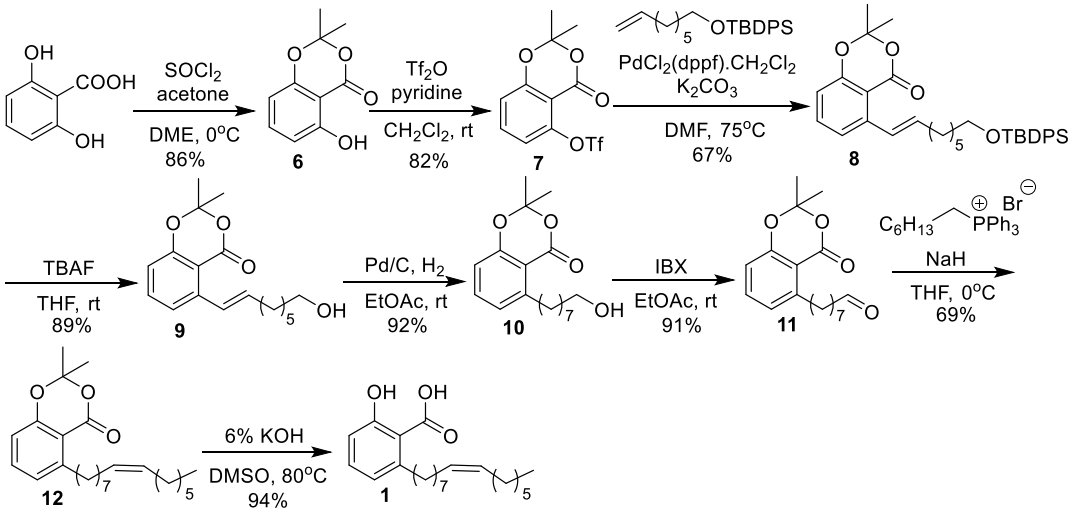

Scheme-1: total synthesis of GA (15:1)

Synthesis of Ginkgolic acid (15:0) and its derivative

Synthesis of GA (15:0) and its derivative **3** were achieved in three steps starting from **7** (**scheme-3**). It involves heck coupling of **7** with 1-octene and 1-pentadecene using $PdCl_2(dppf).CH_2Cl_2$ to get compounds **7a** and **7b**, which were subjected to hydrogenation using Pd/C, H_2 to get compounds **7c** and **7d** followed by basic hydrolysis to obtain desired compounds GA (15:0) and **3**.

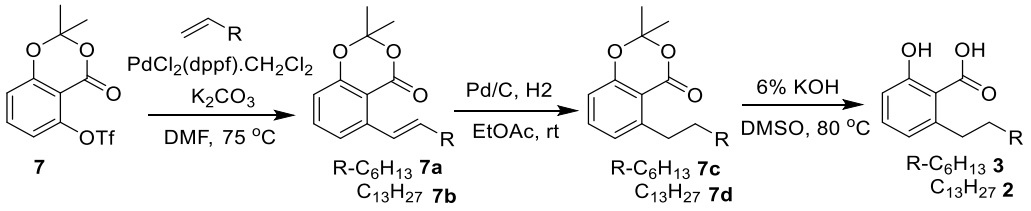

Scheme 2: synthesis of Ginkgolic acid (15:0) and compound **3**

GA (15:1) behaves like inspiring "*sphingo-mimic*"

Moreover, we noticed the structure of GA surprisingly resembles that of sphingosine (**Fig. 2**). We examined the structural similarity between GA, sphingosine and ceramide which is the substrate of SMS, ceramide is biosynthetically obtained by catalytic conversion of sphingosine by ceramide synthase. Sphingosine is an 18-carbon amino alcohol with an unsaturation in the long hydrocarbon chain. It has basically hydrophilic and hydrophobic part, hydrophilic part with two hydroxyl group at 1st and 3rd position and an amine group at 2nd position and hydrophobic part with long hydrocarbon chain with an unsaturation at 4th position. If we compare the structural similarity of sphingosine with GA (15:1), GA acid (15:1) is also having hydrophilic salicylic acid part and hydrophobic long hydrocarbon chain with an unsaturation. Due to these structural similarities of GA, sphingosine and ceramide, we assumed that the inhibitory activity of GA against SMS might be because of substrate like behavior. The 2nd position of GA has carboxylic acid group but sphingosine has amine functionality so, we have decided to replace carboxylic acid by amine group to get more accuracy in terms structural similarity and also we assumed that the expected compound might be more potent inhibitor of SMS inhibitor than GA (15:1). And also we have proposed that GA (15:1) is a natural "sphingo-mimic" due to its structural resemblance with sphingosine and we went ahead to prove its "sphingo-mimic" nature chemically and experimentally. To prove "sphingo-mimic" nature of GA (15:1) chemically, we decided to synthesize compound **13** and its N-acylating derivatives of GA as sphingosine and ceramide mimic respectively by their SMS inhibitory activity.

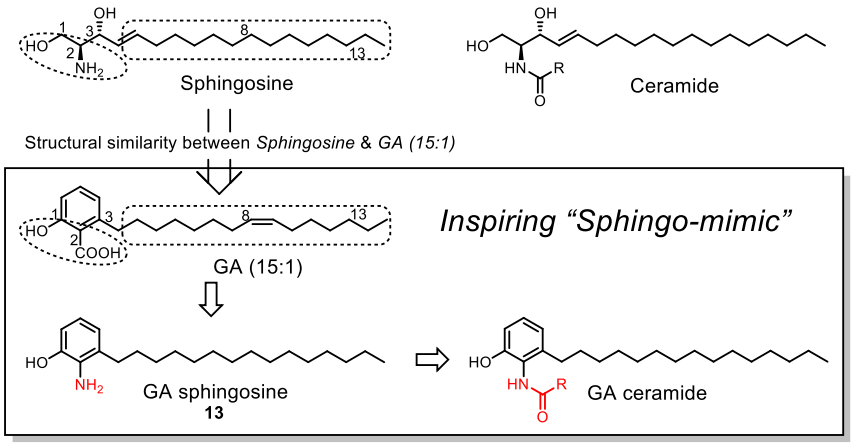

Fig. 2: structural resemblance of GA with sphingosine, ceramide and compound **13** with sphingosine

Sphingosine mimic

Sphingosine mimic **13** and compound **13a** with hydrocarbon chain C-8 were synthesized in three steps starting from commercially available compound, 3-bromo-2-nitro-anisole (**scheme-3**). Sphingosine mimics with two different hydrophobic chain lengths were synthesized to address the length of hydrocarbon chain against SMS activity. All intermediates during the course of synthesis of **13** and **13a** were tested against SMS2. Unfortunately, none of the intermediates were active (1µM-100µM).

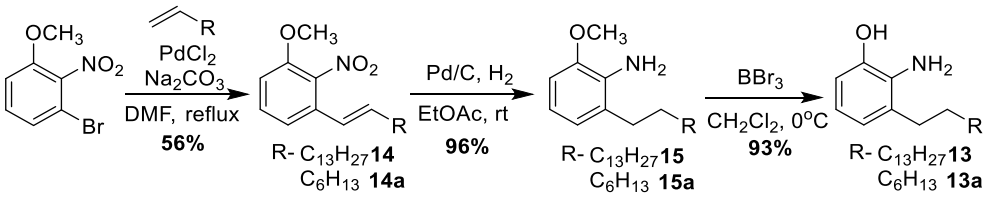

Scheme 3: synthesis of sphingosine mimics

As expected compounds **13** and **13** with hydrocarbon chain C-8 turned out to be SMS2 inhibitors with IC_{50} of 30 µM and 50 µM respectively. The SMS inhibitory activity of compound **13** enhanced our assumption that GA is a "sphingo-mimic". Even though compound **13** is not potent SMS2 inhibitor than GA (15:1), it is slightly selective towards SMS2 (SMS1 IC_{50} is 50 µM). Since SMS2 has been involved in many diseases (metabolic disorders, Alzheimer's disease and tumorigenesis), to identify selective SMS2 inhibitor, we extended our research to synthesize ceramide mimics and also to prove chemically the "sphingo-mimic" nature of GA.

Ceramide mimic

Initially, we tried to synthesize ceramide type derivatives of Ginkgolic acid from **13** and **13a** using coupling agent HATU. Unfortunately, we have got major compound with acylation at both hydroxyl and amine group. To overcome this difficulty we changed the starting materials to **15** and **15a** for N-acylation and followed by *O*-demethylation. The reason behind using both **15** and **15a** was to know the role of hydrocarbon chain length towards the inhibitory activity and also to know role of hydroxyl group towards SMS inhibitory

activity and selectivity. Any drug with shorter hydrocarbon chain length will be better for therapeutic application and also to overcome solubility problems.

Several ceramide mimics of GA were synthesized with two different hydrocarbon chain lengths and by using different carboxylic acids. *N*-acylation was conducted with coupling agents DCC, HBTU and HATU, HATU was showed better result with >90% yield followed by *O*-demethylation using BBr_3 at -78°C. SMS2 assay was performed for ceramide mimics (**scheme-4** &**Table-1**) and also for the intermediates. The Intermediates with methoxy group turned out to be inactive against SMS1 and SMS2. As assumed the ceramide mimics were active against SMS, this might be because of structural resemblance between ceramide and ceramide mimics. As a result we have chemically proved that ceramide mimics might be behaving as substrate and the SMS inhibition is through competitive manner. We have achieved to get two selective SMS2 inhibitors 17d, 17j with IC_{50} of 5 µM and 3 µM respectively with 8 to 10 fold selectivity.

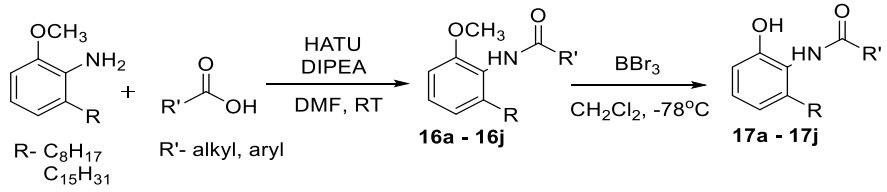

Scheme-4: synthesis of ceramide mimics

Table-1

comp. no	ceramide mimics	IC_{50} (SMS1) (μM)	IC_{50} (SMS2) (μM)	selectivity	yield
17a	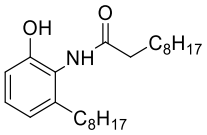	30	>100	SMS1	91%
17b	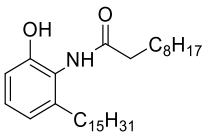	>100	>100	-	87%
17c	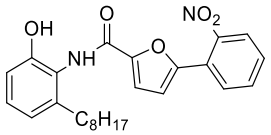	15	5	-	96%
17d	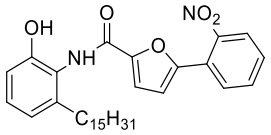	40	5	SMS2	97%
17e	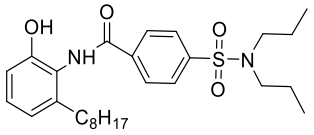	70	20	SMS2	91%
17f	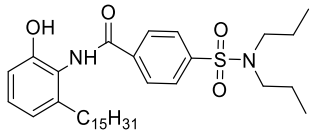	>100	35	SMS2	94%
17g	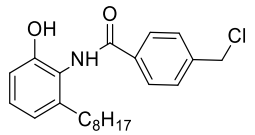	7	10	-	90%
17h	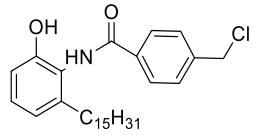	15	7	-	92%
17i	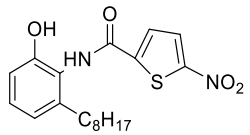	5	3	-	91%
17j	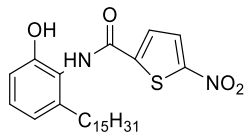	30	3	SMS2	92%

Agonist/antagonist activity of ginkgolic acid

Sphingosine1-phosphate (S1P), a signaling molecule for sphingosine-1-phosphate receptors ($S1P_1$-$S1P_5$) which belongs to the family of G protein coupled receptors (GPCRs). GPCRs represent a major drug target in all the clinical areas and currently about 40% of drugs on the market target GPCRs.[27] GPCRs, $S1P_1$-$S1P_5$ recognize the sphingolipid S1P, which regulates variety of cellular functions and out of five S1PRs, $S1P_1$ is the most important physiologically, especially in the vascular and immune system.[28]

Fingolimod (FTY720) is a S1P mimic and well-known success in the field of drug discovery and in the S1P research field. In 2010 FDA approved FTY720 as the first oral disease-modifying drug for the treatment of *multiple sclerosis*. FTY720 gets phosphorylated (FTY720-P) by sphingosine kinases (SK1 and SK2) *in vivo* and acts as an agonist on four S1P receptors ($S1P_1$, $S1P_3$, $S1P_4$, and $S1P_5$).[29] S1P and Fingolimod-phosphate have been reported to induce lymphopenia through its agonist activity on $S1P_1$ and subsequent internalization of $S1P_1$ in the lymphocytes.[30]

Nizet. V *et al*[31] predicted by *in silico* docking model that GA (15:0) (also called as anacardic acid) mimics S1P. Predicted binding mode suggests that GA (15:0) can establish hydrogen bonding with $S1P_1$ residues, in a similar fashion to the sphingolipid mimic, ML5 (Protein data bank code 3V2Y). ML5 is sphingolipid mimic and an antagonist for $S1P_1$, which was used to generate crystal structure of S1P receptor.[32] We wanted to prove agonist/antagonist activity of GA (15:0) for $S1P_1$ experimentally. To address this phenomenon, we investigated the signaling activities of $S1P_1$ by measuring the ERK (extracellular signal-regulated kinases) phosphorylation up on treatment with GA (15:0) by using stably expressing $S1P_1$ in chinese hamster ovary (CH0) cells. As a result GA (15:0) failed to induce ERK phosphorylation at different concentration (0.1 µM to 10 µM) when compared with S1P as a positive control (**Fig. 4a**). Also GA (15:0) didn't induce $S1P_1$ internalization when subjected to indirect immunofluorescent microscopy using anti-FLAG antibodies (**Fig. 4b**). These results suggest that GA (15:0) neither induces ERK phosphorylation nor $S1P_1$ internalization and also it didn't show antagonist activity also. Hence, GA (15:0) may not mimic S1P and it binds to $S1P_1$ only in case of *in silico* docking studies but not experimentally. The $S1P_1$ signaling assay and immunofluorescence assay were carried out according to Ohno. Y *et al.*[33] To prove

"sphingo-mimic" nature of GA, we went ahead to synthesize S1P mimic, derived from GA (15:0).

Synthesis of phospho-ginkgolic acid

To identify GA (15:0) derived S1P mimic, we decided to synthesize phospho-GA **20** which shows more structural similarity not only with S1P but also with reported S1P mimics FTY720-P and ML5 (**Fig. 3a**). Berg. T *et al*[34] have reported phosphorylation of salicylic acid using PCl_5 (**Fig. 3b**). When we carried out phosphorylation of GA (15:0) using PCl_5, reaction did not proceed may be due to steric hindrance by long hydrophobic chain. We carried out synthesis of **20** in three steps; first step involves the protection of carboxylic acid of GA (15:0) by using benzyl chloride to get compound **18**. The reaction of **18** with dibenzyl phosphite in the presence of DIPEA and DMAP to get compound **19**, followed by hydrogenation using Pd/C, H_2 to get desired compound **20** (**scheme 5**).

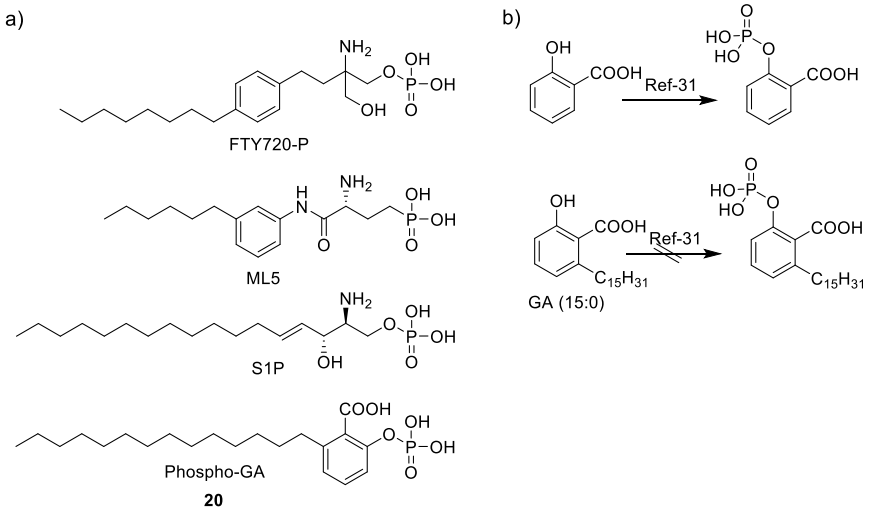

Fig. 3 a) structure of FTY720-P, ML5, S1P and phosphoGA and S1P **b**) phosphorylation of salicylic acid

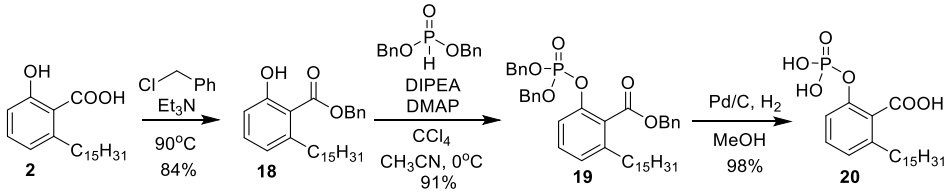

Scheme 5: synthesis of phospho-GA

Agonist activity of phospho-ginkgolic acid

We have assumed that phospho-GA might be a mimic of S1P due to their structural resemblance. To prove experimentally we investigated the signaling activities of $S1P_1$ by measuring the ERK phosphorylation up on treatment with phospho-GA. As a result, phospho-GA induces ERK phosphorylation in a dose dependent manner (**Fig. 4a**) and also it shows partial internalization at 10 µM (**Fig. 4b**). As expected phospho-GA is turned out to be agonist for $S1P_1$ there by proved our assumption that phospho-GA as S1P mimic, and also proved GA (15:1) is natural "sphingo-mimic" and behaves like sphingosine. We will be extending our studies using phospho-GA to identify its selectivity towards $S1P_1$ over other S1PRs and to identify its role in immune response disorders. We are expecting that phospho-GA falls in the same line as FTY720-P and ML5.

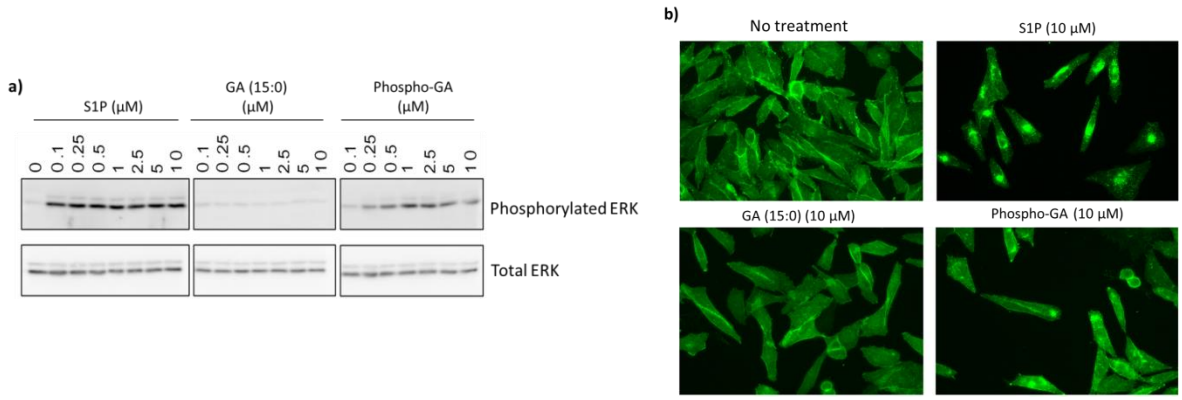

Fig. 4) agonist activity of ginkgolic acid and phospho-GA **a**) When $S1P_1$ expressed CHO cells were treated with phospho-GA, shows dose dependent ERK phosphorylation but not GA (15:0). **b**) Phospho-GA undergoes partial internalization but GA (15:0) failed to internalize.

Docking results of phospho-GA

The protein structure from PDB code 3V2Y was used as the receptor model with the removal of water molecules and bound ligands (ML5 and NAG). Only polar hydrogen atoms were added to the model, and then the input PDBQT file of the receptor was generated by using AutoDockTools(1.5.6).[35] The 3D model of S1P mimic, phospho-GA was generated from its SMILES string by using eLBOW program in Phenix software suite.[36] Then, AutoDockTools merged the non-polar hydrogen atoms and set up the rotatable bonds to create the input PDBQT file of S1P mimic. A grid box with the size of (25Å, 25Å, 25Å) centered at (x=4 Å, y=18 Å, z=-8Å) was set up for the docking simulation of phospho-GA against $S1P_1$, which was

performed by using Autodock Vina(1.1.2).[37] The predicted pose of phospho-GA with the lowest the binding affinity (-8.1 kcal/mol) is shown in **Fig. 5**.

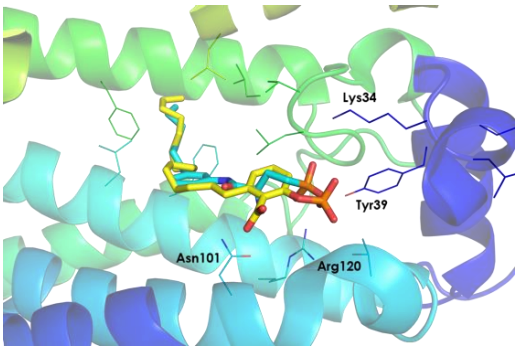

Fig. 5) Docking result of S1P mimic. The protein structure of S1PR (PDB code 3V2Y) is shown in ribbon model and the residues surrounding the binding site are shown in line model. S1P mimic and ML5 (bound ligand in 3V2Y) are represented in stick model. Carbon atoms are highlighted in yellow and cyan for S1P mimic and ML5, respectively. Oxygen, nitrogen and phosphate atoms are shown in red, blue and orange, respectively.

The docking result shows that phospho-GA adopts quite a similar binding pose to the bound ligand ML5. The phosphate group which is supposed to be crucial for binding interaction is located close to that of ML5, surrounded by hydrophilic side chains as shown in (**Fig. 5**). The rest part of phospho-GA representing the hydrophobicity adopts almost the same binding conformation as ML5, located at the hydrophobic region in the binding site. In the complex structure of ML5-$S1P_1$, Lys34 exhibits the possibility of forming a hydrogen bond to the phosphate group while it stays a little far away from that of phospho-ginkgolic acid. Actually, Lys34 could change its conformation to get close to the phosphate group, however the conformation is fixed during docking simulation by Autodock Vina. Docking simulations further confirmed the phospho-GA is a S1P mimic and GA (15:1) is a natural “sphingo-mimic”.

Conclusion

We have succeeded in identifying GA (15:1) and GA (15:0) the first natural inhibitors of SMS by screening library of medicinal plants. SAR studies of GA helped us to deeply understand the sphingosine like behaviour of GA. Ceramide mimic study gave us few selective SMS2 inhibitors which will be useful to understand the SMS2 biology under diseased condition. Our assumption towards GA might be natural “sphingo-mimic” has been proved by ERK phosphorylation, internalization and also by *in silico* docking studies. Finally, Ginkgolic acids role in metabolic disorders and Alzheimer’s disease need to be explored and it will be a platform to identify more effective and selective SMS2 inhibitors.

2.4 Experimental section

Isolation of ginkgolic acid (15:1) from *Ginkgo biloba*

Ginkgo biloba stem (500 g) collected from Hokkaido, Japan were dried, grinded well. The dried powder extracted with methanol (2 L) at room temperature three times after 24 h each. The combined MeOH extract was concentrated under reduced pressure to give a dark brown residue (15.9 g), which was dissolved in 20% MeOH in water (500 mL) and partitioned with hexane (250 mL x 3), Et_2O (250 mL x 3) and EtOAc (250 mL x 3). After removal of solvent, each of residues was used for SMS assay. We found that hexane fraction was more activity than Et_2O fraction but, EtOAc and water fractions turned out to be inactive. The active hexane fraction (3.8 g) was further purified by silica gel column chromatography. The active component was identified as ginkgolic acid (15:1) confirmed by NMR spectroscopy and HRMS. Yield: 0.006% (27.5 mg). Ginkgolic acid (15:1) is one of the major components of *Ginkgo biloba* leaves.

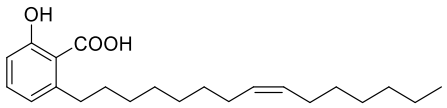

1

Ginkgolic acid (15:1); light yellow oil; ^{1}H NMR ($CDCl_3$, 500 MHz): δ = 10.99 (1H, s), 7.37 (1H, t, 7.9 Hz), 6.88 (1H, d, J=8.3 Hz), 6.78 (1H, d, J=7.5 Hz), 5.32-5.38 (2H, m), 2.97-3.00 (2H, t, J=7.5 Hz), 2.02-2.06 (4H, m), 1.60-1.62 (2H, m), 1.26-1.33 (18H, m), 0.88 (3H, t, J=6.6 Hz). ^{13}C NMR (125 MHz, $CDCl_3$): δ = 176.2, 163.6, 147.8, 135.4, 129.9, 129.8, 122.7, 115.8, 110.4, 36.4, 32.0, 31.9, 29.8, 29.7, 29.7, 29.6, 29.6, 29.5, 29.4, 29.3, 27.2, 26.9, 22.3, 14.0.

HRMS (*m/z*): $[M+H]^+$ calculated for $C_{22}H_{34}O_3$: 347.2580; found 347.2555.

Ginkgolic acid (15:0) (2) from Ginkgolic acid (15:1) (1)

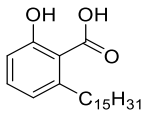

To a stirred solution of ginkgolic acid (15:1) (50 mg, 0.14 mmol) in EtOAc (10 ml) was added 10% Pd/C (30 mg, 0.028 mmol). The reaction mixture was stirred overnight at room temperature under H_2 atmosphere. The solid was filtered off and the filtrate was

concentrated under vacuum to afford a residue that was purified by silica gel column chromatography using hexane/EtOAc (9.0:1.0) to give **2** (48 mg, 96%) as colorless oil.

^{1}H NMR ($CDCl_3$, 500 MHz): δ = 11.13 (1H, s), 7.37 (1H, t, 8.0 Hz), 6.88 (1H, d, J=8.3 Hz), 6.73 (1H, d, J=7.3 Hz), 3.00 (2H, t, J=7.8 Hz), 1.59-1.65 (2H, m), 1.29-1.34 (24H, m), 0.89 (3H, t, J=6.8 Hz). ^{13}C NMR (125 MHz, $CDCl_3$): δ = 176.3, 163.6, 147.8, 135.4, 122.7, 115.8, 110.4, 36.4, 32.0, 31.9, 29.8, 29.7, 29.7, 29.6, 29.6, 29.5, 29.3, 22.7, 14.1

$[M+H]^+$ calculated for $C_{22}H_{36}O_3$: 349.2737; found 349.2712.

Methyl ester of Ginkgolic ester (4)

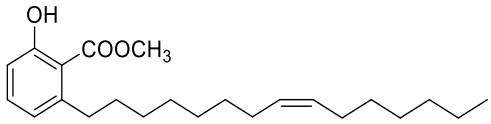

To a stirred solution of ginkgolic acid (15:1) (25 mg, 0.1 mmol) in methanol (2 mL) and diethyl ether (2 mL) was added a solution of TMS-CH_2N_2 in hexane until the color of the solution became yellow at 0 °C. The reaction mixture was stirred at same temperature for 0.5 h. The reaction was quenched with acetic acid and extracted with EtOAc, dried over $MgSO_4$. The organic layer was concentrated under vacuum to afford a residue that was purified by silica gel column chromatography using hexane/EtOAc (9.75:0.25) as an eluent to give the ester **4** (25 mg, 96%) as colorless oil.

^{1}H NMR ($CDCl_3$, 500 MHz): δ = 11.13 (1H, s), 7.29 (1H, t, 7.8 Hz), 6.85 (1H, d, J=8.3 Hz), 6.73 (1H, d, J=7.3 Hz), 5.39-5.33 (2H, m), 3.90 (3H s), 2.89 (2H, t, J=7.8 Hz), 2.03-2.08 (4H, m), 1.51-1.56 (2H, m), 1.29-1.34 (18H, m), 0.91 (3H, t, J=7.1 Hz). ^{13}C NMR (125 MHz, $CDCl_3$): δ = 171.9, 162.5, 146.1, 134.1, 129.8, 129.8, 122.8, 122.4, 115.5, 111.8, 52.0, 36.6, 32.1, 31.9, 29.9, 29.7, 29.6, 29.6, 29.6, 29.5, 29.5, 29.5, 29.5, 29.3, 29.3, 27.2, 26.9, 22.3, 14.0.

HRMS (*m/z*): $[M+H]^+$ calculated for $C_{23}H_{36}O_3$: 361.2737; found 361.2717.

Methyl (*Z*)-2-methoxy-6-(pentadec-8-en-1-yl)benzoate (5)

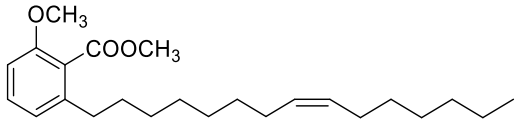

To a stirred solution of Ginkgolic acid (15:1) (100 mg, 0.29 mmol) in DMF (2mL) was added K_2CO_3 (0.73 mmol, 2.5 eq) and iodomethane (0.58 mmol, 2 eq) at room temperature. Then the reaction mixture was stirred at 90 °C under Ar atmosphere overnight. After completion of the reaction the reaction mixture was cooled to room temperature and acidified with 2M HCl and extracted with EtOAc, and dried over $MgSO_4$. The organic layer was concentrated under vacuum to afford a residue that was purified by silica gel column chromatography using hexane/EtOAc (9.5:0.5) to give the ester **5** (103 mg, 95%) as colorless oil.

^{1}H NMR ($CDCl_3$, 500 MHz): δ = 7.28 (1H, t, 8.3 Hz), 6.83 (1H, d, J=7.8 Hz), 6.77 (1H, d, J=8.3 Hz), 5.33-5.37 (2H, m), 3.92 (3H, s), 3.83 (3H, s), 2.55 (2H, t, J=8.0 Hz), 2.01-2.04 (4H, m), 1.56-1.61 (2H, m), 1.29-1.34 (18H, m), 0.90 (3H, t, J=7.0 Hz). ^{13}C NMR (125 MHz, $CDCl_3$): δ = 168.9, 156.2, 141.3, 130.2, 129.9, 129.8, 123.4, 121.4, 108.3, 33.4, 31.7, 31.1, 29.7, 29.7, 29.4, 29.3, 29.1, 28.9, 27.2, 27.1, 22.6, 14.0.

HRMS (*m/z*): $[M+H]^+$ calculated for $C_{24}H_{38}O_3$: 375.2893; found 375.2867.

5-hydroxy-2,2-dimethyl-4H-benzo[d][1,3]dioxin-4-one (6)

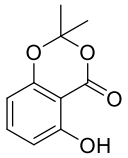

To the stirred solution of 2,6-dihydroxybenzoic acid (8 g, 51.9 mmol) in 1,2-dimethoxyethane (50 mL) at 0 °C was added acetone (4.9 mL, 67.5 mmol), $SOCl_2$ (4.8 mL, 67.5 mmol) and DMAP (316 mg, 2.6 mmol). The reaction mixture was stirred under Ar atmosphere for 1 h at 0 °C and stirred at room temperature overnight. After completion of the reaction saturated $NaHCO_3$ solution was added and extracted with Et_2O (100 mL x 2). The combined organic layer was washed with saturated aqueous NaCl solution, dried over $MgSO_4$ and the solution was concentrated under vacuum. The residue was purified by silica

gel column chromatography using hexane/EtOAc (8:2) to give **6** (9.3 g, Yield 93%) as a white solid.

^{1}H NMR ($CDCl_3$, 500 MHz): δ = 10.31 (1H, s), 7.38 (1H, t, 8.3 Hz), 6.59 (1H, d, 8.35 Hz), 6.41 (1H, d, 8.0 Hz), 1.72 (6H, s). ^{13}C NMR (125 MHz, $CDCl_3$): δ = 165.4, 161.3, 155.5, 137.9, 110.7, 107.2, 107.1, 99.3, 25.5.

HRMS (*m/z*): $[M+H]^+$ calculated for $C_{10}H_{10}O_4$: 195.0651; found 195.0648

2,2-dimethyl-4-oxo-4*H*-benzo[d][1,3]dioxin-5-yl trifluoromethanesulfonate (7)

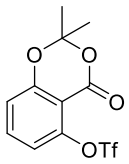

To a stirred solution of **6** (5 g, 25.8 mmol) in CH_2Cl_2 (30 mL) at 0 °C was added anhydrous pyridine (7.4 mL, 92.7 mmol) and trifluoromethanesulfonic anhydride (4.4 mL, 30.9 mmol). The reaction mixture was stirred for additional 1 h at same temperature. After completion of the reaction the reaction mixture was extracted with Et_2O (100 mL x 2) and the combined organic layer was dried over $MgSO_4$ and concentrated under vacuum. The residue obtained was purified by silica gel column chromatography using hexane/EtOAc (7:3) to give **7** (7.6 g, Yield 90%) as a white solid.

^{1}H NMR ($CDCl_3$, 500 MHz): δ = 7.62 (1H, t, 8.3 Hz), 7.0 (1H, d, 8.5 Hz), 7.01 (1H, d, 8.3 Hz), 1.76 (6H, s). ^{13}C NMR (125 MHz, $CDCl_3$): δ = 157.4, 157.0, 148.6, 136.2, 120.0, 117.9, 116.5, 108.2, 106.8, 25.4.

HRMS (*m/z*): $[M+H]^+$ calculated for $C_{11}H_9O_6F_3S$: 327.0144; found 327.0133.

(*E*)-5-(8-((*tert*-butyldiphenylsilyl)oxy)oct-1-en-1-yl)-2,2-dimethyl-4*H*-benzo[*d*][1,3]dioxin-4-one (8)

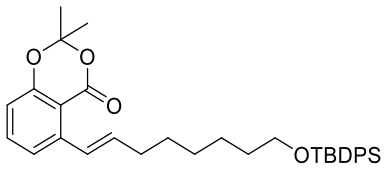

To a stirred solution of *tert*-butyl(oct-7-en-1-yloxy)diphenylsilane (240 mg, 0.68 mmol) in DMF (3 mL) at room temperature was added K_2CO_3 (94 mg, 0.68 mmol) and stirred for 0.5 h. Compound **7** (202 mg, 0.62 mmol) and palladium catalyst $PdCl_2(dppf).CH_2Cl_2$ (15 mg, 0.02 mmol) were added to the reaction mixture. Then the reaction mixture was stirred overnight at 75 °C. The reaction mixture was acidified with 2M HCl and extracted with Et_2O. The organic layer was dried over $MgSO_4$ and concentrated under vacuum. The residue obtained was purified by silica gel column chromatography using hexane/EtOAc (9:1) to give **8** (227 mg, Yield 67%) as colorless oil.

^{1}H NMR ($CDCl_3$, 500 MHz): δ = 7.76 (4H, d, 7.8 Hz), 7.55 (1H, d, J=9.7 Hz), 7.42-7.45 (7H, m), 7.28 (1H, d, 7.8 Hz), 6.87(1H, d, J=8.0 Hz), 6.27-6.33 (1H, m), 3.76 (2H, t, 6.4 Hz), 2.34 (2H, q, 13.9, 7.0, 6.8 Hz), 1.75 (7H, s), 1.69-1.66 (2H, m), 1.43-1.65 (6H, m), 1.14 (9H, m). ^{13}C NMR (125 MHz, $CDCl_3$): δ = 160.3, 158.8, 142.7, 136.6, 135.1, 134.2, 129.5, 128.2, 127.7, 121.3, 115.5, 110.6, 105.1, 64.0, 33.2, 32.6, 31.7, 31.6, 29.2, 29.1, 27.0, 25.7, 22.7, 19.3, 19.3, 14.2.

HRMS (*m/z*): $[M+H]^+$ calculated for $C_{34}H_{42}O_4Si$: 543.2925; found 543.2929.

(*E*)-5-(8-hydroxyoct-1-en-1-yl)-2,2-dimethyl-4*H*-benzo[*d*][1,3]dioxin-4-one (9)

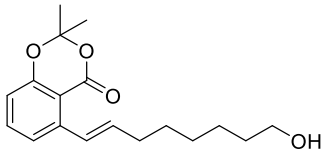

To a stirred solution of **8** (50 mg, 0.1 mmol) in THF (4 mL) at room temperature was added TBAF (36 mg, 0.14 mmol) and stirred for 2 h. After completion of the reaction the THF was evaporated and the residue was extracted with EtOAc. The organic layer was dried over $MgSO_4$ and concentrated under reduced vacuum. The residue obtained was purified by silica

gel column chromatography using hexane/EtOAc (6:4) to give **9** (24 mg, Yield 86%) as colorless oil.

^{1}H NMR ($CDCl_3$, 500 MHz): δ = 7.36-7.41 (2H, m), 7.19 (1H, d, J=7.8 Hz), 6.77 (1H, d, J=8.0 Hz), 6.15-6.21(1H, m), 3.59 (2H, t, J=6.6 Hz), 2.24 (2H, q, 13.9, 7.1, 6.8 Hz), 1.66 (6H, s), 1.49-1.51(4H, m), 1.34-1.37 (4H, m). ^{13}C NMR (125 MHz, $CDCl_3$): δ = 160.4, 156.7, 142.5, 135.4, 135.0, 128.0, 121.2, 115.2, 110.4, 105.0, 62.6, 32.9, 32.6, 28.9, 28.8, 25.5, 25.5.

HRMS (*m/z*): $[M+H]^+$ calculated for $C_{18}H_{24}O_4$: 305.1747; found 305.1772.

5-(8-hydroxyoctyl)-2,2-dimethyl-4*H*-benzo[*d*][1,3]dioxin-4-one (10)

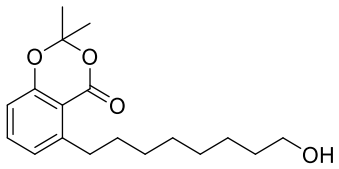

To a stirred solution of **9** (94 mg, 0.31 mmol) in EtOAc (10 ml) was added 10% Pd/C (50 mg, 0.05 mmol). The reaction mixture was stirred overnight at room temperature under H_2 atmosphere. Pd/C was filtered off and the filtrate was concentrated under vacuum to afford a residue that was purified by silica gel column chromatography using hexane/EtOAc (6:4) to give **10** (89 mg, 95%) as colorless oil.

^{1}H NMR ($CDCl_3$, 500 MHz): δ = 7.74 (1H, t, 8.0 Hz), 6.94(1H, d, J=7.5 Hz), 6.81(1H, d, 8.1 Hz), 3.64 (2H, t, 6.5 Hz), 3.09 (2H, t, 7.8 Hz), 1.71 (6H, s), 1.56-1.62 (4H, m), 1.32-1.41 (6H, m). ^{13}C NMR (125 MHz, $CDCl_3$): δ = 160.2, 157.0, 148.4, 135.0, 125.0, 115.0, 112.0, 104.9, 62.8, 34.3, 32.7, 31.1, 29.5, 29.3, 29.2, 25.6, 25.6.

HRMS (*m/z*): $[M+H]^+$ calculated for $C_{18}H_{26}O_4$: 307.1903; found 307.1921.

8-(2,2-dimethyl-4-oxo-4*H*-benzo[*d*][1,3]dioxin-5-yl)octanal (11)

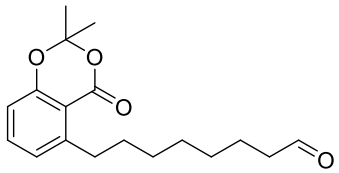

To a stirred solution of **10** (150 mg, 0.49 mmol) in EtOAc (10 ml) was added IBX (412 mg, 1.47 mmol). The reaction mixture was stirred overnight at 40 °C. The white solid was filtered off and the filtrate was concentrated under vacuum. The residue was purified by silica gel column chromatography using hexane/EtOAc (9:1) to give **11** (91 mg, 92%) as colorless oil.

^{1}H NMR ($CDCl_3$, 500 MHz): δ = 9.06(1H, s), 7.33 (1H, t, 8.1), 6.86 (1H, d, J=7.5 Hz), 6.73 (1H, d, 8.3 Hz), 3.01 (2H, t, 7.5 Hz), 2.35 (2H, t, 6.1 Hz), 1.63 (6H, s), 1.49-1.56 (4H, m), 1.27-1.31 (6H, m). ^{13}C NMR (125 MHz, $CDCl_3$): δ = 202.7, 160.1, 157.0, 148.2, 135.6, 125.0, 115.0, 111.9, 111.9, 104.8, 43.7, 34.2, 31.0, 28.9, 28.9, 25.5, 21.9.

HRMS (*m/z*): $[M+H]^+$ calculated for $C_{18}H_{24}O_4$: 305.1747; found 305.1776.

(*Z*)-2,2-dimethyl-5-(pentadec-8-en-1-yl)-4*H*-benzo[*d*][1,3]dioxin-4-one (12)

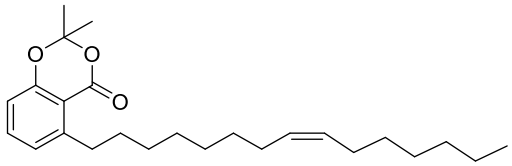

To a stirred solution of bromo(heptyl)triphenylphosphonium ion (50 mg, 0.11 mmol) in THF (5 mL) and DMSO (1 mL) was added NaH (5 mg, 0.23 mmol) at 0 °C under Ar atmosphere. The reaction mixture was stirred at room temperature for 1 h. Compound **11** (17 mg, 0.06 mmol) was added in THF (1 mL) at 0 °C and continued stirring for 1 h at the same temperature. After completion of the reaction, saturated NH_4Cl was added to the reaction mixture and extracted with hexane. The organic layer was dried under $MgSO_4$ and concentrated under vacuum. The residue was purified by silica gel column chromatography using hexane/EtOAc (9.75:0.25) to give **12** (42 mg, 66%) as yellow oil.

^{1}H NMR ($CDCl_3$, 500 MHz): δ = 7.38 (1H, t, 7.8 Hz), 6.92 (1H, d, J=7.8 Hz), 6.79 (1H, d, 8.3 Hz), 5.31-5.35 (2H, m), 3.08 (2H, t, 7.8 Hz), 1.98-2.02 (4H, m), 1.69 (6H, s), 1.55-1.61 (2H, m), 1.27-1.38 (18H, m), 0.87 (3H, t, 6.3 Hz). ^{13}C NMR (125 MHz, $CDCl_3$): δ = 160.2, 157.1, 148.5,

135.0, 129.8, 125.0, 115.0, 112.2, 104.9, 34.3, 31.9, 31.1, 27.2, 27.2, 27.3, 27.4, 27.6, 27.6 28.9, 28.9, 27.2, 25.6, 22.6, 14.1.

HRMS (*m/z*): $[M+H]^+$ calculated for $C_{25}H_{38}O_3$: 387.2893; found 387.2911.

(*E*)-2,2-dimethyl-5-(oct-1-en-1-yl)-4H-benzo[d][1,3]dioxin-4-one (7a)

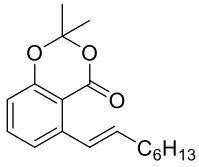

To a stirred solution of 1-pentene (189 mg, 1.68 mmol) in DMF (15 mL) at room temperature was added K_2CO_3 (231 mg, 1.68 mmol) and stirred for 0.5 h. Compound **7** (500 mg, 1.53 mmol) and palladium catalyst $PdCl_2$(dppf). CH_2Cl_2 (37 mg, 0.05 mmol) was added to the reaction mixture. Then the reaction mixture was stirred overnight at 75 °C. After completion of the reaction, the reaction mixture was acidified with 2M HCl and extracted with Et_2O. The organic layer was dried over $MgSO_4$ and concentrated under vacuum. The residue obtained was purified by silica gel column chromatography using hexane/EtOAc (9:1) to give **7a** (295 mg, Yield 67%) as colorless oil.

^{1}H NMR ($CDCl_3$, 500 MHz): δ = 7.39-7.46 (2H, m), 7.23 (1H, d, J=8.0 Hz), 6.81(1H, d, 8.0 Hz), 6.20-6.26 (1H, m), 2.25-2.29 (2H, m), 1.69 (6H, s), 1.46-1.52 (2H, m), 1.28-1.39 (6H, m), 0.88 (3H, t, 6.8 Hz). ^{13}C NMR (125 MHz, $CDCl_3$): δ = 160.3, 156.6, 142.6, 135.6, 134.9, 127.8, 121.1, 115.3, 110.4, 104.9, 33.1, 31.6, 29.0, 28.8, 25.5, 22.5, 14.0.

HRMS (*m/z*): $[M+H]^+$ calculated for $C_{18}H_{24}O_3$: 289.1752; found 289.1747.

(*E*)-2,2-dimethyl-5-(pentadec-1-en-1-yl)-4H-benzo[d][1,3]dioxin-4-one (7b)

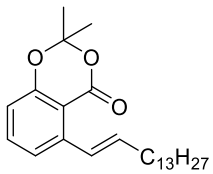

To a stirred solution of 1-pentene (354 mg, 1.68 mmol) in DMF (15 mL) at room temperature was added K_2CO_3 (231 mg, 1.68 mmol) and stirred for 0.5 h. Compound **7** (500 mg, 1.53 mmol) and palladium catalyst $PdCl_2$(dppf).CH_2Cl_2 (37 mg, 0.05 mmol) was added to the reaction mixture. Then the reaction mixture was stirred overnight at 75 °C. After

completion of the reaction, the reaction mixture was acidified with 2M HCl and extracted with Et_2O. The organic layer was dried over $MgSO_4$ and concentrated under vacuum. The residue obtained was purified by silica gel column chromatography using hexane/EtOAc (9:1) to give **7b** (410 mg, Yield 69%) as colorless oil.

^{1}H NMR ($CDCl_3$, 500 MHz): δ = 7.38-7.46 (2H, m), 7.22 (1H, d, J=7.8 Hz), 6.80 (1H, d, 7.0 Hz), 6.19-6.25 (1H, m), 2.24-2.29 (2H, m), 1.69 (6H, s), 1.46-1.52 (2H, m), 1.22-1.30 (20H, m), 0.87 (3H, t, 6.8 Hz). ^{13}C NMR (125 MHz, $CDCl_3$): δ = 160.2, 156.6, 142.6, 135.6, 134.8, 127.8, 121.1, 115.3, 110.4, 104.9, 33.1, 31.8, 29.6, 29.6, 29.6, 29.5, 29.4, 29.2, 29.2, 29.1, 25.5, 22.6, 14.0.

HRMS (*m/z*): $[M+H]^+$ calculated for $C_{25}H_{38}O_3$: 387.2893; found 387.2869.

2,2-dimethyl-5-octyl-4H-benzo[d][1,3]dioxin-4-one (7c)

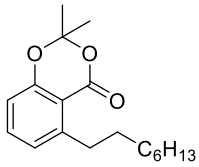

To a stirred solution of **7a** (100 mg, 0.35 mmol) in EtOAc (10 ml) was added 10% Pd/C (40 mg, 0.035 mmol). The reaction mixture was stirred overnight at room temperature under H_2 atmosphere. The solid was filtered off and the filtrate was concentrated under vacuum to afford a residue that was purified by silica gel column chromatography using hexane/EtOAc (9:1) to give **7c'** (95 mg, 94%) as colorless oil.

^{1}H NMR ($CDCl_3$, 500 MHz): δ = 7.38 (1H, t, 8.3 Hz), 6.92 (1H, d, J=8.8 Hz), 6.79 (1H, d, 8.0 Hz), 3.08 (2H, t, 7.8 Hz), 1.68 (6H, s), 1.55-1.61 (2H, m), 1.21-1.32 (10H, m), 0.86 (3H, t, 6.8 Hz). ^{13}C NMR (125 MHz, $CDCl_3$): δ = 160.1, 157.0, 148.4, 134.9, 125.0, 115.0, 112.0, 104.8, 34.3, 31.8, 31.1, 29.4, 29.2, 25.6, 22.6, 14.0. HRMS (*m/z*):

$[M+H]^+$ calculated for $C_{18}H_{24}O_3$: 291.1954; found 291.1949.

2,2-dimethyl-5-pentadecyl-4H-benzo[d][1,3]dioxin-4-one (7d)

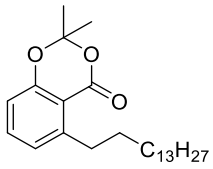

To a stirred solution of **7b** (100 mg, 0.26 mmol) in EtOAc (10 ml) was added 10% Pd/C (30 mg, 0.026 mmol). The reaction mixture was stirred overnight at room temperature under H_2 atmosphere. Pd/C was filtered off and the filtrate was concentrated under vacuum to afford a residue that was purified by silica gel column chromatography using hexane/EtOAc (9:1) as an eluent to give **7d** (92 mg, 91%) as colorless oil.

^{1}H NMR ($CDCl_3$, 500 MHz): δ = 7.39 (1H, t, 8.0 Hz), 6.93 (1H, d, J=7.5 Hz), 6.80 (1H, d, 8.0 Hz), 3.09 (2H, t, 7.6 Hz), 1.70 (6H, s), 1.54-1.62 (2H, m), 1.19-1.31 (24H, m), 0.88 (3H, t, 6.6 Hz). ^{13}C NMR (125 MHz, $CDCl_3$): δ = 159.8, 156.9, 148.2, 134.8, 124.8, 114.8, 111.8, 104.6, 34.2, 31.7, 31.0, 29.5, 29.5, 29.5, 29.5, 29.4, 29.4, 29.4, 29.3, 29.2, 22.5, 13.9.

HRMS (*m/z*): $[M+H]^+$ calculated for $C_{25}H_{40}O_3$: 389.3050; found 387.3046.

2-hydroxy-6-octylbenzoic acid (3)

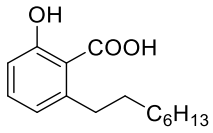

The solution of **7c** (30 mg, 0.10 mmol) in 50% KOH (0.5 mL) and DMSO (1.5 mL) stirred at 80 °C for 1 h. The reaction was cooled to temperature to room temperature and acidified with 2M HCl then extracted with EtOAc. The organic layer was dried under $MgSO_4$ and concentrated under vacuum. The residue was purified by silica gel column chromatography using hexane/EtOAc (7:3) as an eluent to give **3** (25 mg, 96%) as a white solid.

^{1}H NMR ($CDCl_3$, 500 MHz): δ = 10.99 (1H, s), 7.37 (1H, t, 8.0 Hz), 6.88 (1H, d, J=8.3 Hz), 6.79 (1H, d, J=7.1 Hz), 2.98 (2H, t, J=8.0 Hz), 1.58-1.64 (2H, m), 1.28-1.38 (10H, m), 0.88 (3H, t, J=6.6 Hz). ^{13}C NMR (125 MHz, $CDCl_3$): δ = 176.3, 163.6, 147.8, 135.4, 122.8, 115.8, 110.3, 36.4, 31.9, 31.8, 29.7, 29.4, 29.2, 22.6, 14.0. HRMS (*m/z*):

$[M+H]^+$ calculated for $C_{15}H_{22}O_3$: 251.1641; found 251.1636.

Ginkgolic acid (15:0) (2)

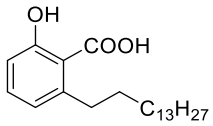

The solution of **7d** (50 mg, 0.13 mmol) in 50% KOH (0.75 mL) and DMSO (2 mL) stirred at 80 °C for 1 h. The reaction was cooled to temperature to room temperature and acidified with 2M HCl then extracted with EtOAc. The organic layer was dried under $MgSO_4$ and concentrated under vacuum. The residue was purified by silica gel column chromatography using hexane/EtOAc (7:3) as an eluent to give **2** (41 mg, 91%) as a white solid.

^{1}H NMR ($CDCl_3$, 500 MHz): δ = 11.13 (1H, s), 7.37 (1H, t, 8.0 Hz), 6.88 (1H, d, J=8.3 Hz), 6.73 (1H, d, J=7.3 Hz), 3.00 (2H, t, J=7.8 Hz), 1.59-1.65 (2H, m), 1.29-1.34 (24H, m), 0.89 (3H, t, J=6.8 Hz). ^{13}C NMR (125 MHz, $CDCl_3$): δ = 176.3, 163.6, 147.8, 135.4, 122.7, 115.8, 110.4, 36.4, 32.0, 31.9, 29.8, 29.7, 29.7, 29.6, 29.6, 29.5, 29.3, 22.7, 14.1.

HRMS (*m/z*): $[M+H]^+$ calculated for $C_{22}H_{36}O_3$: 349.2737; found 349.2712.

(*E*)-1-methoxy-2-nitro-3-(oct-1-en-1-yl)benzene (14a)

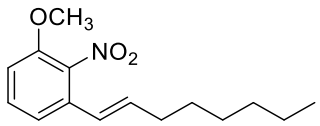

To a stirred solution of 3-bromo-2-nitro-anisole (750 mg, 3.23 mmol) in DMF (10 mL) was added 1-octene (725 mg, 6.46 mmol), Na_2CO_3 (536 mg, 3.87 mmol) and $PdCl_2$ (28 mg, 0.16 mmol). The reaction mixture was refluxed overnight. The reaction mixture was cooled to room temperature, neutralized with 2M HCl and extracted with Et_2O. The organic layer was dried under $MgSO_4$ and concentrated under vacuum. The residue was purified by silica gel column chromatography using hexane/EtOAc (9.5:0.5) to give **14a** (410 mg, 48%) as yellow oil.

^{1}H NMR ($CDCl_3$, 500 MHz): δ = 7.23 (1H, t, 8.3 Hz), 6.04(1H, d, J=7.85 Hz), 6.78(1H, d, 8.3 Hz), 6.20-6.26 (1H, m), 5.28- 3.53 (1H, m), 3.78 (3H, s), 2.45 (1H, t, 8.0 Hz), 2.13 (1H, q, 14.4, 7.1, 7.3) 1.65-1.84 (1H, m), 1.37-1.57 (1H, m), 1.20-1.35 (6H, m), 0.80 (3H, t, 6.6 Hz). ^{13}C NMR

(125 MHz, $CDCl_3$): δ = 150.6, 137.5, 131.1, 130.4, 121.8, 121.6, 117.8, 110.3, 56.3, 56.2, 33.1, 31.6, 29.1, 28.8, 22.5, 14.0.

HRMS (*m/z*): $[M+H]^+$ calculated for $C_{15}H_{21}NO_3$: 264.1594; found 264.1575.

(*E*)-1-methoxy-2-nitro-3-(pentadec-1-en-1-yl)benzene (14)

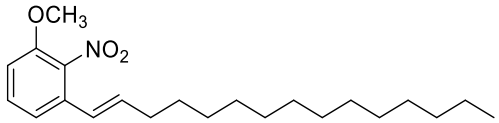

^1H NMR ($CDCl_3$, 500 MHz): δ = 7.31 (1H, t, 8.0 Hz), 6.86 (2H, d, 8.2 Hz), 6.21-6.34 (1H, m), 5.34-5.42 (1H, m), 3.87 (3H, s), 2.53(2H, t, 7.8 Hz), 2.15-2.18 (1H, m), 1.96-1.99 (2H, m), 1.57-1.60 (4H, m), 1.25-1.32 (16H, m), 0.87 (3H, t, 6.6 Hz). ^{13}C NMR (125 MHz, $CDCl_3$): δ = 150.6, 150.5, 137.5, 130.5, 130.4, 121.8, 121.6, 117.8, 110.3, 109.8, 56.3, 56.2, 43.8, 33.8, 33.2, 31.9, 30.8, 32.9, 30.5, 29.8, 28.7, 29.6, 29.3, 29.1, 28.2, 23.8, 22.6, 14.1. HRMS (*m/z*): $[M+Na]^+$ calculated for $C_{22}H_{35}NO_3Na$: 384.2509; found 384.2518.

2-methoxy-6-octylaniline (15a)

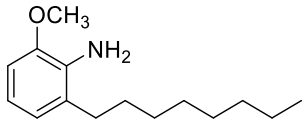

To a stirred solution of **14a** (275 mg, 1.04 mmol) in EtOAc (10 ml) was added 10% Pd/C (220 mg, 0.21 mmol). The reaction mixture was stirred overnight under H_2 atmosphere at room temperature. Pd/C was filtered off and the filtrate was concentrated under vacuum. The residue was purified by silica gel column chromatography using hexane/EtOAc (9:1) to give **15a** (235 mg, 96%) as yellow oil.

^1H NMR ($CDCl_3$, 500 MHz): δ = 6.67-6.70 (3H, m), 3.84 (3H, s), 3.78(2H, s), 2.49 (2H, t, 7.6 Hz), 1.54-1.64 (2H, m), 1.21-1.37 (24H, m), 0.87 (3H, t, 6.8 Hz). ^{13}C NMR (125 MHz, $CDCl_3$): δ = 147.2, 133.5, 127.4, 121.6, 117.7, 108.1, 55.5, 55.5, 55.4, 31.9, 31.2, 29.7, 29.7, 29.9, 29.6, 29.4, 28.8, 27.8, 27.6, 22.7, 14.1.

HRMS (*m/z*): $[M+H]^+$ calculated for $C_{15}H_{25}NO$: 236.2008; found 236.1998,

2-methoxy-6-pentadecylaniline (15)

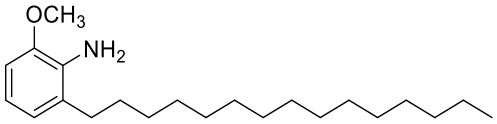

^{1}H NMR ($CDCl_3$, 500 MHz): δ = 6.67-6.70 (3H, m), 3.84 (3H, s), 3.78(2H, s), 2.49 (2H, t, 7.6 Hz), 1.54-1.64 (2H, m), 1.21-1.37 (24H, m), 0.87 (3H, t, 6.8 Hz). ^{13}C NMR (125 MHz, $CDCl_3$): δ = 147.2, 133.5, 127.4, 121.6, 117.7, 108.1, 55.5, 55.5, 55.4, 31.9, 31.2, 29.7, 29.7, 29.9, 29.6, 29.4, 28.8, 27.8, 27.6, 22.7, 14.1. HRMS (*m/z*): $[M+H]^+$ calculated for $C_{22}H_{39}NO$: 334.3104; found 334.3122.

2-amino-3-octylphenol (13a)

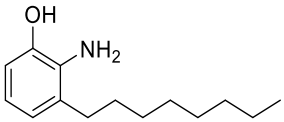

To a stirred solution of **15a** (100 mg, 0.426 mmol) in CH_2Cl_2 (5 ml) under Ar atmosphere was added BBr_3 (320 mg, 1.28 mmol) at 0°C. The reaction mixture was stirred at 0 °C for additional 2h. After completion of the reaction, reaction mixture was quenched with EtOAc/H_2O (1:1) and extracted with EtOAc. The organic layer was dried with $MgSO_4$ and concentrated under vacuum. The residue was purified by silica gel column chromatography using hexane/EtOAc (8:2) to give **13a** (410 mg, 96%) as yellow oil.

^{1}H NMR ($CDCl_3$, 500 MHz): δ = 6.57-6.70 (3H, m), 4.61 (3H, s), 2.50-2.53 (2H, t, 7.6 Hz), 1.60-1.64 (2H, m), 1.22-1.40 (10H, m), 0.91 (3H, t, 6.8 Hz). ^{13}C NMR (125 MHz, $CDCl_3$): δ = 144.3, 131.7, 129.6, 121.5, 119.1, 112.9, 31.9, 31.6, 29.7, 29.7 29.3, 29.0, 22.8, 14.1. HRMS (*m/z*): $[M+H]^+$ calculated for $C_{14}H_{23}NO$: 222.1852; found 222.1831.

2-amino-3-pentadecylphenol (13)

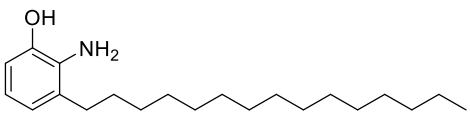

^{1}H NMR ($CDCl_3$, 500 MHz): δ = 6.59-6.70 (3H, m), 4.36 (2H, s), 2.55 (2H, t, 7.8 Hz), 1.56-1.64 (4H, m), 1.22-1.39 (25H, m), 0.90 (3H, t, 7.0 Hz). ^{13}C NMR (125 MHz, $CDCl_3$): δ = 144.2, 131.9,

129.6, 121.6, 118.9, 112.8, 31.9, 31.2, 29.7, 29.7, 29.7, 29.7, 29.6, 29.6, 29.5, 29.0, 22.7, 14.1.

HRMS (*m/z*): $[M+H]^+$ calculated for $C_{21}H_{37}NO$: 320.2947; found 320.2967.

General procedure for acid and amine coupling reaction (16a to 16j)

To a stirred solution of acid (0.315 mmol) in DMF under Ar atmosphere was added *N,N*-diisopropylethylamine (1.1 mmol) at room temperature. To the reaction mixture amine (0.21 mmol) and HATU (0.42 mmol) was added. The reaction mixture was stirred under Ar atmosphere at room temperature for additional 2h. After completion of the reaction, the reaction mixture was diluted with water and extracted with EtOAc. The organic layer was dried with $MgSO_4$ and concentrated under vacuum. The residue was purified by silica gel column chromatography using hexane/EtOAc to give desired compound.

***N*-(2-methoxy-6-octylphenyl)decanamide (16a)**

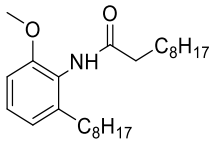

(As a white solid, 92%) ^{1}H NMR ($CDCl_3$, 500 MHz): δ = 7.17 (1H, t, 7.8 Hz), 6.87 (1H, d, 7.8 Hz), 6.76 (1H, d, 7.8 Hz), 6.68 (1H, s), 3.80(3H, s), 2.56 (2H, t, 7.8), 2.41 (2H, t, 7.3 Hz), 1.73-1.78 (2H, m), 1.54-1.60 (2H, m), 1.41-1.43 (2H, m), 1.21-1.29 (20H, m), 0.84-0.89 (6H, m).

HRMS (*m/z*): $[M+H]^+$ calculated for $C_{25}H_{43}NO_2$: 390.3366; found 390.3363.

***N*-(2-methoxy-6-pentadecylphenyl)decanamide (16b)**

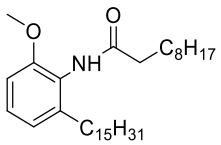

(As white solid, 93%) ^{1}H NMR ($CDCl_3$, 500 MHz): δ = 7.15 (1H, t, 7.8 Hz), 6.85 (1H, d, 7.8 Hz), 6.74 (1H, d, 7.8 Hz), 6.67 (1H, s), 3.79 (3H, s), 2.55 (2H, t, 7.6), 2.40 (2H, t, 7.3 Hz), 1.73-1.77 (2H, m), 1.55-1.51 (2H, m), 1.42-1.44 (1H, m), 1.19-1.26 (36H, m), 0.87 (6H, t, 7.1 Hz).

HRMS (*m/z*): $[M+H]^+$ calculated for $C_{32}H_{57}NO_2$: 488.4462; found 488.4442.

***N*-(2-methoxy-6-octylphenyl)-5-(2-nitrophenyl)furan-2-carboxamide (16c)**

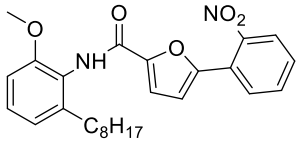

(As yellow oil, 87%) ^{1}H NMR ($CDCl_3$, 500 MHz): δ = 8.01 (1H, s), 7.76 (2H, t, 8.1 Hz), 6.64 (1H, t, 8.0 Hz), 7.50-754 (2H, m), 7.28 (1H, d, 7.8 Hz), 6.89 (1H, d, 7.3), 6.78-6.82 (2H, m), 3.84(3H, s), 2.64 (2H, t, 7.8 Hz), 1.20-1.33 (10H, m), 0.83(3H, t, 6.8 Hz). HRMS (*m/z*):

$[M+H]^+$ calculated for $C_{26}H_{30}N_2O_5$: 451.2267; found 451.2247.

***N*-(2-methoxy-6-pentadecylphenyl)-5-(2-nitrophenyl)furan-2-carboxamide (16d)**

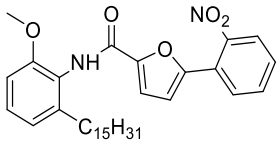

(As a yellow solid, 94%) ^{1}H NMR ($CDCl_3$, 500 MHz): δ = 7.75-7.79 (2H, m), 7.65 (1H, t, 8.1 Hz), 7.58 (1H, s), 7.52 (1H, t, 8.0 Hz), 7.21-7.3 (2H, m), 6.91 (1H, d, 7.8), 6.79-6.84 (2H, m), 3.85 (3H, s), 2.66 (2H, t, 7.8 Hz), 1.60-1.64 (2H, m), 1.33-1.22 (24H, m), 0.89 (3H, t, 6.8 Hz).

HRMS (*m/z*): $[M+H]^+$ calculated for $C_{33}H_{44}N_2O_5$: 549.3323; found 549.3316.

4-(*N*,*N*-dipropylsulfamoyl)-*N*-(2-methoxy-6-octylphenyl)benzamide (16e)

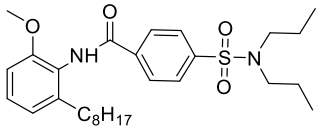

(As a white solid, 88%) ^{1}H NMR ($CDCl_3$, 500 MHz): δ = 8.02 (1H, d, 7.8 Hz), 7.90 (2H, d, 7.3 Hz), 7.55 (1H, s), 7.23 (1H, t, 8.0 Hz), 6.92 (1H, d, 7.8 Hz), 6.80 (1H, d, 7.5 Hz), 3.80 (3H, s), 3.10 (4H, t, 7.8 Hz), 2.62 (2H, t, 7.8 Hz), 1.55-1.61 (6H, m), 1.55-1.61(10H, m), 0.83-0.90 (9H, m).

HRMS (*m/z*): $[M+H]^+$ calculated for $C_{28}H_{42}N_2O_4S$: 503.2938; found 503.2929.

4-(*N*,*N*-dipropylsulfamoyl)-*N*-(2-methoxy-6-pentadecylphenyl)benzamide (16f)

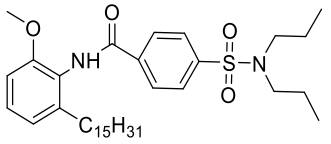

(As a yellow solid, 86%) ^{1}H NMR ($CDCl_3$, 500 MHz): δ = 8.01 (1H, d, 5.4 Hz), 7.89 (2H, d, 7.1 Hz), 7.53 (1H, s), 7.22 (1H, t, 8.0 Hz), 6.91 (1H, d, 7.8 Hz), 6.79 (1H, d, 7.5 Hz), 3.79 (3H, s), 3.10 (4H, t, 7.6 Hz), 2.62 (2H, t, 7.8 Hz), 1.53-1.62 (6H, m), 1.22-1.30 (25H, m), 0.86-0.90 (9H, m).

HRMS (*m/z*): $[M+H]^+$ calculated for $C_{35}H_{56}N_2O_4S$: 601.4033; found 601.4031.

4-(chloromethyl)-*N*-(2-methoxy-6-octylphenyl)benzamide (16g)

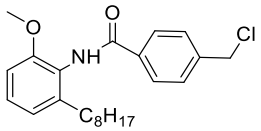

(As a yellow solid, 90%) ^{1}HNMR ($CDCl_3$, 500 MHz): δ = 8.69 (1H, d, 4.3 Hz), 8.33 (1H, d, 8.3 Hz), 7.9 (1H, s), 7.92 (1H, d, 8.3 Hz), 7.61 (2H, d, 7.1 Hz), 7.38 (1H, t, 4.0 Hz), 6.89 (1H, d, 7.8 Hz), 6.76 (1H, d, 8.0 Hz), 5.69 (2H, s), 3.76 (3H, s) 2.60 (2H, t, 7.8 Hz) 1.56-1.60 (2H, m), 1.20-1.24 (10H, m), 0.83 (3H, t, 6.8Hz).

HRMS (*m/z*): $[M+H]^+$ calculated for $C_{23}H_{30}ClNO_2$: 388.2037; found 388.2033.

4-(chloromethyl)-*N*-(2-methoxy-6-pentadecylphenyl)benzamide (16h)

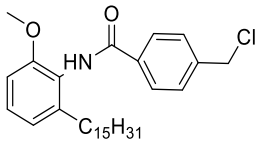

(As a yellow solid, 93%) ^{1}H NMR ($CDCl_3$, 500 MHz): δ = 7.93 (2H, s), 7.48-7.53 (3H, m), 7.23 (1H, t, 8.0 Hz), 6.93 (1H, d, 7.8 Hz), 6.80 (1H, d, 7.8 Hz), 4.65 (2H, s), 3.81 (3H, s), 2.65 (2H, t, 7.5 Hz), 1.59-1.65 (2H, m), 1.24-1.27 (24H, m), 0.90 (3H, t, 6.8Hz).

HRMS (*m/z*): $[M+H]^+$ calculated for $C_{30}H_{44}ClNO_2$: 48603133; found 486.3133.

***N*-(2-methoxy-6-octylphenyl)-5-nitrothiophene-2-carboxamide (16i)**

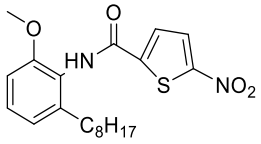

(As a light yellow solid, 87%) ^{1}H NMR ($CDCl_3$, 500 MHz): δ = 7.90 (1H, s), 7.53 (1H, s), 7.25-7.37 (2H, m), 6.93 (1H, d, 7.8 Hz), 6.81 (1H, d, 8.0 Hz), 3.81 (3H, s), 2.61 (2H, t, 7.8 Hz), 1.55-1.60 (2H, m), 1.23-1.28 (10H, m), 0.86 (3H, t, 6.8 Hz).

HRMS (*m/z*): $[M+H]^+$ calculated for $C_{20}H_{26}N_2O_4S$: 391.1686; found 391.1675.

***N*-(2-methoxy-6-pentadecylphenyl)-5-nitrothiophene-2-carboxamide (16j)**

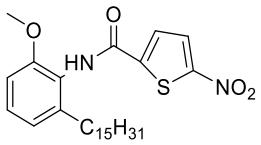

(As a yellow solid, 88%) ^{1}H NMR ($CDCl_3$, 500 MHz): δ = 8.89 (1H, s), 7.53 (1H, s), 7.26-7.39 (2H, m), 6.92 (1H, d, 7.5 Hz), 6.81 (1H, d, 7.3 Hz), 3.81 (3H, s), 2.60 (2H, t, 8.1 Hz), 1.56-1.61 (2H, m), 1.23-1.31 (25H, m), 0.88 (3H, t, 6.8Hz).

HRMS (*m/z*): $[M+H]^+$ calculated for $C_{27}H_{40}N_2O_4S$: 489.2781; found 489.2754.

General procedure for *O*-methyl deprotection (17a to 17j)

To a stirred solution of methyl phenyl ethers (0.06 mmol) in CH_2Cl_2 under Ar atmosphere was added BBr_3 (320 mg, 1.28 mmol) at 78°C. The reaction mixture was stirred for 1h at 0°C. After completion of the reaction, the reaction mixture was cooled to room temperature and quenched with EtOAc/H_2O (1:1) and extracted with EtOAc. The organic layer was dried with $MgSO_4$ and concentrated under vacuum. The residue was purified by silica gel column chromatography using hexane/EtOAc

***N*-(2-hydroxy-6-octylphenyl)decanamide (17a)**

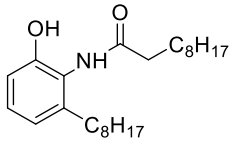

(As yellow oil, 90%) ^{1}H NMR ($CDCl_3$, 500 MHz): δ = 7.31 (1H, d, 8.3 Hz), 7.20 (1H, t, 7.8 Hz), 7.11 (1H, d, 7.3 Hz), 2.91-2.98 (4H, m), 1.83-1.89 (2H, m), 1.71-1.77 (2H, m), 1.27-1.43 (22H, m), 0.87-0.89 (6H, m).

HRMS (*m/z*): $[M+H]^+$ calculated for $C_{24}H_{41}NO_2$: 376.3210; found 376.3198.

***N*-(2-hydroxy-6-pentadecylphenyl)decanamide (17b)**

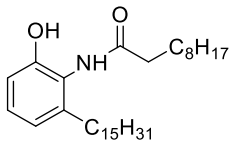

(As a white solid, 87%) ^{1}H NMR ($CDCl_3$, 500.MHz): δ = 7.08 (1H, t, 7.7 Hz), 6.91 (1H, d, 7.0 Hz), 6.75 (1H, d, 8.5 Hz), 2.54 (2H, t, 7.8), 2.47 (2H, t, 7.6 Hz), 1.74-1.78 (2H, m), 1.52-1.58 (2H, m), 1.23-1.41 (40H, m), 0.86-0.89 (6H, m).

HRMS (*m/z*): $[M+H]^+$ calculated for $C_{31}H_{55}NO_2$: 474.4305; found 474.4286.

***N*-(2-hydroxy-6-octylphenyl)-5-(2-nitrophenyl)furan-2-carboxamide (17c)**

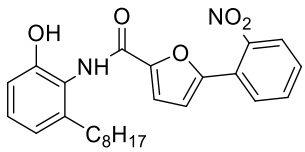

(As a red solid, 95%) ^{1}H NMR ($CDCl_3$, 500 MHz): δ = 8.34 (1H, s), 8.10 (1H, d, 3.9 Hz), 7.79 (1H, d, 8.0 Hz), 7.72 (1H, d, 7.8 Hz), 7.67 (1H, t, 7.3 Hz), 7.57 (1H, t, 7.6 Hz), 7.14 (1H, t, 7.8 Hz), 6.97 (1H, s), 6.88 (1H, d, 3.6 Hz), 6.82 (1H, d, 7.6 Hz), 2.69 (2H, t, 7.5 Hz), 6.61-6.66 (2H, m), 1.04-1.40 (2H, m), 1.16-1.30 (10H, m), 0.83 (3H, t, 6.8 Hz).

HRMS (*m/z*): $[M+H]^+$ calculated for $C_{25}H_{28}N_2O_5$: 437.2071; found 437.2056.

_N_-(2-hydroxy-6-pentadecylphenyl)-5-(2-nitrophenyl)furan-2-carboxamide (17d)

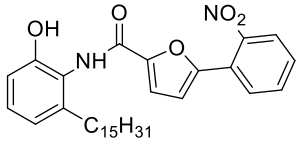

(As an orange solid, 97%) ^{1}H NMR ($CDCl_3$, 500 MHz): δ = 8.35 (1H, s), 8.1 (1H, s), 7.81 (1H, d, 6.8 Hz), 7.73 (1H, d, 6.8 Hz), 7.68 (1H, t, 7.3), 7.57 (1H, t, 7.6 Hz), 7.40 (1H, d, 3.6), 7.15 (1H, t, 7.8 Hz), 6.98 (1H, t, 7.3) (2H, m), 6.90 (1H, d, 3.6 Hz), 6.83 (1H, d, 8.3 Hz), 2.70 (2H, t, 7.6 Hz), 1.62-1.67 (2H, m), 1.38-1.41 (2H, s), 1.19-1.31 (24H, m), 0.88 (3H, t, 6.6 Hz).

HRMS (*m/z*): $[M+H]^+$ calculated for $C_{32}H_{42}N_2O_5$: 535.3166; found 535.3162.

4-(_N_,_N_-dipropylsulfamoyl)-_N_-(2-hydroxy-6-octylphenyl)benzamide (17e)

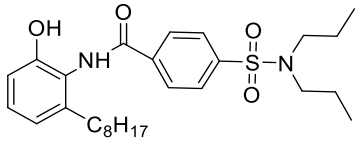

(As a yellow solid, 90%) ^{1}H NMR ($CDCl_3$, 500 MHz): δ = 8.0 (2H, d, 8.5 Hz), 7.97 (3H, t, 8.3 Hz), 6.99 (1H, d, 8.3 Hz), 6.84 (1H, d, 8.5 Hz), 3.13 (4H, t, 7.8 Hz), 2.67 (2H, t, 7.6 Hz), 1.55-1.61 (6H, m), 1.21-1.30 (10H, m), 0.85-0.90 (9H, m).

HRMS (*m/z*): $[M+H]^+$ calculated for $C_{27}H_{40}N_2O_4S$: 489.2781; found 489.2785.

4-(_N_,_N_-dipropylsulfamoyl)-_N_-(2-hydroxy-6-pentadecylphenyl)benzamide (17f)

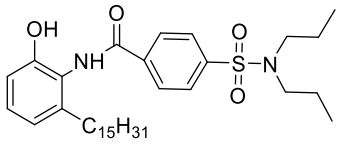

(As yellow oil, 92%) ^{1}H NMR ($CDCl_3$, 500 MHz): δ = 7.96-8.03 (4H, m), 7.18 (1H, t, 7.8 Hz), 7.00 (1H, d, 5.6 Hz), 6.85 (1H, d, 7.3 Hz), 3.14 (4H, t, 7.8 Hz), 2.68 (2H, t, 7.3 Hz), 1.55-1.65 (6H, m), 1.25-1.35 (24H, m), 0.89 (9H, t, 7.3 Hz).

HRMS (*m/z*): $[M+H]^+$ calculated for $C_{34}H_{54}N_2O_4S$: 587.3877; found 587.3855.

4-(chloromethyl)-*N*-(2-hydroxy-6-octylphenyl)benzamide (17g)

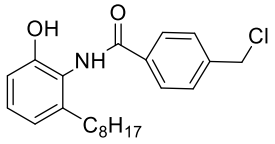

(As yellow oil, 90%) ^{1}H NMR ($CDCl_3$, 500 MHz): δ = 8.30 (1H, s), 7.94 (1H, s), 7.88 (2H, d, 8.3 Hz), 7.56 (2H, d, 8.3 Hz), 7.14 (1H, t, 7.8 Hz), 6.8 (1H, d, 8.3 Hz), 6.81 (1H, d, 8.5 Hz), 4.53 (2H, s), 2.66 (2H, t, 7.6 Hz), 1.59-1.65 (2H, m), 1.21-1.39 (12H, m), 0.86 (3H, t, 7.0 Hz).

HRMS (*m/z*): $[M+H]^+$ calculated for $C_{22}H_{28}ClNO_2$: 374.1881; found 374.1873.

4-(chloromethyl)-*N*-(2-hydroxy-6-pentadecylphenyl)benzamide (17h)

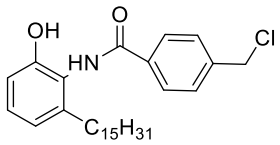

(As a white solid, 95%) ^{1}H NMR (CDCl3, 500 MHz): δ = 8.33 (1H, s), 7.91-8.00 (3H, m), 7.58 (2H, d, 7.5 Hz) 7.16 (1H, t, 8.0 Hz), 6.99 (1H, d, 7.8 Hz), 6.82 (1H, d, 7.5 Hz), 4.66 (2H, s), 2.67 (2H, t, 7.0 Hz), 1.56-1.68 (2H, m), 1.26-1.42 (25H, m), 0.88 (3H, t, 6.8Hz). HRMS (*m/z*): $[M+H]^+$ calculated for $C_{29}H_{42}ClNO_2$: 472.2976; found 472.2973.

***N*-(2-hydroxy-6-octylphenyl)-5-nitrothiophene-2-carboxamide (17i)**

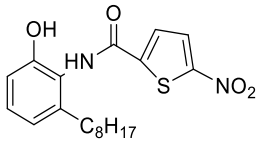

(As a yellow solid, 92%) ^{1}H NMR (CDCl3, 500 MHz): δ = 8.41 (1H, s), 7.4 (1H, s), 7.28 (1H, d, 7.3), 7.12 (1H, t, 7.8 Hz), 6.96 (1H, d, 8.0 Hz), 6.79 (1H, d, 7.3 Hz), 4.55 (1H, s), 2.63 (2H, t, 7.5 Hz), 1.50-1.64 (2H, m), 1.26-1.41 (10H, m), 0.88 (3H, t, 6.5 Hz).

HRMS (*m/z*): $[M+H]^+$ calculated for $C_{19}H_{24}N_2O_4S$: 377.1529; found 377.1528.

_N_-(2-hydroxy-6-pentadecylphenyl)-5-nitrothiophene-2-carboxamide (17j)

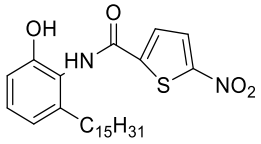

(As a yellow solid, 92%) ^{1}H NMR ($CDCl_3$, 500 MHz) δ = 8.41 (1H, s), 7.45 (1H, s), 7.28 (1H, s), 7.11 (1H, d, 7.8 Hz), 6.96 (1H, d, 7.6 Hz), 6.79 (1H, d, 7.5 Hz), 4.56 (1H, s), 2.63 (2H, t, 7.3 Hz), 1.58-1.63 (2H, m), 1.26-1.40 (24H, m), 0.88 (3H, t, 6.8Hz).

HRMS (*m/z*): $[M+H]^+$ calculated for $C_{26}H_{38}N_2O_4S$: 475.0562; found 475.0548.

Synthesis of phosphorylated ginkgolic acid

Benzyl 2-hydroxy-6-pentadecylbenzoate (18)

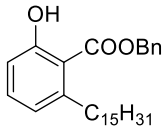

To a stirred solution of ginkgolic acid **2** (100 mg, 0.29 mmol) in triethylamine (1:1 v/v) was stirred at 90 °C for few minutes. Then benzyl chloride (36 mg, 0.29 mmol) was added to the reaction mixture at 90 °C and stirred for additional 1.5 hours at 90 °C. After completion of the reaction, the reaction mixture was cooled to room temperature and acidified with 2M HCl, extracted with EtOAc and dried over $MgSO_4$. The organic layer was concentrated under vacuum to afford a residue that was purified by silica gel column chromatography using hexane/EtOAc (9.25:0.75) to give desired compound **18** (118 mg, 94%) as colorless oil.

^{1}H NMR ($CDCl_3$, 500 MHz): δ = 11.21 (1H, s), 7.47 (2H, d, 6.11 Hz), 7.40-7.44 (3H, m), 7.30 (1H, t, 8.0 Hz), 6.86 (1H, d, J=8.3 Hz), 6.72 (1H, d, J=7.3 Hz), 5.41 (2H, s), 2.83 (2H, t, 9.8 Hz), 1.40-1.47 (2H, m), 1.30-1.37 (18H, m), 1.09-1.20 (6H, m), 0.92 (3H, t, J=6.8 Hz). ^{13}C NMR (125 MHz, $CDCl_3$) δ = 171.3, 162.7, 146.3, 134.8, 134.2, 129.0, 128.7, 122.4, 115.5, 111.8, 67.7, 29.8, 29.7, 29.7, 29.7, 29.7, 29.7, 29.6, 29.6, 29.4, 22.7, 14.1.

HRMS (*m/z*): $[M+H]^+$ calculated for $C_{29}H_{42}O_3$: 439.3206; found 439.3215.

Benzyl 2-((bis(benzyloxy)phosphoryl)oxy)-6-pentadecylbenzoate (19)

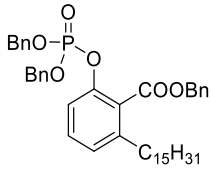

To a stirred solution of **18** (60 mg, 0.18 mmol) in CH_3CN (5 mL) was stirred at 0 °C for few minutes under Ar atmosphere. DIPEA (57 mg, 0.44 mmol), DMAP (catalytic amount 0.05 eq), CCl_4 (270 mg, 1.75 mmol) and dibenzylphosphite (55 mg 0.21 mmol) were added to the reaction mixture at 0 °C and stirred at room temperature for 2 h. After completion of the reaction, the reaction mixture was cooled to room temperature and acidified with 2M HCl, extracted with EtOAc and dried over $MgSO_4$. The organic layer was concentrated under vacuum. The residue was purified by silica gel column chromatography using chloroform (100%) as an eluent to get **19** (86 mg, 91%) as colorless oil.

^{1}H NMR ($CDCl_3$, 500 MHz): δ = 7.40 (2H, t, 6.8 Hz), 7.25-7.31 (15H, m), 7.03 (1H, d, 7.5 Hz), 5.29 (2H, s), 5.01-5-10 (4H, m), 2.57 (2H, t, 7.8 Hz), 1.51-1.56 (2H, m), 1.17-1.32 (24H, m), 0.90 (3H, t, J=6.6 Hz). ^{13}C NMR (125 MHz, $CDCl_3$): δ = 166.6, 147.4, 142.5, 135.5, 135.4, 135.3, 130.5, 128.7, 128.5, 128.5, 128.5, 128.5, 128.4, 127.9, 127.9, 125.9, 117.2, 70.0, 67.2, 33.6, 31.9, 31.3, 29.7, 29.7, 29.7, 29.7, 29.6, 29.5, 29.4, 29.4, 22.7, 14.1.

HRMS (*m/z*): $[M+H]^+$ calculated for $C_{43}H_{55}O_6P$: 699.3809; found 699.3816.

Phospho-ginkgolic acid (20)

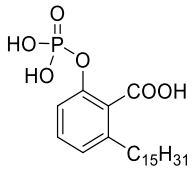

To a stirred solution of **9** (40 mg, 57 µmol) in MeOH (5 ml) was added 10% Pd/C (45 mg, 0.052 mmol). The reaction mixture was stirred overnight at rt under H_2 atmosphere. The solid was filtered off and the filtrate was concentrated under vacuum to afford a residue that was washed with non-polar solvents to get pure **10** (23 mg, 96%) as white solid.

^{1}H NMR ($CDCl_3$, 500 MHz): δ = 7.26-7.32 (2H, t, m), 7.01 (1H, d, 7.0 Hz), 2.66 (2H, t, 8.0 Hz), 1.57-1.61 (2H, m), 1.28-1.32 (24H, m), 0.89 (3H, t, J=7.1 Hz).

HRMS (*m/z*): $[M+H]^+$ calculated for $C_{22}H_{37}O_6P$: 451.2220; found 451.2214.

SMS assay

Cell lysates were prepared as follows: ZS/SMS1 and ZS/SMS2 cells (protein concentration 0.1 µg/µL) were diluted by Tris-buffer (pH 7.5) 20 mM and sonicated. Aiquots of the cell lysates 100 µL were added 1 µL of inhibitor of desired concentration and incubated at 37°C. After 30 min, the solutions were added 1 µL of C6-NBD-ceramide and incubated for 3 h at 37°C. The reaction was stopped by addition of 400 µL of MeOH/CHCl3 [1/2 (v/v)]; the mixture was shaken and centrifuged (1500 rpm x 5 min). The formation of C6-NBD-sphingomyelin was quantified by determination of the peak area of C6-NBD-sphingomyelin using HPLC. A reverse phase HPLC assay using a JACSO HPLC system was developed for the quantitative analysis of the inhibitory activity. The system was equipped with a PU-2089 Plus and FP-2020 Plus set at λex = 470 nm and λem = 530 nm. A 50 x 4.6 YMC-Pack Diol-120-NP column (5-µm particle size) was used with mobile phase (IPA/hexane/water) at a flow rate of 1.0 mL/min

^{1}H and ^{13}C NMR of ginkgolic acid (15:1) **1**

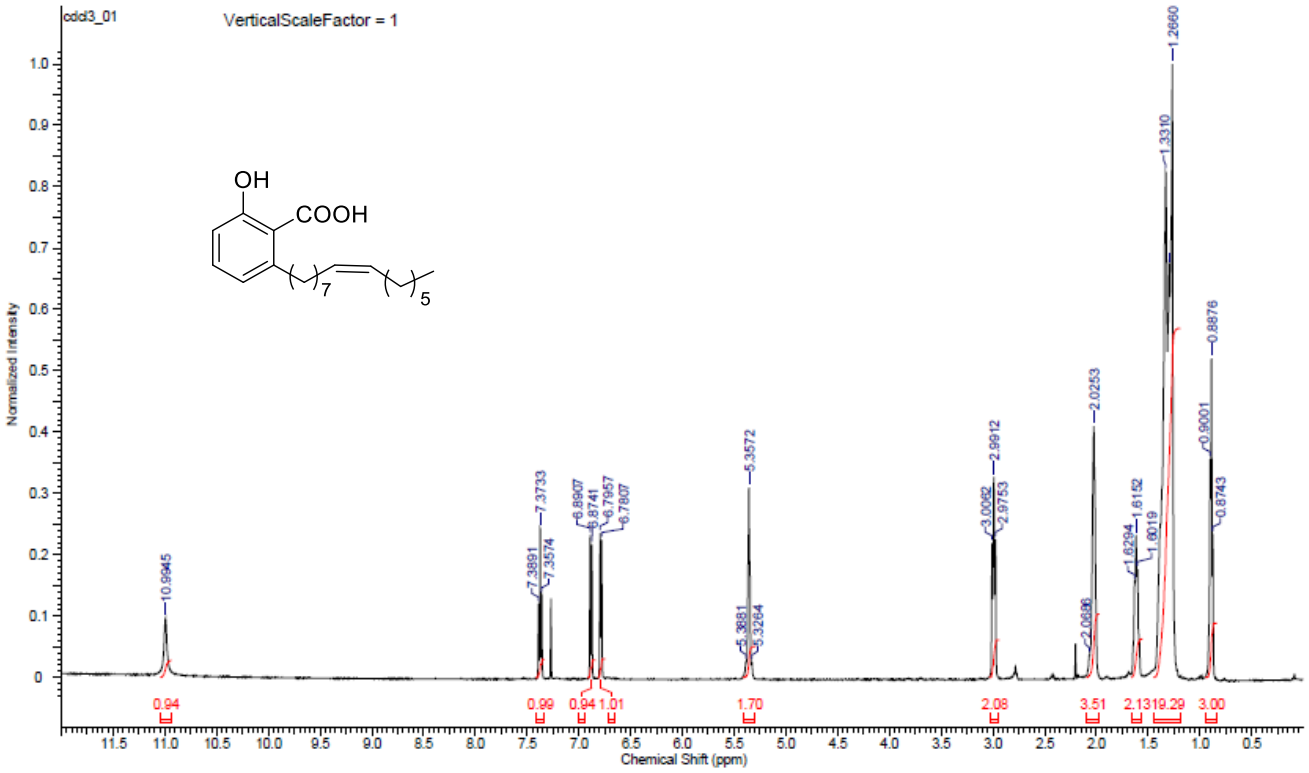

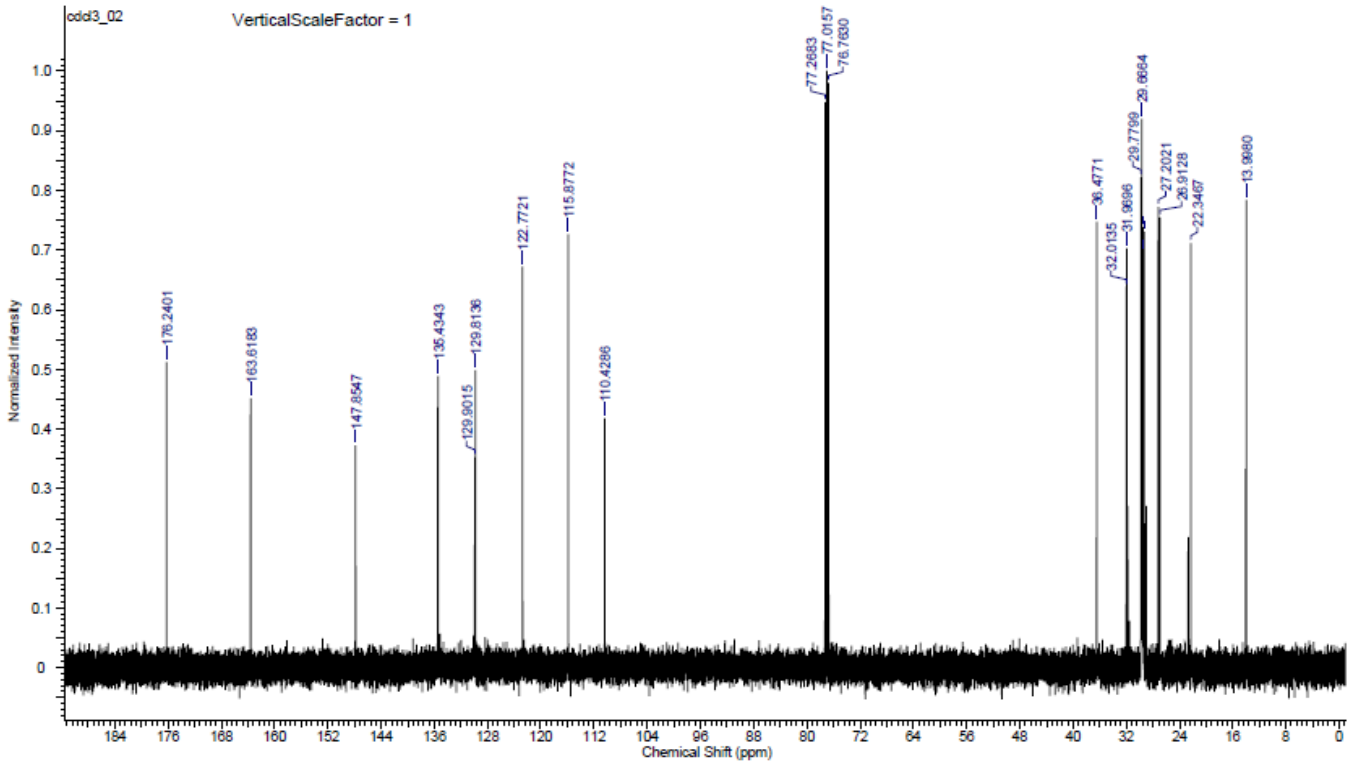

^{1}H and ^{13}C NMR of ginkgolic acid (15:0) **2**

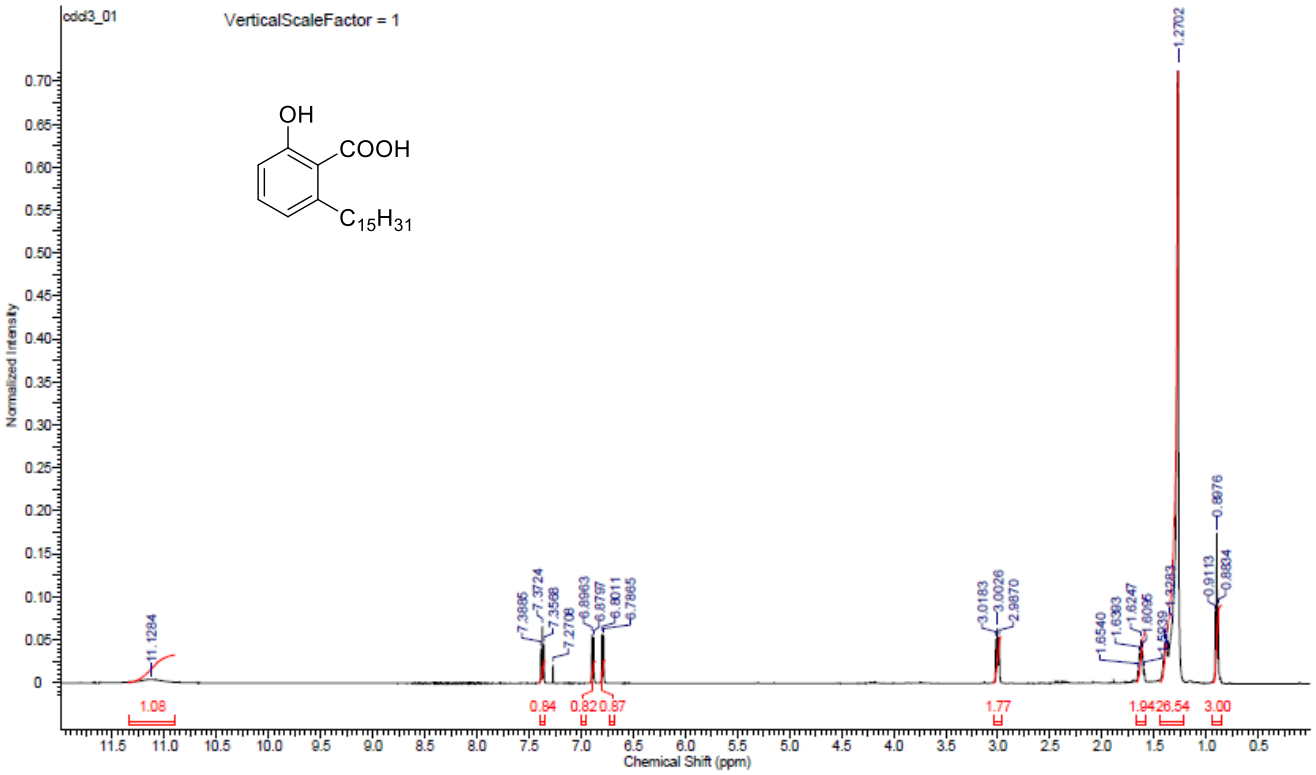

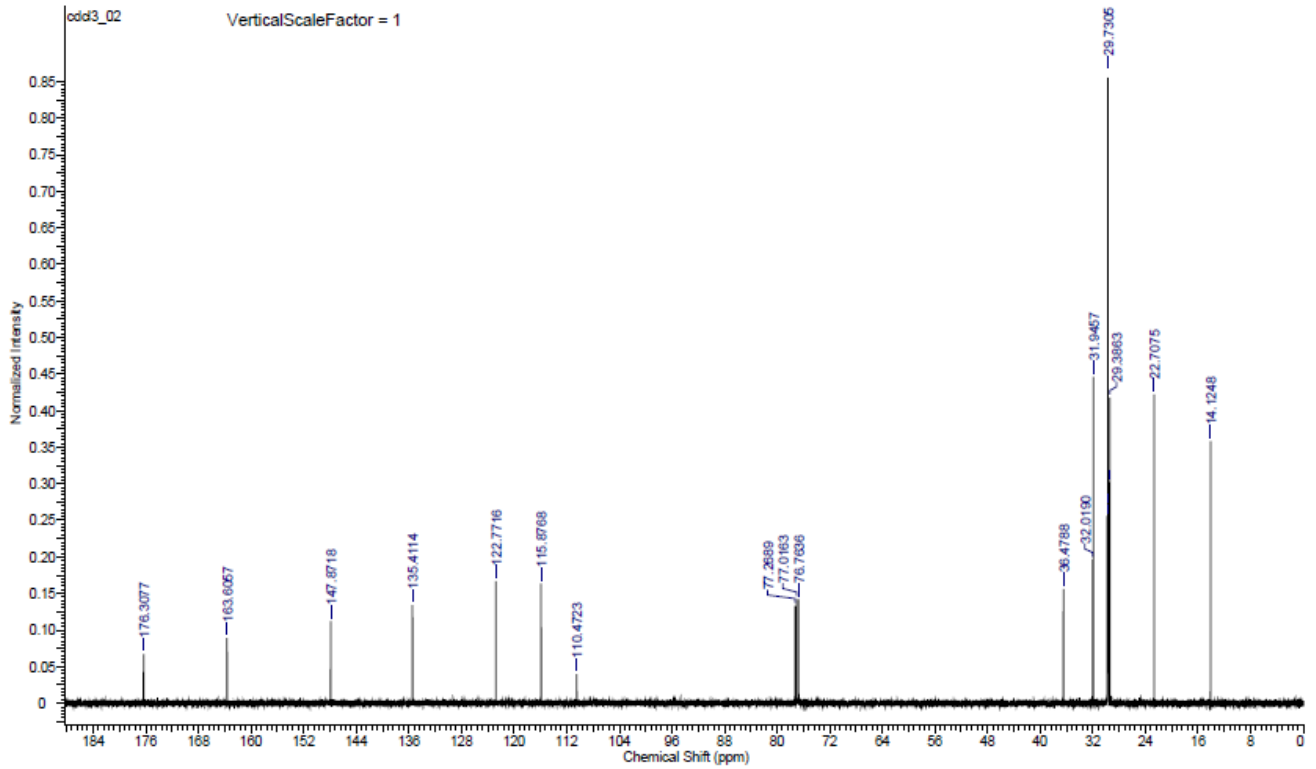

^{1}H and ^{13}C NMR of **13**

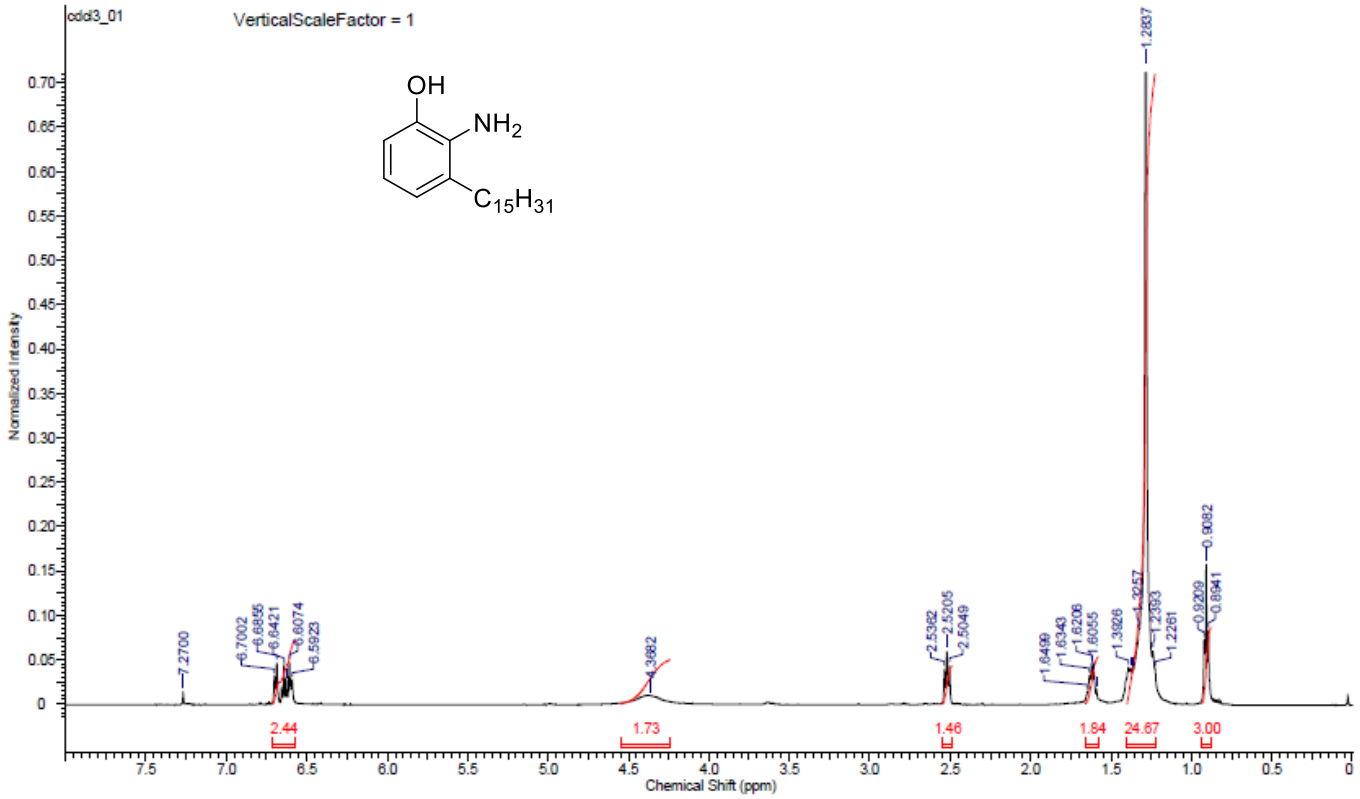

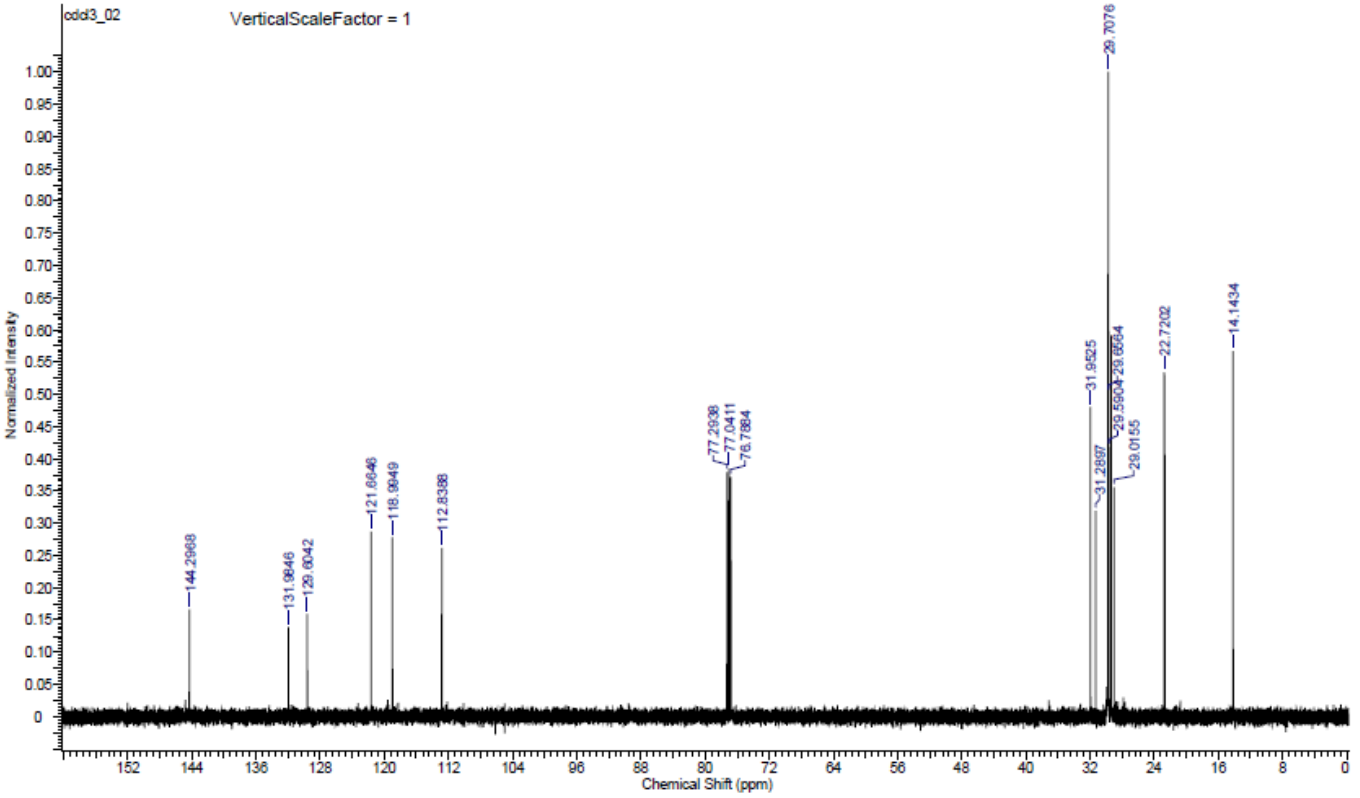

^{1}H NMR of **17b and 17d**

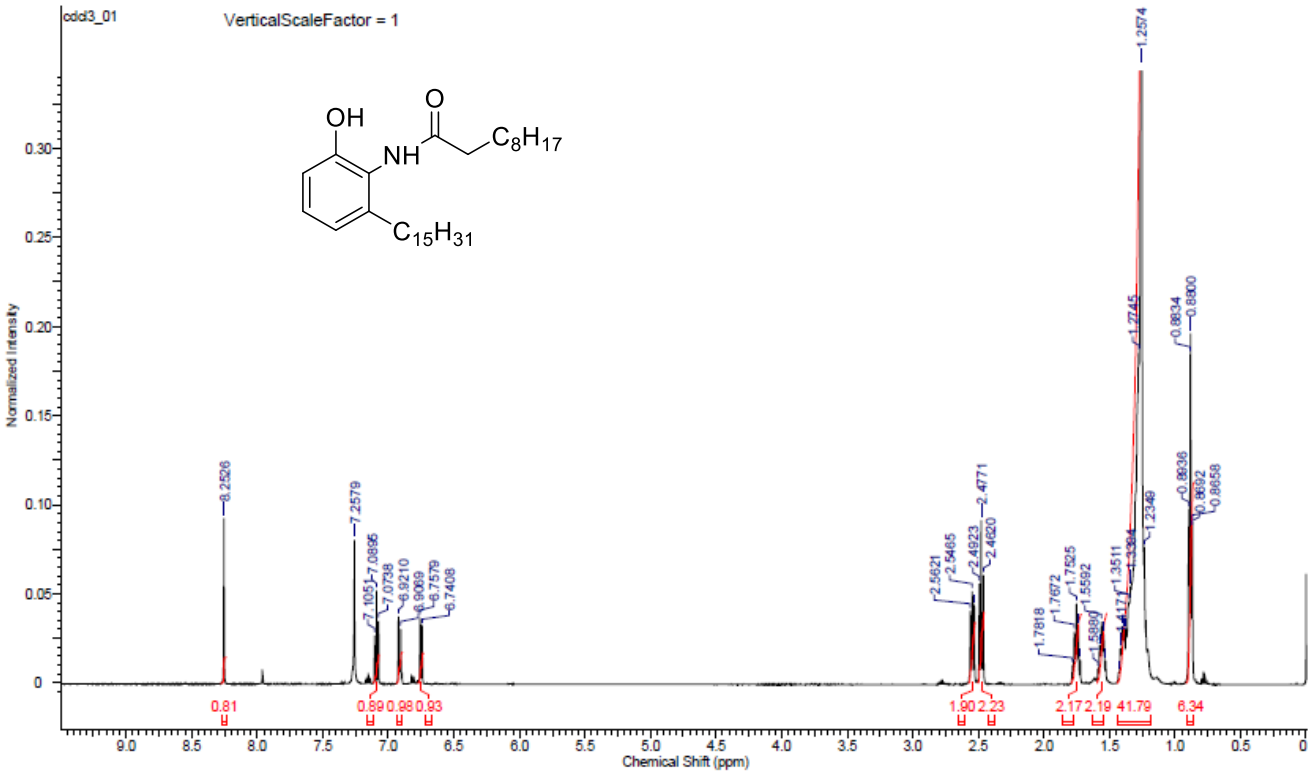

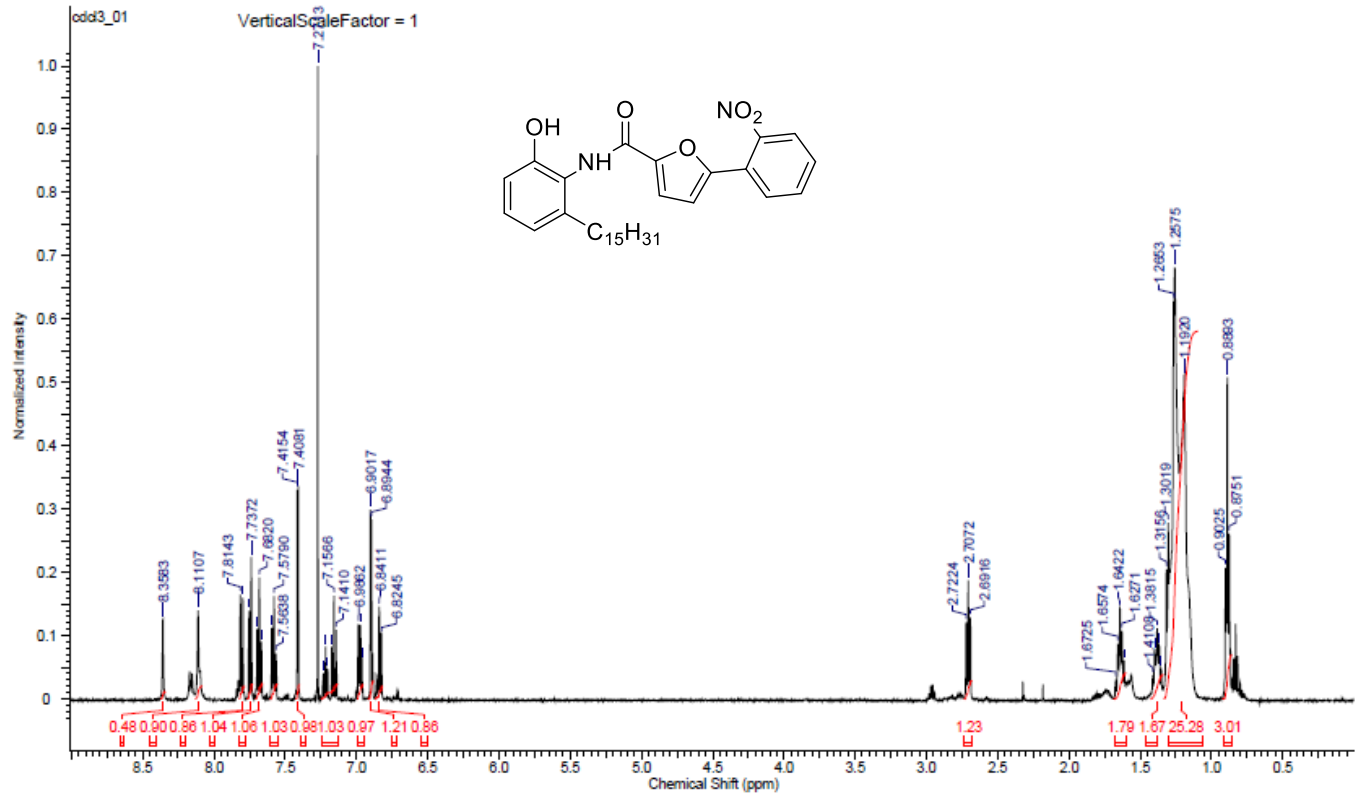

^{1}H NMR of **17f and 17h**

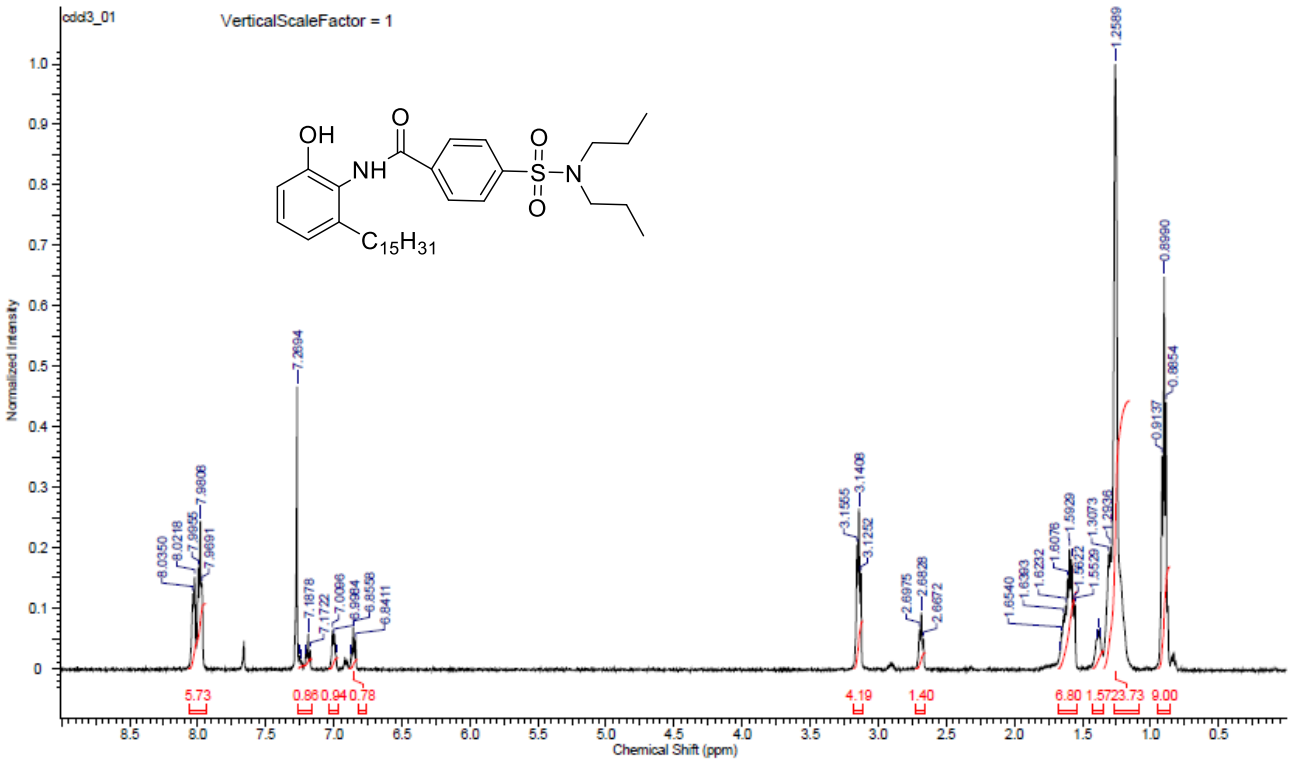

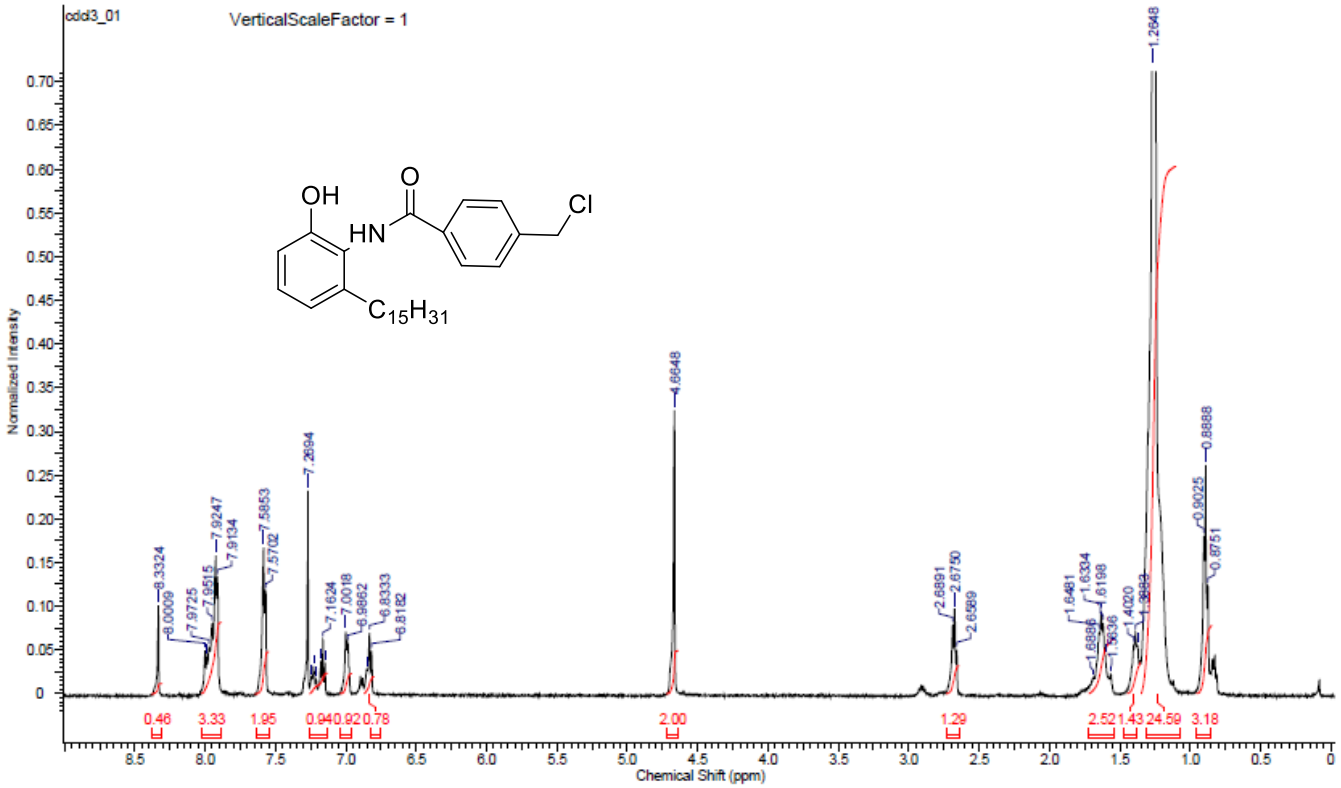

^{1}H and NMR of **17j**

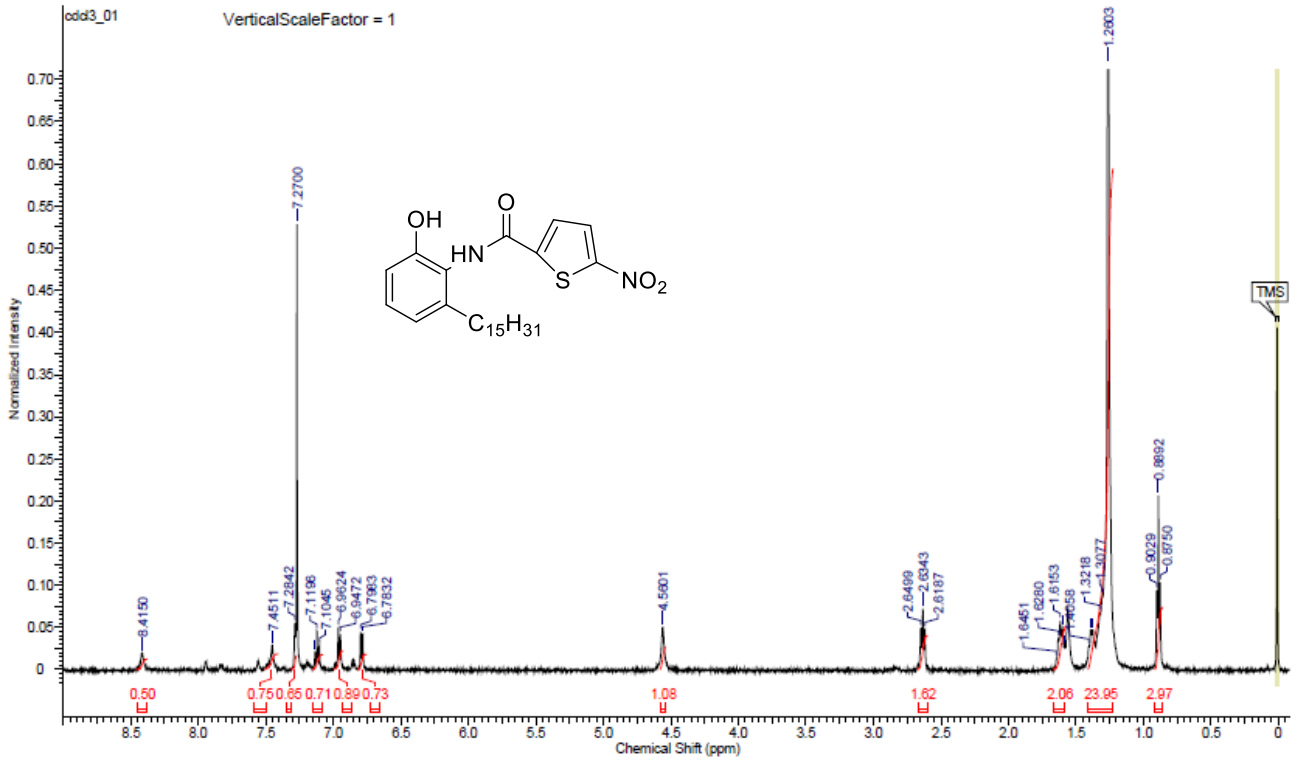

^{1}H and ^{13}C NMR of **18**

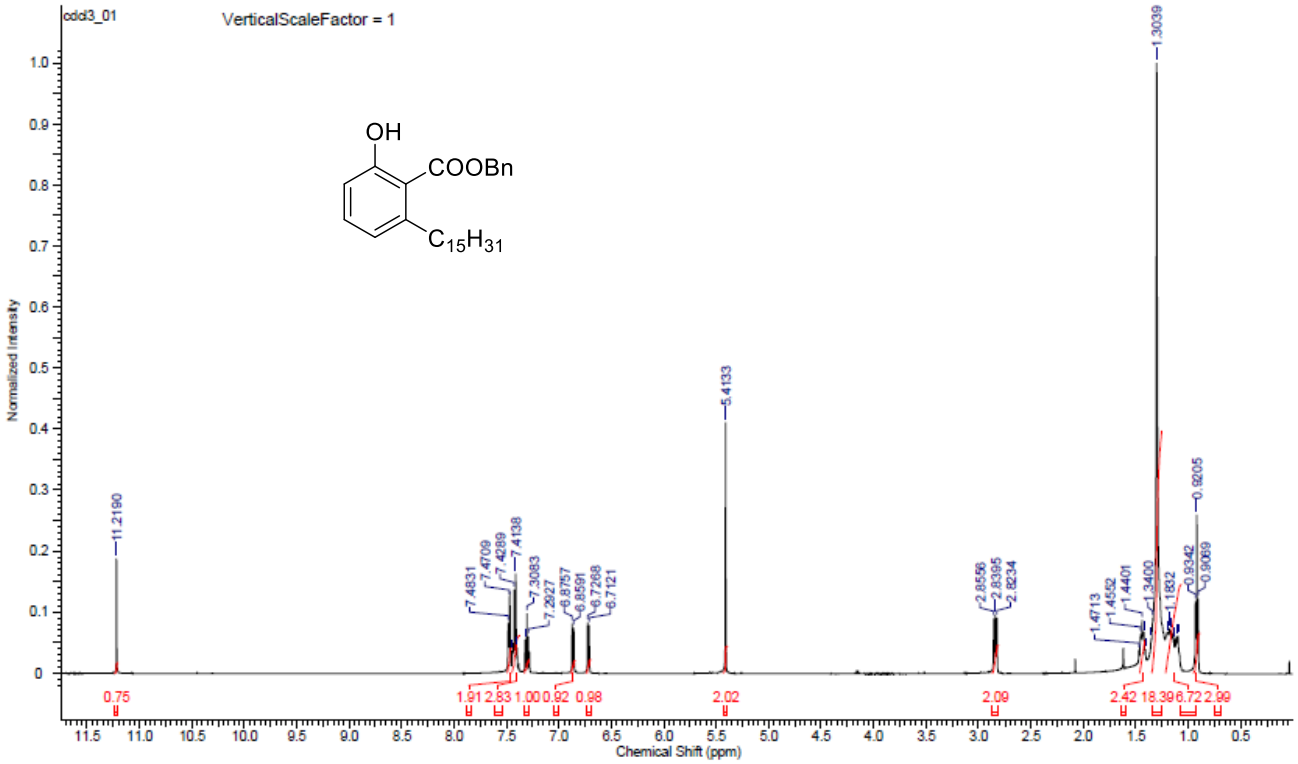

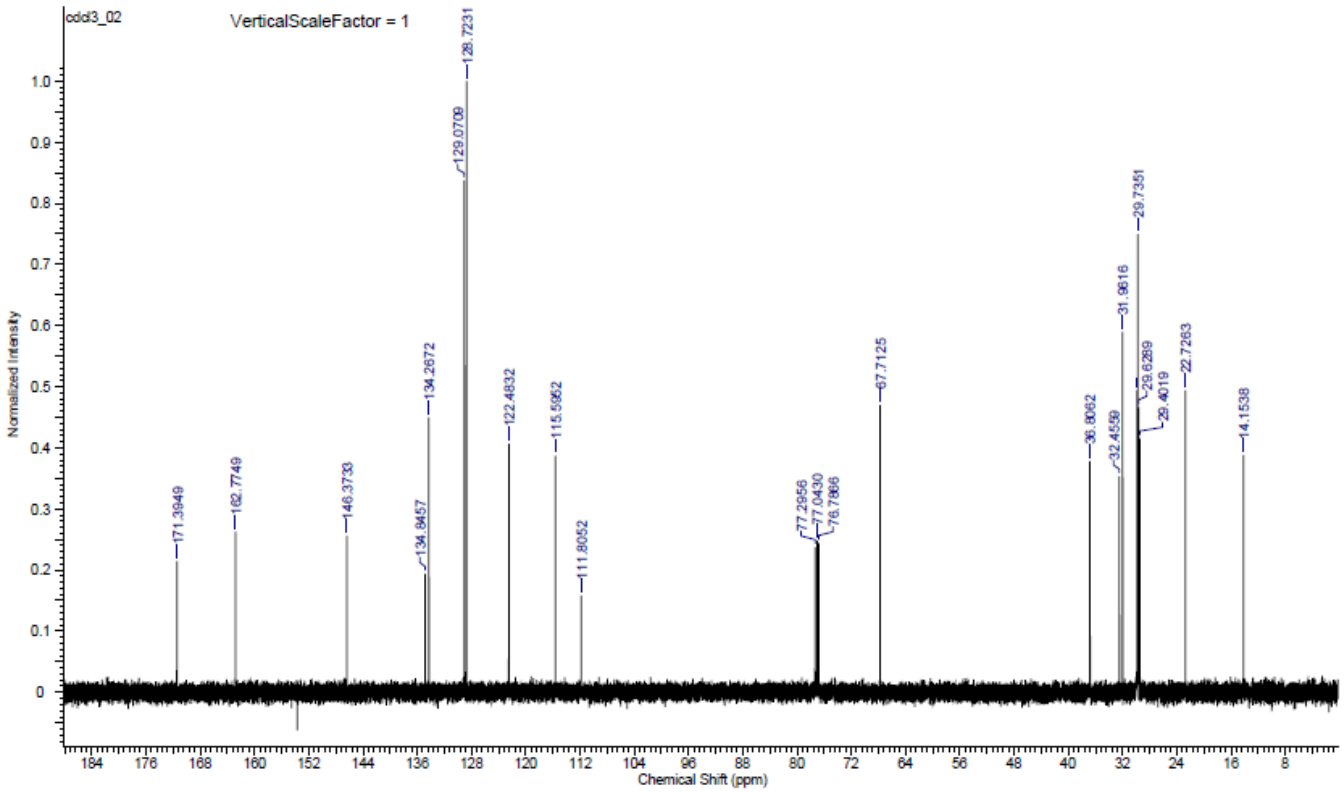

^{1}H and ^{13}C NMR of **19**

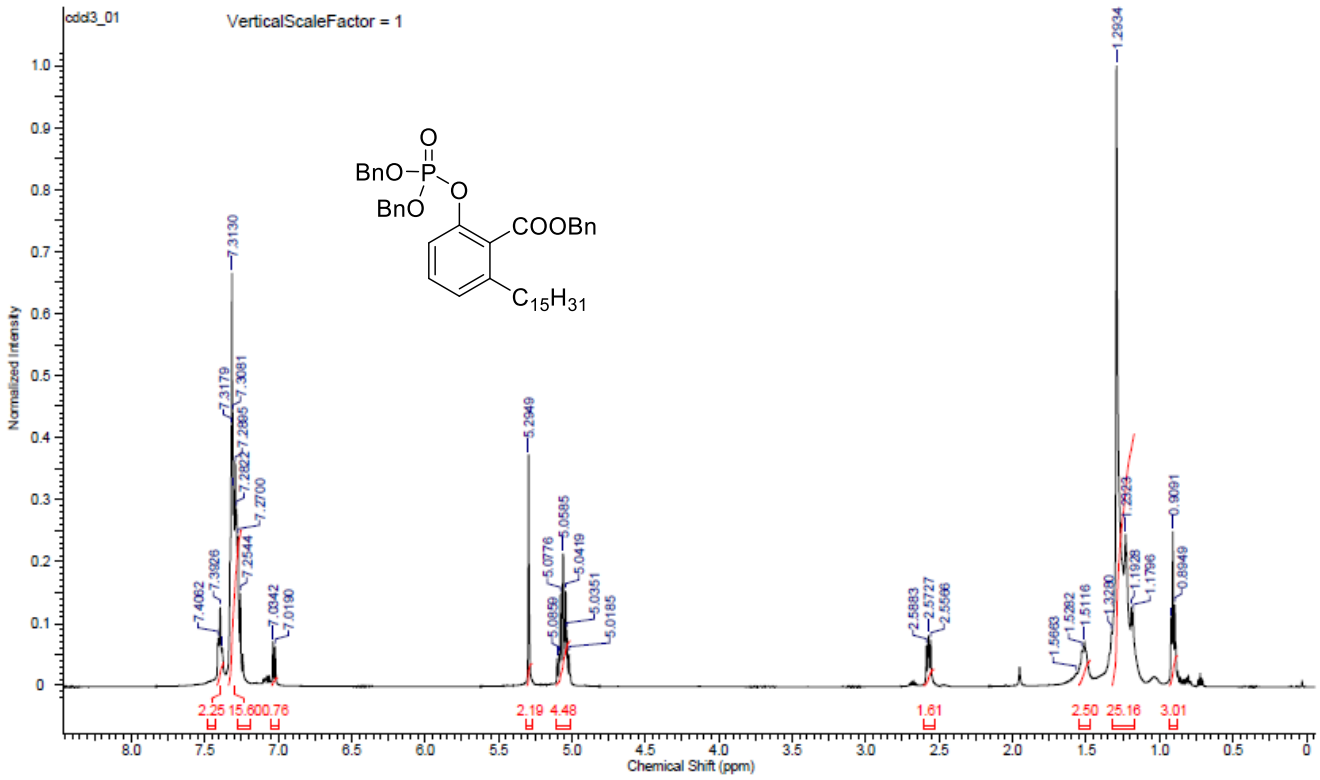

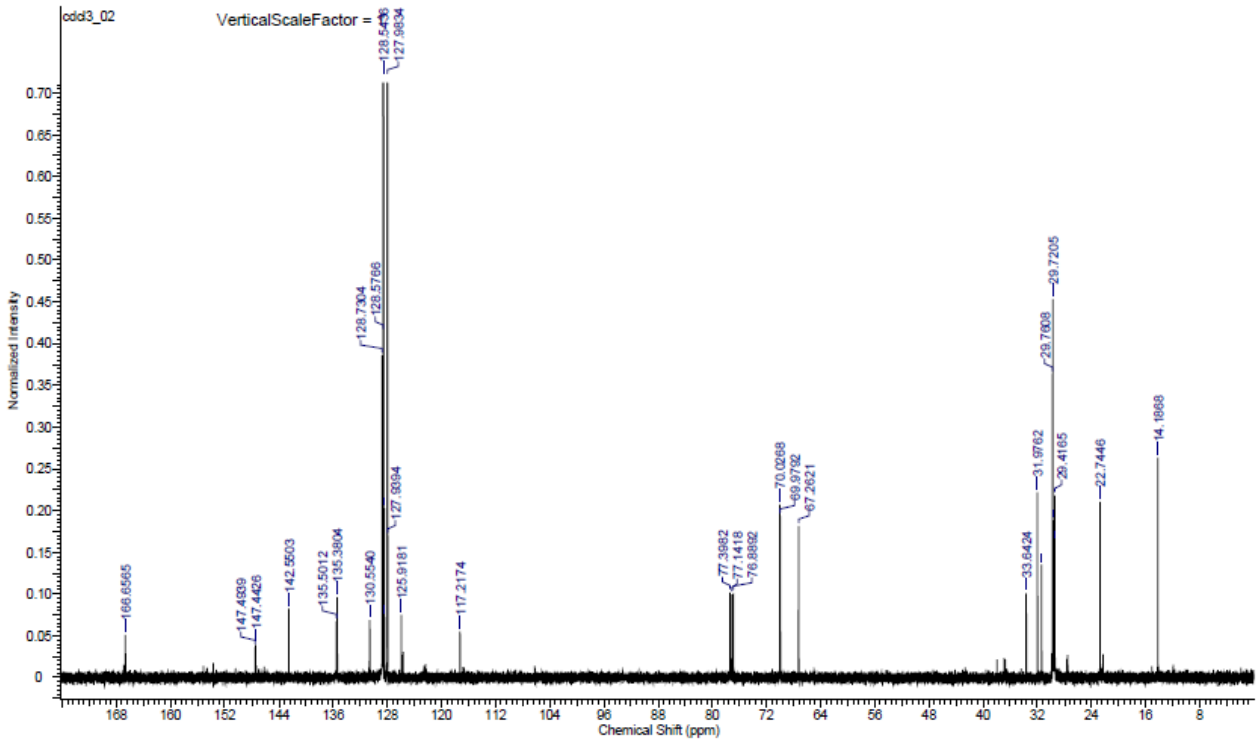

^{1}H NMR of **20**

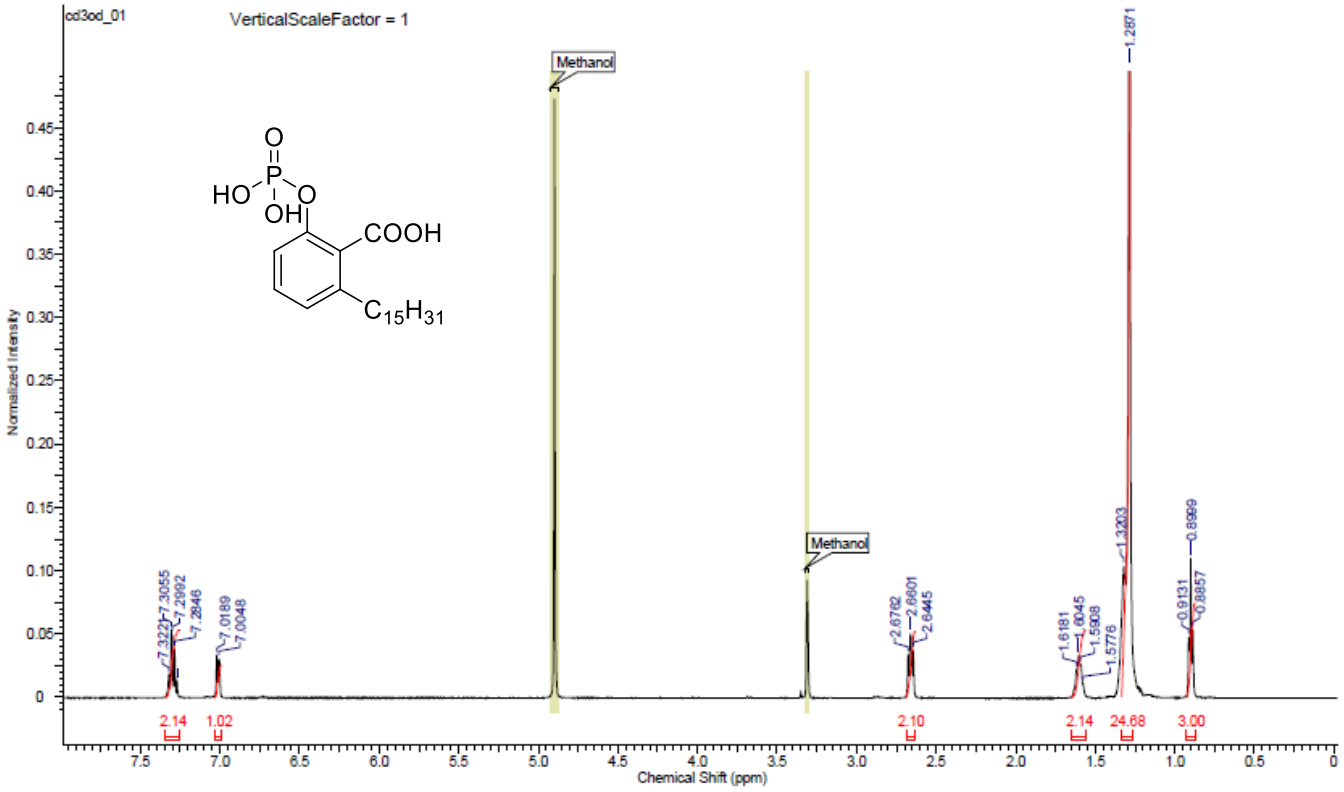
cd3od_01
VerticalScaleFactor = 1
Methanol
Methanol
HO
O
P
O
OH
COOH
$C_{15}H_{31}$
Normalized Intensity
Chemical Shift (ppm)
7.3221
7.3055
7.2992
7.2846
7.0189
7.0048
2.6762
2.6601
2.6445
1.6181
1.6045
1.5908
1.5776
1.3203
1.2871
0.9131
0.8999
0.8857
2.14
1.02
2.10
2.14
24.68
3.00

2.5 References

1) Y. A. Hannun and L. M. Obeid, ***Nature reviews***, 2008, 9, 139
2) F. G. Tafesse, P. Ternes and J. C. M. Holthuis, ***J. Biol. Chem***., 2003, 281, 29421
3) S. Mitsutake, K. Zama, H. Yokota, T. Yoshida, M. Tanaka, M. Mitsui, M. Ikawa, M. Okabe, Y. Tanaka, T. Yamashita, H. Takemoto, T. Okazaki, K. Watanabe and Y. Igarashi, ***J. Biol. Chem.***, 2011, 286, 28544
4) Z. Li, H. Zhang, J. Liu, C. Liang, Y. Li, G. Teitelman, T. Beyer, H. H. Bui, D. A. Peake, Y. Zhang, P. E. Sanders, M. Kuo, T. Park, G. Cao and X. Jiang, ***Mol. Cell. Biol.***, 2001, 21, 4205
5) Z. Li, Y. Fan, J. Liu, C. Huan, H. H. Bui, M. Kuo, T. Park, G. Cao, X. Jiang, ***Arterioscler. Thromb. Vasc. Biol.***, 2012, 32, 1577
6) J. T. Hsiao, Y. Fu, A. Hill, G. M. Halliday and W. S. Kim, ***PLOS ONE***, 8, e74016
7) Y. Hayashi, Y. Nemoto-Sasaki, T. Tanikawa, S.Oka, K. Tsuchiya, K. Zama, S. Mitsutake, T. Sugiura, and A. Yamashita, ***J. Biol. Chem.***, 2014, 289, 30842
8) T. Ohnishi, C. Hashizume, M. Taniguchi, H. Furumoto, J. Han, R. Gao, S. Kinami, T. Kosaka and T. Okazaki, ***The FASEB Journal,*** 2017, 31, 3816
9) C. Luberto and Y. A. Hannun, ***J. Biol. Chem.***, 1998, 273, 14550
10) G. Sauer, E. Amtmann, K. Melber, A. Knapp, K. Muller, K. Hummel and A. Scherm, ***Proc. Natl. Acad. Sci.***, 1984, 81, 3263
11) K. Muller-Decker, ***BBRC***, 1989, 162, 198
12) X. Deng, F. Lin, Y. Zhang, Y. Li, L. Zhou, B. Lou, Y. Li, J. Dong, T. Ding, X. Jiang, R. Wang, D. Yea, ***Eur. J. Med. Chem.***, 2014, 73, 1
13) R. Adachi, K. Ogawa, S. Matsumoto, T. Satou, Y. Tanaka, J. Sakamoto, T. Nakahata, R. Okamoto, M. Kamaura, T. Kawamoto ***Eur. J. Med. Chem.***, 2017, 136, 283.
14) D. J. Newman, G. M. Cragg, and K. M. Snader, ***J. Nat. Prod.,*** 2003, 66, 1022
15) G. M. Cragg, D. J. Newman and K. M. Snader, ***J. Nat. Prod.***, 1997, 60, 52
16) W. Zheng, X. Li, L. Zhang, Y. Zhang, X. Lu and J. Tian, ***Proteomics,*** 2015, ***15***, 1868
17) Y. Fu, S. Hong, D. Li, and S. Liu, ***J. Agric. Food Chem.***, 2013, 61, 5347
18) I. Fukuda, A. Ito, G. Hirai, S. Nishimura, H. Kawasaki, H. Saitoh, K. Kimura, M. Sodeoka and M. Yoshida, ***Chem. Biol.***, 16, 133

19) S. H. Baek, J. Ko, J. H. Lee, C. Kim, H. Lee, D. Nam, J. LEE, S. Lee, W. M. Yang, J. Um, G. Sethi, and K. S. Ahn, ***J. Cell. Physiol.,*** 2017, 232, 346

20) D. Mango, F. Weisz and R. Nisticò, ***Front. Pharmacol.***, 2016, 7, 401

21) S. H. Baek, J. Ko, J. H. Lee, C. Kim, H. Lee, D. Nam, J. LEE, S. Lee, W. M. Yang, J. Um, G. Sethi, and K. S. Ahn ***J. Cell. Physiol.,*** 2017, 232, 346

22) Y. Yahagiwa, K. Oiiaski, Y. Sakamoto, S. Hirakawa and T. Kamikawa, ***Tetrahedron***, 1987, **43**, 3387

23) M. Satoh, N. Takeuchi, T. Nishimura, T. Ohta and S. Tobinaga, ***Chem. Pharm. Bull.***, 2001, **49**, 18

24) I. R. Green and F. E. Tocoli, ***Synth. Communications***, 2002, 32, 947

25) J. S. Yadav, A. K. Mishra, S. S. Dachavaram, S. G. Kumar, S. Das, ***Tetrahedron. Lett.***, 2014, 55, 2921

26) T. Maegawa, Y. Koutani, K. Otake and H. Fujioka, ***J. Org. Chem.***, 2013, 78, 3384

27) S. Park and D. Im, ***Biomol. Ther.***, 2017, 25, 80

28) A. Kihara, S. Mitsutake, Y. Mizutani, Y. Igarashi, ***Prog. Lipid Res.***, 2007, 46, 126

29) A. Billich, F. Bornancin, P. De´vay, D. Mechtcheriakova, N. Urtz, and T. Baumruker, ***J. Biol. Chem.***, 2003, 278, 47408

30) V. Brinkmann, J. G. Cyster and T. Hla ***Am. J. Transplant.***, 2004, 4, 1019

31) A. Billich, F. Bornancin, P. De´vay, D. Mechtcheriakova, N. Urtz, and T. Baumruker ***J. Biol. Chem.***, 2003, 278, 47408

32) M. A. Hanson, C. B. Roth, E. Jo, M. T. Griffith, F. L. Scott, G. Reinhart, H. Desale, B. Clemons, S. M. Cahalan, S. C. Schuerer, M. G. Sanna, G. W. Han, P. Kuhn, H. Rosen, R. C. Stevens, ***Science,*** 2012, 335, 851

33) Y. Ohno, A. Ito, R. Ogata, Y. Hiraga, Y. Igarashi and A. Kihara, ***Genes Cells***, 2009, 14, 911

34) M. Graber, W. Janczyk, B. Sperl, N. Elumalai, C. Kozany, F. Hausch, T. A. Holak, and T. Berg, ***ACS Chem. Biol***., 2011, 6, 1008

35) G. M. Morris, R. Huey, W. Lindstrom, M. F. Sanner, R. K. Belew, D. S. Goodsell, A. J. Olson, ***J. Comput. Chem.***, 2009, 16, 2785

36) P. D. Adams, P. V. Afonine, G. Bunkóczi, V. B. Chen, I. W. Davis, N. Echols, J. J. Headd, L.-W. Hung, G. J. Kapral, R. W. Grosse-Kunstleve, A. J. McCoy, N. W. Moriarty, R.

Oeffner, R. J. Read, D. C. Richardson, J. S. Richardson, T. C. Terwilliger and P. H. Zwart, ***Acta Cryst.,*** 2010, D66, 213

37) O. Trott and A. J. Olson, ***J. Comput. Chem.***, 2010, 31, 455

Chapter-3

Daurichromenic acid, a novel SMS inhibitor: stereochemical studies of rhododaurichromanic acid A and Hongoquercin A

3.1 Abstract

Sphingomyelin synthase (SMS) is an important enzyme to biosynthesize sphingomyelin that regulates membrane fluidity and microdomain structure. SMS plays crucial roles in mediating metabolic syndrome, Alzheimer's disease and tumorigenesis. In search of identifying a new scaffold as SMS inhibitor, we screened a library of medicinal plants. As a result we could obtain daurichromenic acid (DA) as a potent inhibitor of SMS. Structural activity relationship validation of DA helped us to understand the role of functional group against SMS activity. Herein we report Hongoquercin A as another natural product as potent SMS inhibitor obtained by SAR studies of DA. DA is a flexible natural product with long hydrophobic chain so, it is difficult to use for circular dichroism calculations (CD) because of large number of low-energy conformers and ambiguous Boltzmann distributions. Here we report, through electronic circular dichroism (ECD) and vibrational circular dichroism (VCD) spectroscopic studies on DA, we demonstrate that derivatization of a flexible molecule can dramatically reduce its flexibility and we were able to assign absolute configuration of unnatural hongoquercin A. This work also shows the usefulness of derivatization for diminishing computational expense required for optimization and CD calculation and for increasing the reliability of the assignment of absolute configuration. On the other hand we derivatized DA in to a less flexible rhododaurichromanic acid A derivative to elucidate its absolute configuration by CD method.

3.2 Introduction

SMS enzyme catalyzes the conversion of ceramide and phosphatidylcholine to sphingimyelin (SM) and diacylglycerol. Ceramide and SM are emerged has key components of cell membrane, regulate diverse cell functions such as cell adhesion, migration, cell growth, inflammation and angiogenesis.[1] The SMS isoforms SMS1 and SMS2 are localized Golgi apparatus and plasma membrane respectively. Both SMS1 and SMS2 activity are involved in atherosclerosis,[2] but SMS2 alone is involved in obesity mediated metabolic disorders,[3] Alzheimer's disease[4,5] and also colon cancer.[6] Thus, SMS1 and SMS2 are expected to be potential target for the treatment of many diseases. To understand SMS biology in disease condition we need potent and selective SMS inhibitors. Natural products have been emerging as source of potential drug candidates since few decades.[7] However, the inhibitor of SMS from natural resources has not been discovered at all. Identification of inhibitors from natural resources to target molecules involved in human diseases is a big and attractive challenge in the field of chemical biology, because natural products have been had good track record in application of drug discovery.[8] Here, we describe the identification of natural inhibitor daurichromenic acid (DA) and confirmation of structure-activity relationship (SAR) study toward SMS.

On the other hand, we have thought to explore the usefulness of derivatization (cyclization) to reduce the flexible molecule. The flexible (*S*)-(+)-daurichrmenic acid has been applied for CD studies to test the feasibility of the derivatization approach. By cyclization of (S)-(+)-DA to rigid hongoquercin A derivative, we demonstrated that the number of the possible stable conformers of a molecule can be reduced to less than 5% by using cyclization of a molecule and that can lead to reliable structural assignment. Rhododaurichromenic acid A is a potent anti-HIV component of *Rhododendron dauricum*.[9] Its synthetic information from DA using UV-light irradiation was described in several studies.[10,11] In 2006 Kurdyumov et al applied an unnatural cationic [2+2] cycloaddition reaction and synthesized a racemic micture of its 15,16-dihydro-16-(2,2,2-trifluoroacetoxy)methyl ester derivative[12] from racemic mixture of DA obtained by synthesis. Herein, we report a modified synthesis of rhododaurichromenic acid A derivative from natural DA and its stereochemistry, 2*S*,3*S*,4*S*,11*R*,12*S*, elucidated by VCD and ECD studies aided by DFT calculations.

3.3 Result and discussion

Isolation of daurichromenic acid (DA) from Rhododendron dauricum: Leaves of Rhododendron dauricum was collected from Hokkaido, Japan were dried and powdered well (81 g). The dried powder was extracted with methanol (400 mL x 3) at room temperature three times after 24 hours each. The combined MeOH extract was concentrated under reduced pressure to give a black residue (24.2 g), which was dissolved in 20% MeOH in water (500 mL) and partitioned with hexane (200 mL x 3) Et2O (200 mL x 3) and EtOAc (200 mL x 3). After removal of solvent by evaporation, the hexane, Et2O, EtOAc and water residues were used for SMS assay. We found that hexane fraction was active than Et_2O fraction but, EtOAc and water fractions turned out to be inactive. The active Hexane fraction (3.8 g) was further fractionated and sub-fractionated by silica gel column chromatography guided by bio-assay. The active component was identified as daurichromenic acid, which was confirmed by ^{1}H, ^{13}C NMR and ESI-MS. Yield: 1.53% (1.24 g).

SAR studies of DA

After obtaining DA **1** as potent inhibitor of SMS by screening library of medicinal plants, SAR study was applied to identify the role of carboxylic acid and hydroxyl group towards SMS activity (**Figure-1**). Compound **2** was synthesized by methylating reagent TMS-CH_2N_2, which was turned out to be inactive derivative of DA. It gave a hint that carboxylic acid functional group is very important for SMS inhibition. To further confirm its role compounds **3** and **4** were synthesized, as we expected compound **4** with free carboxylic acid group turned out to be an inhibitor of SMS

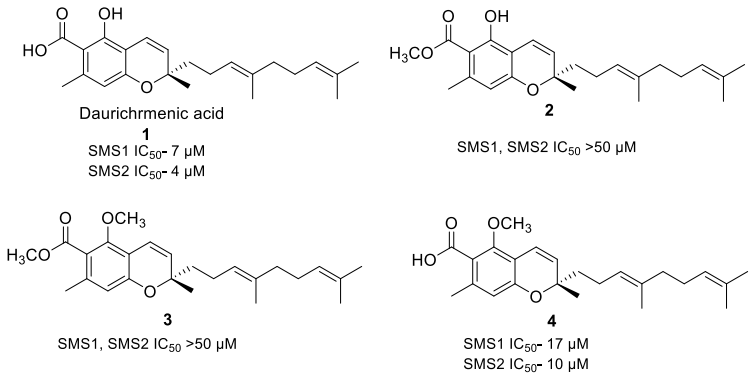

Figure-1: SAR studies of daurichromenic acid and SMS inhibition IC_{50} values

Synthesis of unnatural hongoquercin A

Kurdyumov *et al.* synthesized Hongoquercin A by divergent total synthesis. Hongoquercin A was isolated from an unidentified terrestrial fungus[13] and exhibits antibacterial properties toward methicillin-resistant *Staphylococcus aureus* and vancomycin-resistant *Enterococcus faecium*.[14,15] When we performed Lewis acid catalyzed cycloaddition of DA, reaction didn't proceed might be due to electron withdrawing effect of carboxylic acid group. We synthesized methyl ester of DA to perform cycloaddition reaction, as a result we could synthesize compound **3** from **2** by cycloaddition reaction using $FeCl_3$. Finally, hydrolysis of 5 followed by Pd/C catalyzed reduction of olefin leads to obtain unnatural hongoquercin A. We performed SMS assay of all intermediates during Hongoquercin A synthesis, we obtained compound **6** and **7** as potent SMS inhibitors. Collectively, from SAR study of DA, we obtained compounds **1**, **4**, **6** and **7** as potent SMS inhibitors. In future these SMS inhibitors need to be explored in cell based assays and to address their efficacy in metabolic disorders and Alzheimer's disease.

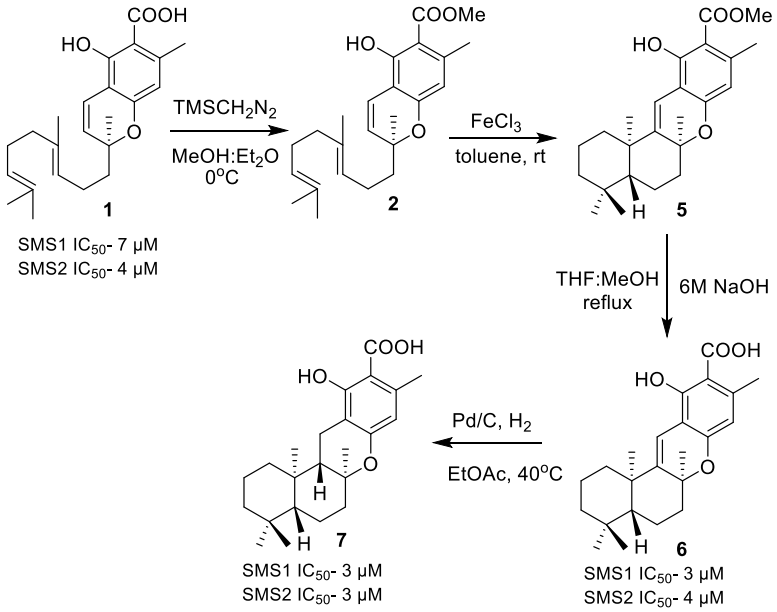

Scheme-1: synthesis of unnatural hongoquercin A from natural daurichromenic acid

ECD and VCD experiment and calculation of 5 and 6

Because of the same single or a few rather similar low energy conformers one would expect that the computed ECD and VCD spectra of **5** and **6** were also similar at all applied levels. Indeed, as shown in **Figure 3a**, ECD calculations for the DFT optimized CONFLEX conformer of (5*R*,8*S*,10*R*)-**5** reproduced the observed transitions well, except the differences around 280 nm and below 225 nm. A similar tendency was observed for the ECD curves of (5*R*,8*S*,10*R*)-**3** (**Figure 3b**). Overall agreement between the calculated and observed spectra of **5** and **6** revealed their absolute configurations. The same conclusion was obtained with confidence for the optimized structures generated by SPARTAN. Meanwhile, VCD calculations of the optimized CONFLEX conformer of (5*R*,8*S*,10*R*)-**2** also reproduced its major transitions with subtle wavenumber shifts above 1300 cm^{-1} at all applied levels (**Figure 3c**). Representative transitions were ascribed as follows: skeletal vibrations (~975 cm^{-1}), CH/CH_2 bendings (~1275 cm^{-1}), and CH_2 bending coupled with aromatic/ester vibrations (~1300 cm^{-1}). VCD calculations of the optimized SPARTAN conformers also well predicted the experimental spectrum. These results clearly showed that VCD calculation of **5** could also elucidate its absolute configuration with high confidence while minimizing computational cost. Our attempt to calculate the VCD spectrum of (5*R*,8*S*,10*R*)-**6** was not as successful as the case for **5**, probably because of intermolecular interactions of **6** due to its carboxylic acid moiety, which could not be taken into account in computation (50 chirality). Our study has verified the reported absolute configuration of(+)-1 as S through the assignment of the absolute configuration of (–)-**5** as 5R,8S,10R with minimized computational cost and high reliability.[9,12] In the only reference on 12, Kurdyumov and Hsung synthesized the 9,15-saturated derivative of **6**, hongoquercin A, as an enantiopure form. Our current study verified the assumption that naturally occurring (5*S*,8*R*,9*R*,10*S*)-(+)-hongoquercin A is not synthesized from (*S*)-(+)-**1** but from (*R*)-(–)-**1**, which has not been found in nature.

This kind of derivatization may be applied to test the correctness of some of the recently reported studies with truncation of unsaturated side-chains,[16] but more importantly it can facilitate elucidation of the absolute configuration of some derivatives not possible with regular methods. Lastly, it is worthwhile mentioning that **1** is a liquid sample while **5** and **6** are solid samples. This kind of derivatization may afford crystalline materials applicable for solid-state ECD and VCD studies.

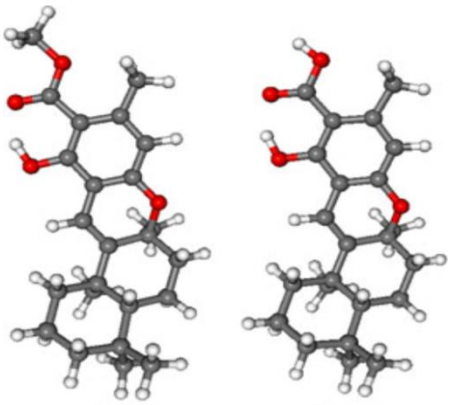

Figure-2: The lowest-energy conformers of (5*R*,8*S*,10*R*)-**2** and (5*R*,8*S*,10*R*)-**3** obtained by optimization of the MMFF94S (CONFLEX) conformers at all applied levels of theory.

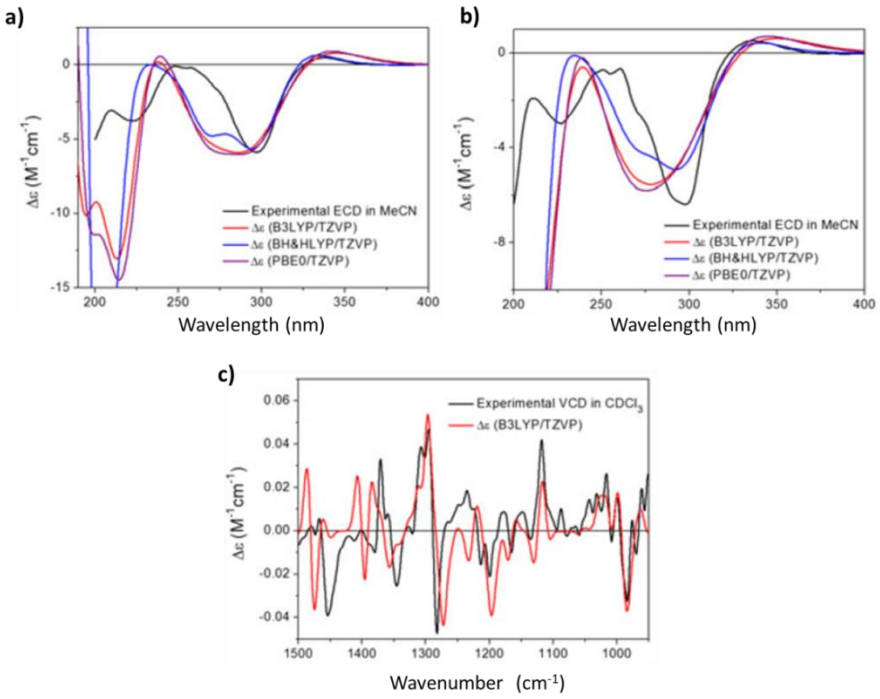

Figure-3: Experimental and calculated ECD spectra of (**a**) (5*R*,8*S*,10*R*)-**5** and (**b**) (5*R*,8*S*,10*R*)-**6** at various levels with PCM for MeCN computed for the lowest-energy B3LYP/TZVP level PCM/MeCN optimized conformer. Experimental and calculated VCD OF (**c**) (5*R*,8*S*,10*R*)-**5** at the B3LYP/TZVP level gas phase.

Synthesis of rhododaurichromenic acid A derivative

$FeCl_3$ catalyzed cycloaddition of **2** gives only compound **5** but trifluoroacetic acid (TFA) mediated reaction of **2** gives mixture of **5** and 2+2 cycloaddition product **8 (Scheme-2**). The modified synthesis of rhododaurichromenic acid A derivative from natural DA and its stereochemistry, 2*S*,3*S*,4*S*,11*R*,12*S*, elucidated by VCD and ECD studies aided by DFT calculations.

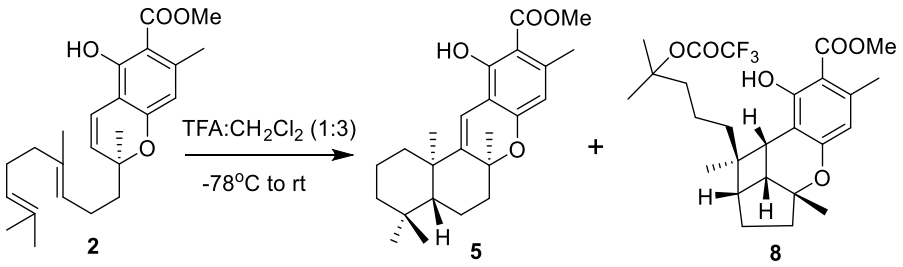

Scheme-2: synthesis of hongoquercin A derivative and rhododaurichromenic acid A derivative from natural DA

Although the relative configuration of **8** was elucidated by X-ray crystallography, conformational analysis, VCD and ECD calculations of **8** were performed on the arbitrarily chosen 2*S*,3*S*,4*S*,11*R*,12*S* enantiomer in order to determine its absolute configuration. The MMFF conformational search yielded 59 conformers in a 21 kJ/mol energy window, the B3LYP/6-31G(d) in vacuo reoptimization of which resulted in 13 low-energy (≥2%) conformers (**Figure 4**). These conformers differed in the orientation of the C-12 side-chain. The Boltzmann-averaged VCD spectrum (**Figure 5**) calculated for these structures at the B3LYP/TZVP level reproduced all the main transitions suggesting a 2S,3S,4S,11R,12S absolute configuration.[17] ECD calculations for the same conformers at various levels (B3LYP/TZVP, BH&HLYP/TZVP and PBE0/TZVP) gave good agreement with the experimental spectrum verifying the VCD results (**Figure 6**).

Because of the moderate flexibility of **3** another conformational search algorithm and program suite.[18] was also utilized for generating initial conformers.[19,20] Although CONFLEX found some new low-energy conformers, VCD and ECD data obtained in these calculations were in line with the herein presented results. In both ECD and VCD the orientation of the C-12 side chain has minor influence on the calculated spectra.

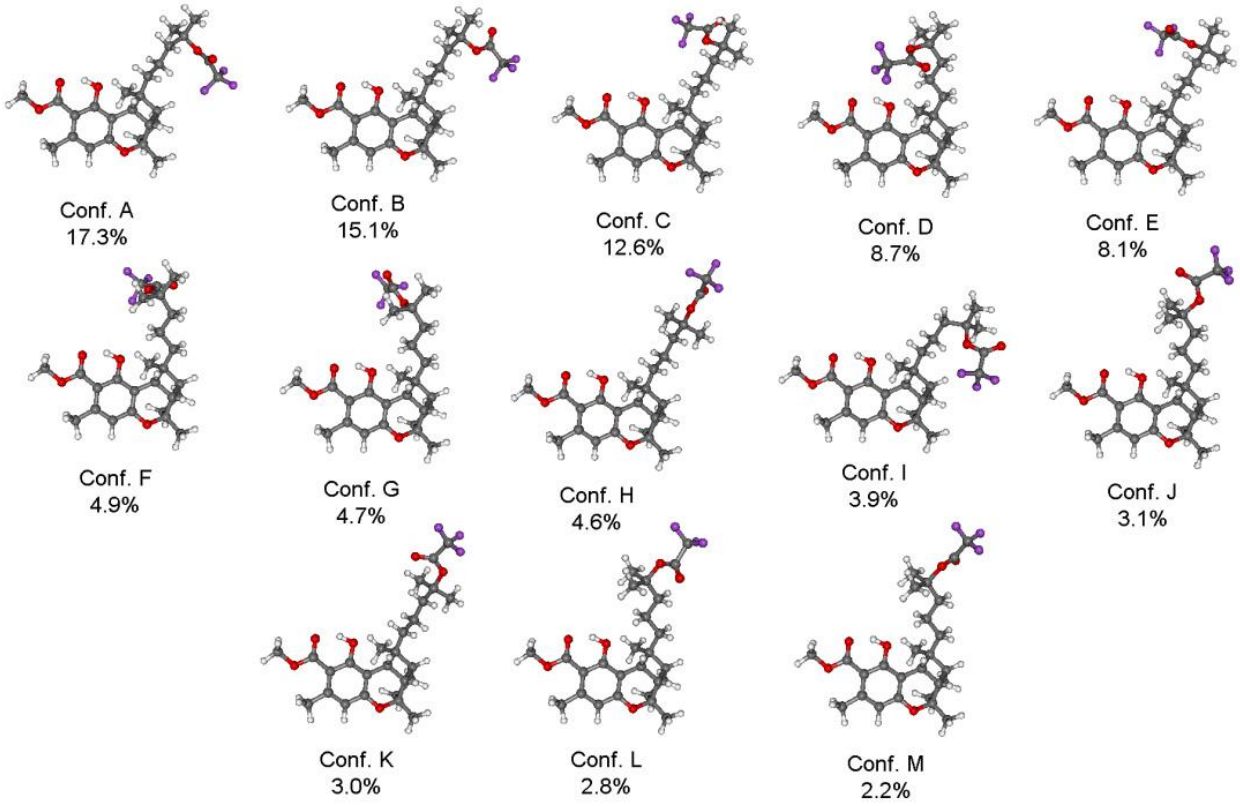

Figure-4: Low-energy conformers (≥2%) of (2*S*,3*S*,4*S*,11*R*,12*S*)-3 obtained by B3LYP/6-31G(d) *in vacuo* reoptimization of the MMFF geometries.

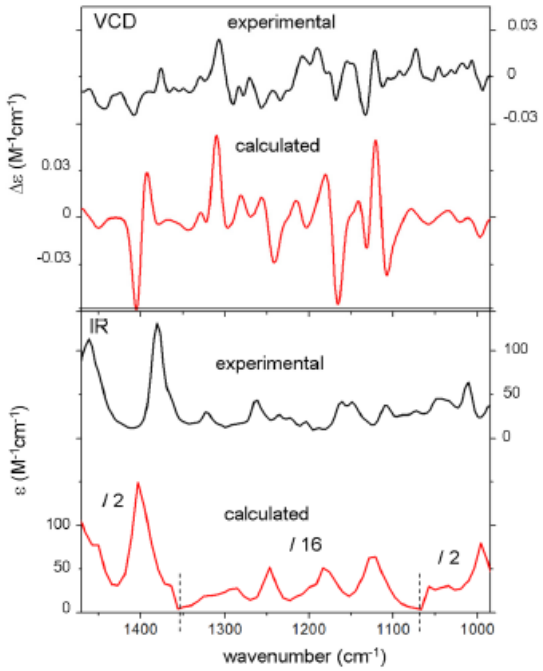

Figure-5: Experimental and calculated VCD and IR spectra of (2*S*,3*S*,4*S*,11*R*,12*S*)-**8** at the B3LYP/TZVP level gas-phase (Boltzmann-average of the B3LYP/6-31G(d) gasphase reoptimized low-energy MMFF conformers)

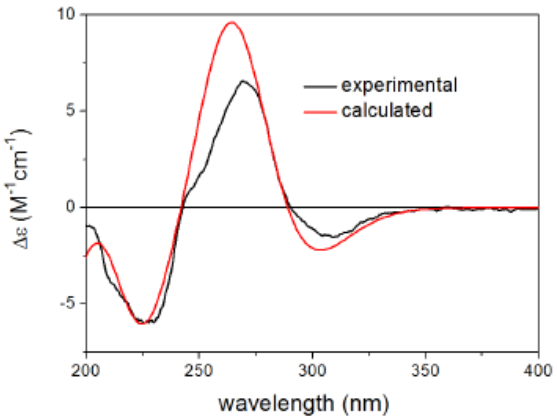

Figure-6: Experimental and calculated ECD spectra of (2*S*,3*S*,4*S*,11*R*,12*S*)-**8** at PBE0/TZVP level gas-phase (Boltzmann-average of the B3LYP/6-31G(d) gas-phase reoptimized low-energy MMFF conformers).

Conclusion

Medicinal plants library screening identified daurichromenic acid as a novel SMS inhibitor. Structural activity relationship studies of DA leads to synthesize unnatural hongoquercin A which turned out to be another novel SMS inhibitor, their efficacy *in vivo* need to be explored. We demonstrated how derivatization couldminimize computational time by lowering molecular flexibility and help elucidate molecular stereostructure. In this study, the conformational freedom of a flexible molecule was reduced to less than 5% upon cyclization. Furthermore, the parameter dependency of the ECD and VCD spectra of derivatized compounds was dramatically decreased, which makes the assignmentmore reliable. Although such a derivatization strategy may not be applicable to all molecules, discussion between organic and theoretical chemists should facilitate the determination of molecular stereostructure that could not otherwise be elucidated. On the other hand, the elucidated 2*S*,3*S*,4*S*,11*R*,12*S* absolute configuration of **8** synthesized from the methyl ester **2** of naturally occurring (+)-(*S*)-1 is in line with the proposed assumption of Kurdyumov et al., that from the unnatural (*R*)-daurichromenic ester (2*R*,3*R*,4*R*,11*S*,12*R*)-3 can be formed. This study is another possibility for reducing flexibility of daurichromenic acid. Despite the moderate flexibility of **3**, experimental spectra could be reproduced with confidence.

3.4 Experimental section

Methyl ester of daurichromenic acid (2)

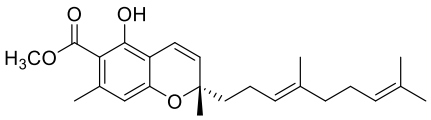

2

To a solution of Daurichromenic acid **1** (100 mg, 0.2699 mmol) in methanol (5 mL) and diethyl ether (5 mL) was added a solution of TMS-CH_2N_2 in hexane until the color of the solution became yellow at 0°C. The reaction mixture was stirred at same temperature for 0.5 h and at room temperature for 1 h. The reaction was quenched with acetic acid and concentrated under vacuum to afford a residue that was purified by silica gel column chromatography using hexane/ ethyl acetate (9.5:0.5) as an eluent to give the ester **2** with yield 97% **(**ref. ***Eur. J. Org. Chem.*** 2010, 1033–36).

Compound **2**; colorless oil; ^{1}H NMR ($CDCl_3$, 500 MHz) δ 11.97 (1H, s), 6.72 (1H, d, 10 Hz), 6.18 (1H, s), 5.47 (1H, d, J=10.2 Hz), 5.05-5.11 (2H, m), 3.91 (3H, s), 2.45 (3H, s), 1.93-2.10 (6H, m) 2.97-3.00, 1.57-1.76 (2H, m), 1.66 (3H, s), 1.56-1.58 (6H, 2s), 1.39 (3H, s).

Methyl(*S*,*E*)-2-(4,8-dimethylnona-3,7-dien-1-yl)-5-methoxy-2,7-dimethyl-2*H*-chromene-6 carboxylate (3)

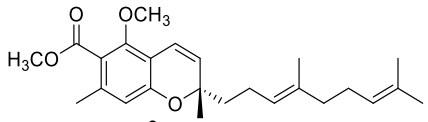

3

To a solution of **2** (59 mg, 0.16mmol) in DMF (3 mL) was added MeI (55 mg, 0.40 mmol) at room temperature. The reaction mixture was stirred at 90°C for overnight. After completion of the reaction, the reaction mixture was brought to room temperature and extracted with EtOAc. Organic layer was concentrated and residue was purified by silica gel column chromatography using hexane/ ethyl acetate (9:1) as an eluent to give the **3** with 59 mg (yield 94%).

Compound **3**; colorless oil; ^{1}H NMR ($CDCl_3$, 500 MHz) δ 6.55 (1H, d, 10 Hz), 6.42 (1H, s), 5.56 (1H, d, J=10 Hz), 5.06-5.11(2H, m), 3.89 (3H, s), 3.78 (3H, s), 2.24 (3H, s), 1.94-2.05 (6H, m), 1.56-1.58 (2H, m), 1.67 (3H, s), 1.56-1.58 (6H, 2s), 1.38 (3H, s).

(*S*,*E*)-2-(4,8-dimethylnona-3,7-dien-1-yl)-5-methoxy-2,7-dimethyl-2H-chromene-6-carboxylic acid (4)

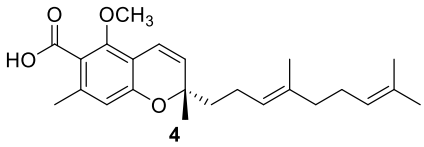

4

To a solution of **3** (50 mg, 0.13mmol) in MeOH (2 mL) and THF (2 mL) was added NaOH (6M, 2.5 mL) at room temperature. The reaction mixture was stirred at 100oC for 1-2 h. After completion of the reaction, the reaction mixture was brought to room temperature, solvent was evaporated and neutralized with 2N HCl and extracted with EtOAc. Organic layer was concentrated and residue was purified by silica gel column chromatography using hexane/ ethyl acetate (9.5:0.5) as an eluent to give the **4** with 59 mg (yield 83%).

Compound **4**; colorless oil; 1H NMR (CDCl3, 500 MHz) δ 10.50 (1H, s), 6.55 (1H, d, 10.2 Hz), 6.53 (1H, s), 5.63 (1H, d, J=9.2 Hz), 5.06-5.11(2H, m), 3.87 (3H, s), 2.50 (3H, s), 1.94-2.15 (6H, m) 2.97-3.00, 1.65-1.80 (2H, m), 1.67 (3H, s), 1.56-1.58 (6H, 2s), 1.41 (3H, s).

(–)-(5*R*,8*S*,10*R*)-9,15-didehydro hongoquercin A methyl ester (5)

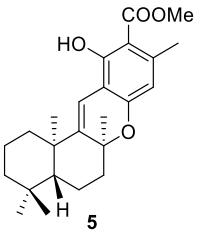

5

To a solution of **2** (194 mg, 505 µmol) in fluorobenzene (10 mL) at room temperature was added ferric chloride ($FeCl_3$) (81 mg, 499 µmol) and stirred for 8 h until the disappearance of the starting material. After evaporation of fluorobenzene, to the residue was added 10 mL of water and extracted with ethyl acetate. The combined organic layer was dried with Na_2SO_4, and the residue was purified by silica gel column chromatography using 5% EtOAc in hexane, which yielded **5** as a white solid (46%).

^{1}H NMR ($CDCl_3$, 500 MHz) δ 11.99 (1H, s), 6.50 (1H, s), 6.19 (1H, s), 3.91 (3H, s), 2.45 (3H, s), 2.20 (1H, ddd, J = 3.5, 3.5, 13.0Hz), 2.05 (1H, d, J = 12.5Hz), 1.90 (1H, ddd, J = 4.5, 13.0, 13.0Hz), 1.80 (1H, d, J = 13.5Hz), 1.65–1.70 (1H, m), 1.58–1.62 (1H, m), 1.44 (3H, s), 1.41–1.52 (3H, m), 1.17 (3H, s), 1.09– 1.20 (2H, m), 0.92 (3H, s), 0.86 (3H, s); ^{13}C NMR (125MHz, CDCl3) δ 172.5, 159.5, 156.3, 148.8, 141.6, 111.4, 108.9, 108.3, 105.0, 79.2, 52.2, 41.5, 41.4, 39.3, 38.0, 33.6, 33.3, 26.9, 24.4, 23.5, 21.6, 19.3, 18.8; ESIMS m/z calcd for $C_{24}H_{33}O_4$ (M^++H) 384.5, found 385.1; $[\alpha]_D$ –176.1 (c 0.10, CHCl3); ECD (MeCN, λ [nm] (Δε), c 0.466mM): 338 (+0.53), 299 (–6.08), 292sh (–5.73), 268sh (–1.42), 255 (–0.46), 236sh (–1.87), 225 (–3.87), < 200 (< –6.06).

(–)-(5*R*,8*S*,10*R*)-9,15-didehydro hongoquercin A (6).

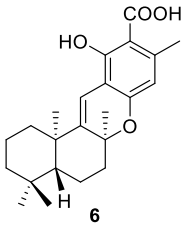

6

To a solution of **5** (27.0 mg, 69.9 µmol) in methanol (1 mL) and THF (2 mL) was added 6M aq NaOH (1.5 mL) and refluxed for 2 h. The reaction mixture was then acidified with 2% aq HCl and extracted with CH_2Cl_2. The combined organic layer was washed with brine, dried over Na_2SO_4, and concentrated. The crude residue was purified by silica gel column chromatography using 20% EtOAc in hexane, which yielded **6** as a white solid (84%).

^{1}H NMR ($CDCl_3$, 500 MHz) δ 11.69 (1H, s), 6.50 (1H, s), 6.24 (1H, s), 2.53 (3H, s), 2.20 (1H, ddd, J = 3.5, 3.5, 13.0 Hz), 2.05 (1H, d, J = 12.5 Hz), 1.90 (1H, ddd, J = 4.5, 13.0, 13.0 Hz), 1.79 (1H, d, J = 13.5 Hz), 1.64–1.70 (1H, m), 1.56–1.61 (1H, m), 1.42 (3H, s), 1.37–1.51 (3H, m), 1.16 (3H, s), 1.08–1.20 (2H, m), 0.91 (3H, s), 0.86 (3H, s); ^{13}C NMR (125 MHz, $CDCl_3$) δ 176.4, 160.5, 157.5, 148.8, 143.4, 112.1, 108.9, 108.2, 103.7, 79.5, 52.2, 41.5, 39.3, 38.0, 33.6, 33.3, 27.1, 24.5, 23.5, 21.6, 19.3, 18.8; ESI-MS m/z calcd for $C_{23}H_{30}NaO_4$ (M^++Na) 393.5, found 393.3; $[\alpha]_D$ –164.6 (c 0.10, CHCl3); ECD (MeCN, λ [nm] (Δε), c 0.421 mM): 335 (+0.54), 298 (–6.48), 290sh (–6.18), 270sh (–2.49), 256 (–1.10), 235sh (–2.36), 228 (–3.07), < 200 (<–7.27).

Unnatural Hongoquercin A (7)

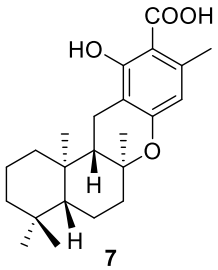

7

To a stirred solution of **6** (0.14 mmol) in EtOAc (10 ml) was added 10% Pd/C (0.028 mmol). The reaction mixture was stirred overnight at 40 °C under H_2 atmosphere. The solid was filtered off and the filtrate was concentrated under vacuum to afford a residue that was purified by silica gel column chromatography using hexane/EtOAc (8.0:2.0) to give **7** (74%) white solid.

^{1}H NMR (500 MHz, $CDCl_3$) δ 11.78 (1H, s), 6.14 (1H, s), 2.63 (1H, dd, J=16.8 Hz), 2.44 (3H, s), 2.19-2.25 (m, 1H), 2.01 (1H, dt, 3.1, 13.0 Hz), 1.69 (2H, m), 1.54-1.60 (3H, m), 1.48 (1H, dd, J= 5.4, 13.0 Hz), 1.38-1.43 (1H, m), 1.28-1.35 (2H, m), 1.13 (3H, s), 0.96 (1H, dd, J= 2.2, 12.4 Hz), 0.90 (1H, dd, J= 3.2, 13.0 Hz), 0.85 (3H, s), 0.83 (3H, s), 0.78 (3H, s). $[\alpha]_D$: +109.1 (c 1.00, $CHCl_3$).

Rhododaurichromenic acid A derivative (8)

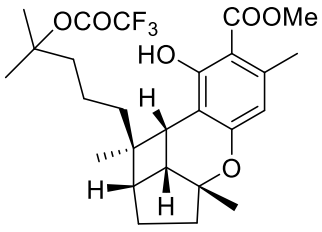

8

To a solution of **2** (24 mg, 0.062 mmol) in CH_2Cl_2 (5 mL) at –78 °C was added TFA (0.5 mL, 6.58 mmol) drop wise. The mixture was stirred at –78 °C for 30 min and then at rt for 30 min. Reaction was then quenched by pouring it to the sat aq $NaHCO_3$, the organic phase was separated, washed with sat aq NaCl, dried over Na_2SO_4, and concentrated under reduced pressure. The crude residue was purified by column chromatography using (hexane:EtOAc) (9.5:0.5) gave **8** as white powder (7.8 mg, 33%).

^{1}H NMR (500 MHz, CDCl3) δ 11.86 (s, 1H), 6.26 (s, 1H), 3.90 (s, 3H), 3.09 (d, 1H, J = 10.0 Hz), 2.56 (t, 1H), 2.45 (s, 3H), 2.41–2.48 (m, 1H), 1.83–1.95 (m, 4H), 1.46–1.70 (m, 4H), 1.56 (s, 3H), 1.55 (s, 3H), 1.38 (s, 3H), 1.25–1.44 (m, 2H), 0.72 (s, 3H), 13C NMR (75 MHz, CDCl3) δ 14.7, 18.5,24.0, 25.5, 27.2, 29.0, 29.3, 35.4, 38.4, 38.8, 42.2, 44.2, 44.6, 46.5, 51.5, 71.1, 84.1, 104.4, 109.4, 113.1, 115.3 (q, J = 105 Hz), 127.8, 140.0, 158.1, 163.2, 172.6 ppm. ESI-MS: 498.53. $[\alpha]_D$: +3.4 (c 1.00, $CHCl_3$). CD (MeCN, λ [nm] (Δε), c = 0.261 mM): 310 (-1.51), 269 (+6.57), 226 (-6.00).

1H NMR of Daurichromenic acid (**1**) and **2**

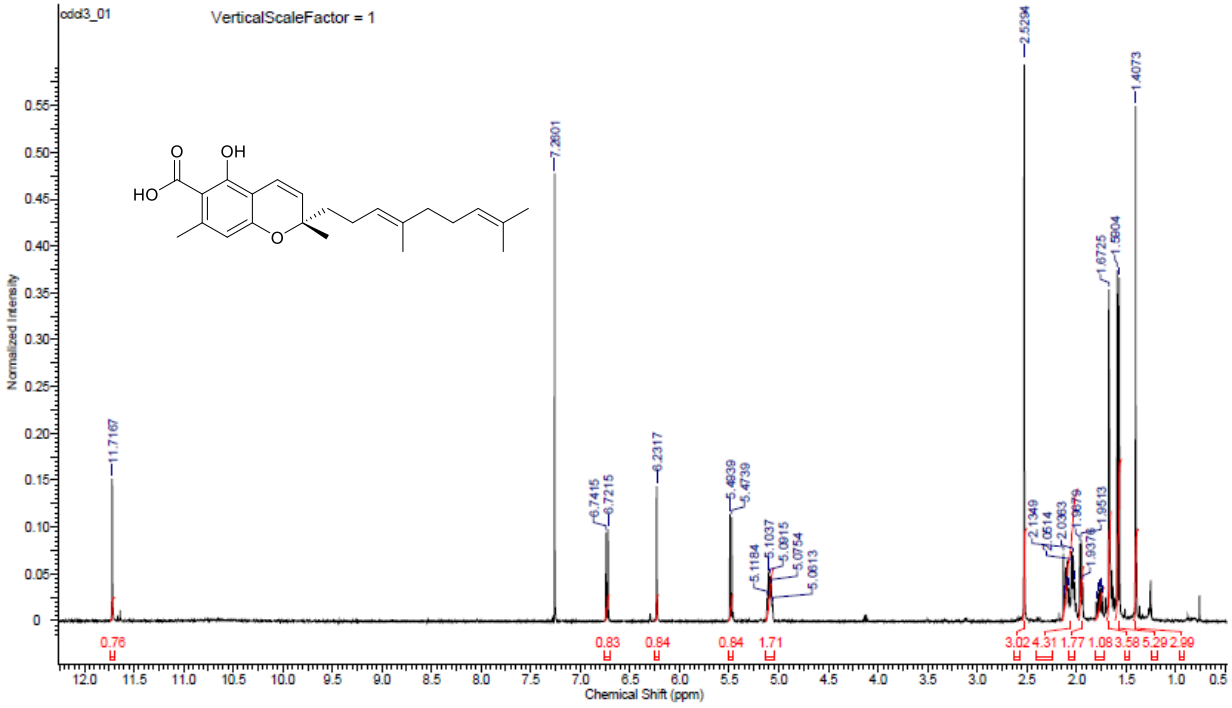

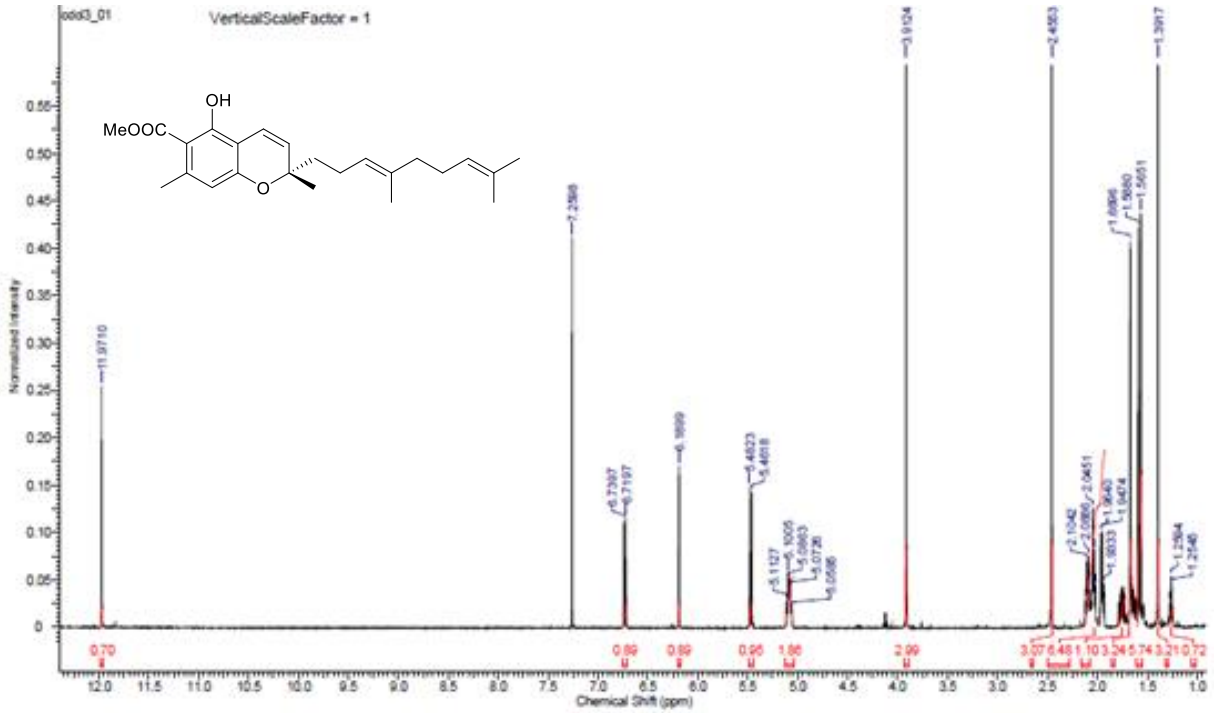

^{1}H NMR of **3** and **4**

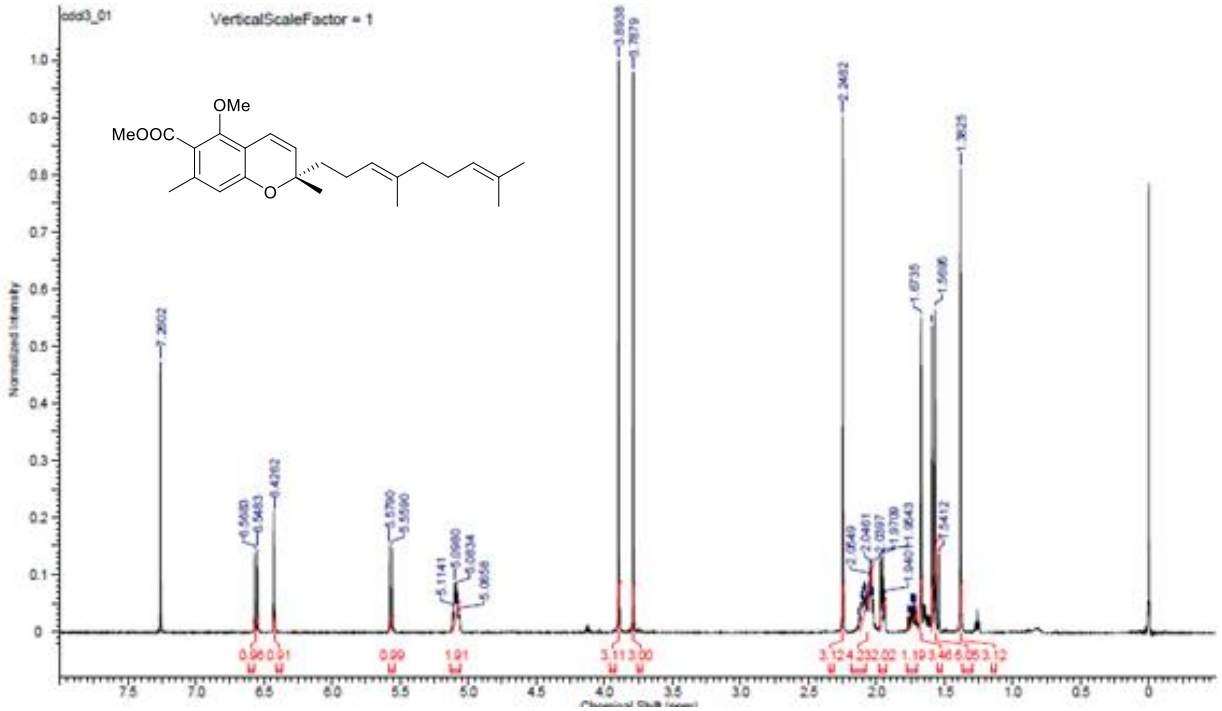

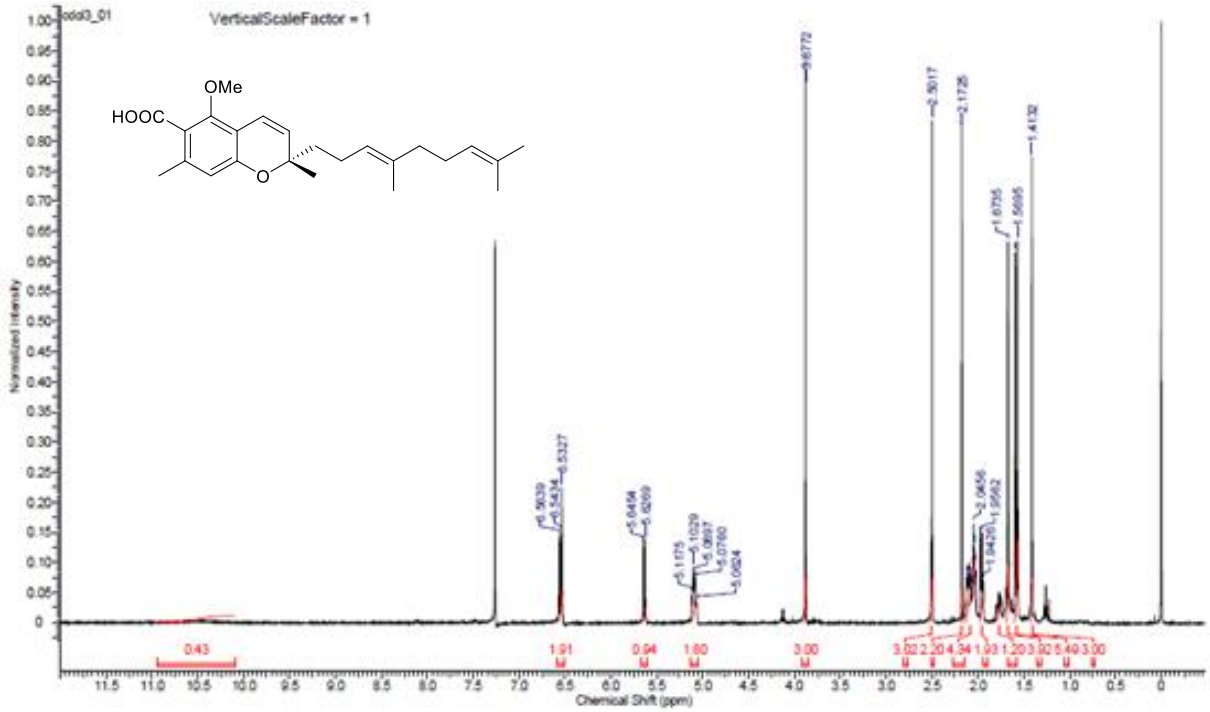

^{1}H NMR of **5** and **6**

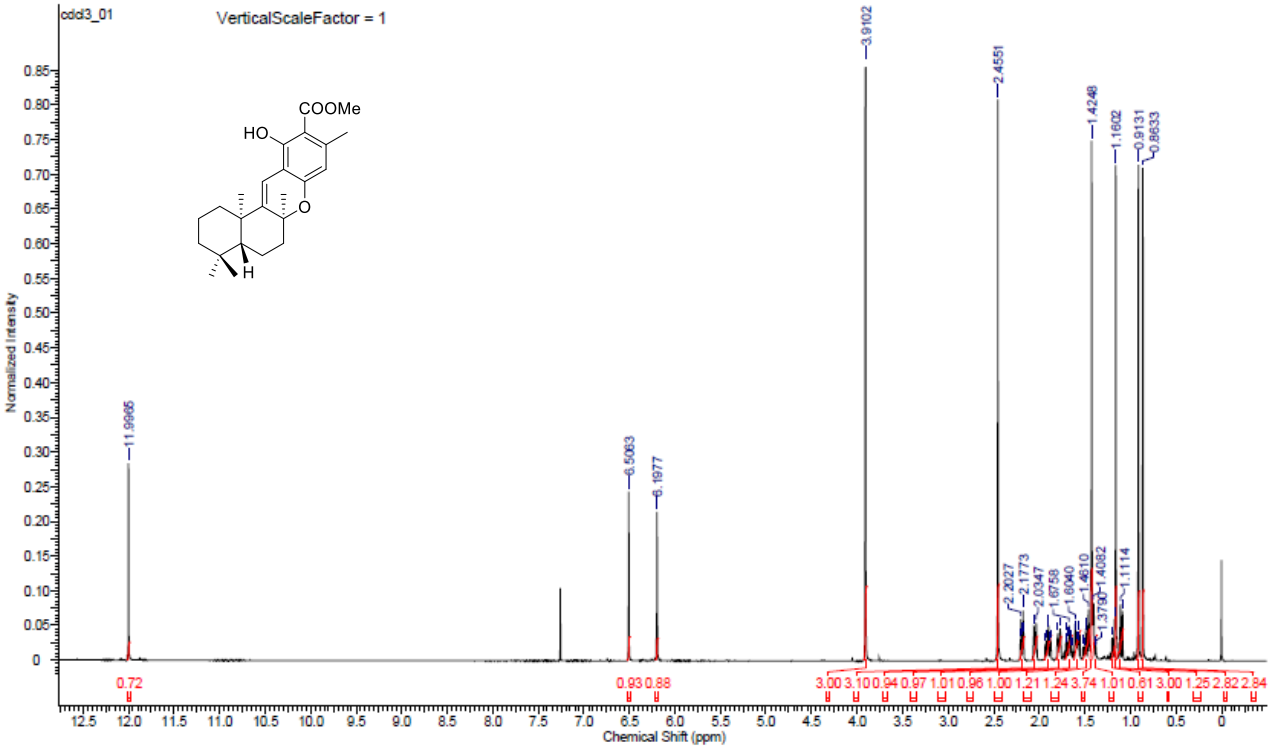

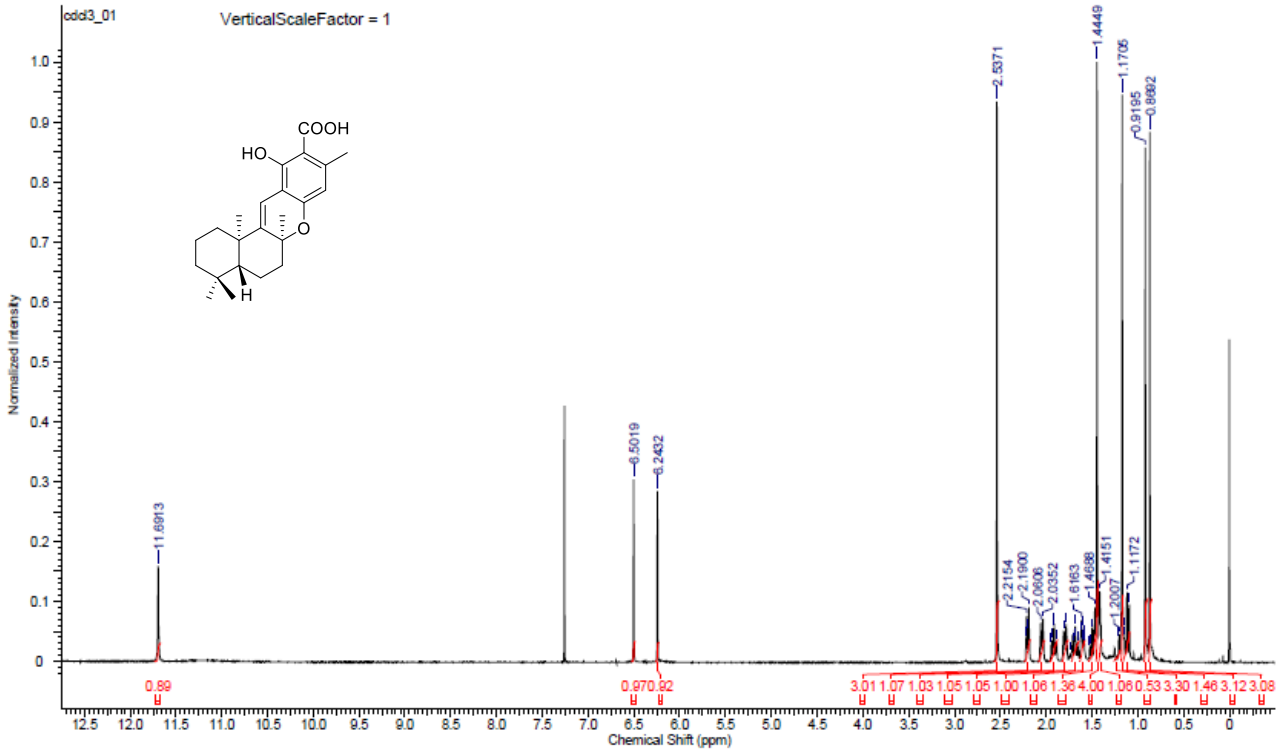

^{1}H NMR of unnatural hongoquercin A **7**

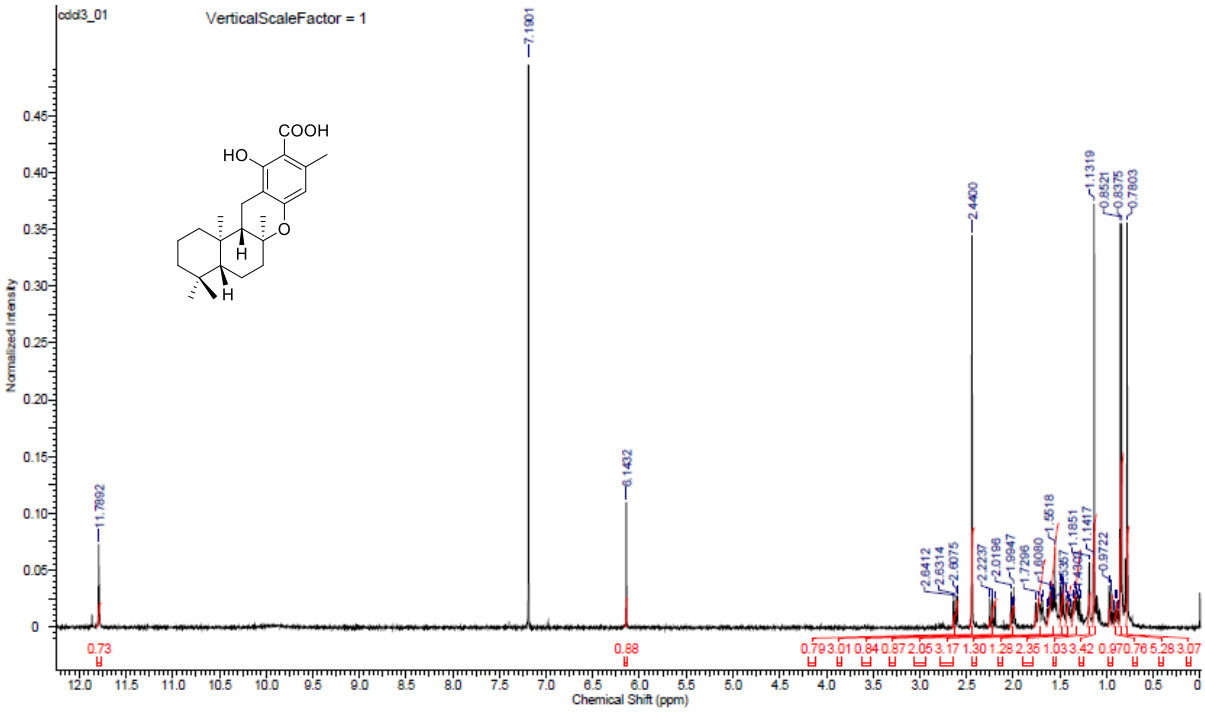

3.5 References

1) Y. A. Hannun and L. M. Obeid, ***Nature reviews***, 2008, 9, 139.
2) Z. Li, Y. Fan, J. Liu, C. Huan, H. H. Bui, M. Kuo, T. Park, G. Cao, X. Jiang, *Arterioscler. **Thromb. Vasc. Biol.,*** 2012, 32, 1577.
3) Z. Li, H. Zhang, J. Liu, C. Liang, Y. Li, G. Teitelman, T. Beyer, H. H. Bui, D. A. Peake, Y. Zhang, P. E. Sanders, M. Kuo, T. Park, G. Cao and X. Jiang, ***Mol. Cell. Biol.,*** 2001, 21, 4205.
4) J. T. Hsiao, Y. Fu, A. Hill, G. M. Halliday and W. S. Kim, ***PLOS ONE***, 8, e74016.
5) K. Yuyama, H. Sun, S. Mitsutake and Y. Igarashi, ***J. Biol. Chem.***, 2012, 287, 10977.
6) T. Ohnishi, C. Hashizume, M. Taniguchi, H. Furumoto, J. Han, R. Gao, S. Kinami, T. Kosaka and T. Okazaki, ***The FASEB Journal***, 2017, 31, 3816.
7) D. J. Newman, G. M. Cragg, and K. M. Snader, ***J. Nat. Prod.***, 2003, 66, 1022.
8) G. M. Cragg, D. J. Newman and K. M. Snader, ***J. Nat. Prod.***, 1997, 60, 52.
9) Y. Kashiwada, K. Yamazaki, Y. Ikeshiro, T. Yamagishi, T. Fujioka, K. Mihashi, K. Mizuki, L. M. Cosentino, K. Fowke, S. L. Morris-Natschkef, K. H. Lee. ***Tetrahedron***, 2001, 57, 1559.
10) A. V. Kurdyumov, R. P. Hsung, K. Ihlen, J. Wang, ***Organic Letters***, 2003, 5, 3935.
11) Y. Kang, Y. Mei, Y. Du, Z. Jin, Organic Letters, ***2003***, 5, 4481.
12) A. V. Kurdyumov, R. P. Hsung***, J. Am. Chem. Soc.,***2006, 128, 6272.
13) D. M. Roll, J. K. Manning, G. T. Carter***, J. Antibiot***., 1998, 51, 635.
14) H. Tsujimori, M. Bando, K. Mori, ***Eur. J. Org. Chem.***, 1999, 2000, 297.
15) D. A. Abbanat, M. P. Singh, M. Greenstein***, J. Antibiot.***, 1998, 51, 708.
16) J. M. Jr Batista, E. W. Blanch, V. S. Bolzani, ***Nat. Prod. Rep.***, 2015, 32, 1280.
17) The calculated and experimental IR spectra were not in good agreement due to over-estimation of their transitions in the region 1360-1070 cm^{-1}.
18) H. Goto, E. Osawa, ***J. Chem. Soc. Perk.Trans. 2***, 1993, 187.
19) Y. Ye, A. Minami, A. Mándi, C. Liu, T. Taniguchi, T. Kuzuyama, K. Monde, K. Gomi, H. Oikawa, ***J. Am. Chem. Soc.***, 2015, 137, 11846.
20) P. L. Polavarapu, E. A. Donahue, G. Shanmugam, G. Scalmani, E. K. Hawkins, C. Rizzo, I. Ibnusaud, G. Thomas, D. Habel, D. Sebastian, ***J. Phy. Chem. A***, 2011, 115, 5665.

Acknowledgement

It is my pleasure to acknowledge roles of several individuals who were instrumental for completion of my doctoral research.

First of all, I would like to express my gratitude to Prof. Kenji Monde, who encouraged for me to pursue this research and taught me throughout my PhD course. I truly enjoyed working in a research environment that stimulates original thinking and initiative, which he created. Prof. Monde's skillful guidance, innovative ideas and stoic patience are greatly appreciated.

My special thanks to my associate supervisors Prof. Shin-Ichiro Nishimura, Prof. Makato Demura and Prof. Akio Kihara for their valuable suggestions and inputs for progress of my research. I would like to express my gratitude to Dr. Yuta Murai, Dr. Tohru Taniguchi, Ms. Yusuke Suga, Prof. Masaki Anetai, Kazuhiko Orito, Dr. Yusuke Ohno, Prof. Min Yao and Dr. Jian Yu and, who contributed to my research and involved in valuable discussion. They always helped me in resolving the most difficult experimental issues.

I would like to thank my colleagues and friends. It was a great pleasure working with them and appreciate their ideas, help and humor. Special thanks go to Keiko Abe and Asana Sugawara for their patience and understanding during administrative work.

My deepest appreciation belongs to my family members for their support and understanding.

I would like convey my special thanks to financial support from MEXT through IGP and JASSO. This work would not have been completed without their financial support.

Publications

(1) **Mahadeva M. M. Swamy**, Attila Mándi, Masaki Anetai and Kenji Monde, “Stereochemistry of a Rhododaurichromanic Acid Derivative” ***Natural product communications***, 2016, 11, 193-195.

(2) Attila Mandi, **Mahadeva M. M. Swamy**, Tohru Taniguchi, Masaki Anetai, and Kenji Monde, “Reducing Molecular Flexibility by Cyclization for Elucidation of Absolute Configuration by CD Calculations: Daurichromenic Acid” ***Chirality***, 2016, 28, 453-459.

(3) **Mahadeva Swamy M. M**, Yuta Murai, Yusuke Ohno, Yoshiko Suga, Masaki Anetai, Jian Yu, Min Yao, Akio Kihara, and Kenji Monde “Structure-inspired design of S1P mimic from natural sphingomyelin synthase inhibitor”(to be submitted)

Patents

(1) 門出　健次、村井 勇太、**マカナハリ マデゴウダ　マハデバ スワミィ**, 天然より得られたＳＭＳ阻害剤ギンコール酸, (**特許公開** 2017-236846, 2017/12/11)

(2) 門出　健次、村井 勇太、**マカナハリ マデゴウダ　マハデバ スワミィ**, 天然より得られたＳＭＳ阻害剤ダウリクロメン酸, (**特許公開** 2017-236847, 2017/12/11)